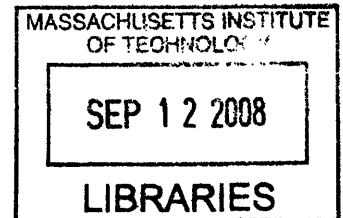# Self Assembly of Block Copolymers: Applicability in Microelectronics and Gains for Patterned Media

By

Anay Chaube

B.Tech., Polymer Technology and Engineering (2007)
Institute of Chemical Technology (ICT), Bombay

Submitted to the Department of Materials Science and Engineering
in partial fulfillment of the requirements for the Degree of

Master of Engineering in Materials Science and Engineering
at the
Massachusetts institute of technology

September 2008

Signature of Author: ..

Department of Materials Science and Engineering
August 15th, 2008

Certified by: ....

Caroline Ross
Professor of Materials Science and Engineering
Thesis Advisor

Accepted by: ....

Samuel M. Allen
POSCO Professor of Physical Metallurgy
Chair, Departmental Committee on Graduate Students

Self Assembly of Block Copolymers: Applicability in Microelectronics and Gains for Patterned Media

By
Anay Chaube

Submitted to the Department of Material Science and Engineering
in partial fulfillment of the requirements for the Degree of
Master of Engineering in Materials Science and Engineering

Abstract

As device size decreases, conventional lithographic methods are finding it increasingly hard to keep up. Introduction of newer method such as E-beam, X-ray lithography etc. has demonstrated possibility of scaling to lower dimensions. However most of these methods are too expensive, too complex or too slow. Hence a method is required which can provide high resolutions at low cost, is easy to implement and can be integrated with current processing technologies. Block copolymer self assembly promises to do just that. An immiscible block copolymer will microphase separate into individual domains due to unfavorable mixing enthalpy. These microphase-separated blocks can have domain sizes of very low dimensions, to the order of 15-20 nms. By careful preparation, microphase-separated thin films of immiscible block copolymers can act as nanomasks for a variety of applications in electronic, optoelectronic and storage media fields. One such application is patterned media. With ever increasing areal densities, there is a limit to which the grain size within a bit can be decreased, for a conventional thin film media. Beyond a certain limit, which is dictated by the superparamagnetic effect, these grains will spontaneously reverse, resulting in undesired data loss. Patterned media has been proposed as an alternative to surpass this thermal instability criterion. In patterned media, lithographically defined nano-scale magnetic elements form single bits onto which the data is stored. Due to its unique structure in which each magnetic dots act as a single magnetic domain it can postpone the arrival of superparamagnetic effect beyond densities much higher than 10 Terabits/inch^2. However, very high resolutions and strict positioning control is required for its fabrication so as to attain a marketable 1Tb/inch^2 advantage. Block Copolymer self assembly holds great promise in fabrication of such devices requiring periodic, high resolution pattern generation. If issues such as long range order, pattern uniformity and placement accuracy of magnetic dots can be effectively resolved, block copolymer self assembly enabled lithography can quickly become the main stay of the multimillion dollar hard disk industry.

Thesis Supervisor: Caroline. A. Ross
Title: Professor of Materials Science and Engineering

Acknowledgements

To start with, I would like to thank my advisor Prof. Ross, for taking me under her wings, and allowing me the freedom to pursue my interest. I thank her for her constant guidance, and quick replies to my all my queries, many of which seem naive to me in hindsight, but were yet patiently answered. I also thank her for giving me direction every time I lost mine. I am in debt for all that I have learnt from her both in and out of class, which increased my understanding of the subject and took my thought process to a different level.

Besides her, I would also like to thank Yeon Sik Jung at MIT, who got me started off with my thesis at MIT, in being kind enough in providing me with the most basic of notes; and also answering my doubts on subsequent many occasions. Also to Dr Fernando Castano at MIT (who incidentally was introduced to me, by Yeon), who took time out to answer a rather lengthy mail of mine. Thanks for that.

I would also like to mention Prof. Yoon of SMA for connecting me to Dr Lui Chongyang at Data Storage institute (Singapore) who provided me with crucial bits of figures, which along with the help I received from my good friend Rajamouly shaped my cost model. Thank you.

Special thanks to my roommate Omkar for helping me sort and organize my references. Thanks also to friends and classmates here, most notably Raghavan, for all their support and fun.

Last but not least, I would like to thank my family back home, for their understanding, support and love, which made all of this much easier.

Table of Contents

List of figures

List of tables

Abbreviations

1D- One dimensional

2D- Two dimensional

3D- Three dimensional

BA- Benzoic acid

BCPs- Block Copolymers

CPS- Close-packed spheres

C- Cylinder

EBL/e-beam- Electron beam lithography

G- Gyroid

HDD- hard disk drive

L- Lamellae

NIL- Nano-Imprint Lithography

P2VP- Poly(2-vinylpyridine)

PB- Poly(butadiene)

PDMS- Poly(dimethylsiloxane)

PEO- Poly(ethylene oxide)

PFS- Poly(ferrocenyl dimethylsilane)

PI- Polyisoprene

PM – patterned media

PMMA- Poly(methylmethacrylate)

PMS Poly(para-methylstyrene)

PS- Polystyrene

SAM- Self-assembled monolayer

SFIL- Step and Flash Imprint Lithography

SSL- strong segregation limit

TSA – template self assembly

S- Sphere

-b- -Block-

-r- -Random

f_A- Volume ratio

L_0 -Natural period of block copolymers

t -Film thickness

WSL – weak segregation limit

χ- Flory–Huggins parameter

Chapter 1: Introduction

With the constant scaling down of electronic, optoelectronic and magnetic devices, and device feature becoming smaller and smaller, the limits of conventional lithography are continuously being challenged. Conventional optical lithography is set to plateau at 45 nm, with alternative methods suggested like X-Ray lithography(1) and E-beam lithography(2) being far too expensive or slow for applicability in the microelectronic industry. Hence to obtain higher density circuits, storage devices or displays, and to keep up with Moore's law, the fabrication community is constantly looking for innovative routes to circumvent costs as well as manufacturing issues. An optimum process would be one that can easily be integrated with current manufacturing techniques and also serve resolution demands of the industry for a long time. Lithography using self assembly of block copolymers is one such technique that aims to do just that.

Block copolymers (BCPs) are composed of two or more homogenous polymers blocks covalently bonded together. On account of the number of different polymers involved one can have di-/tri-/multi-block copolymers. Self assembly is a phenomenon associated with immiscible blocks which separate or self assemble into distinct microphases owing to their unfavorable mixing enthalpy(3). However at the same time macrophase separation is prevented owing to their covalent bonding. When deposited as thin films, these immiscible block copolymers self assemble into a variety of highly ordered morphologies, such that the size scale of individual domains is of the order of 15-50 nms(4).

With a little consideration, a thin film as formed above can be utilized as a self organizing template for a variety of nanostructures having periodic order on the nanometer scale. However to do this other parameters such as microdomain orientation and long range order need to be effectively tailored. If implemented successfully, the combination of "bottom up" self assembly with "top down" microfabrication processes can blend to satisfy the ever growing thirst of the industry fuelled by consumer demands, in a simple, economical and hardy way.

One such application where BCP self assembly can prove especially successful is patterned media (5) . Patterned media consists of small magnetic dots placed at close proximity to each other. It has been proposed as a method to attain areal densities greater than 1 Terabit/inch ^{2} (6). The need for patterned media is twofold, one stemming from the rapid rise of areal density (6) with each passing year and the other stemming from the current conventional thin film media's inability to provide it. (7)

The current conventional thin film media consists of small, single domain grain boundary, generally 10 to 20 nanometers in diameter, which are exchange decoupled from one another having individual grains with randomly oriented magnetic easy axis. To overcome this randomnesss, bits consisting of many grains are written by the magnetic head of a hard disk drive. With increasing areal densities,

manufacturers have so far successfully reduced the size of the bits and grains. However beyond a certain limit, the grain size cannot be reduced due to the effect of superparamagnetism where the magnetic energy of the grain becomes comparable to its thermal energy. When this occurs the magnetization state of the grain can spontaneously reverse leading to thermal erasure or data loss. (7)

Patterned media with its lithographically defined bit positions can circumvent this limitation. In patterned media each bit is a single magnetic domain, with uniaxial magnetic anisotropy in any one direction of remanance. Also the grains within a nano scaled magnetic element are coupled, such that each magnetic element acts as a single magnetic domain(8), Owing to, the 'bit' format of patterned media, very high areal densities can be achieved as the thermal stability criterion now extends to the volume of the entire magnetic element as opposed to individual grains inherent to conventional thin film media. (8, 9)

BCP self assembly's efficacy as a lithographic tool to achieve very high resolutions can be implemented here, either by additive or subtractive patterning, to define the nano periodic magnetic dots/bits.
The key to the success of BCP self assembly lies in attaining sufficient long range order, coupled with uniform placement accuracy of the bits, at extremely small dimensions, so as to get densities of 1 Tb/inch^2

Chapter 2: Self Assembly of Block Copolymers (BCPs)

2.1 Self Assembly

Block copolymers (BCPs or BCs) as they are known; in their simplest form can be considered to be consisting of two or more homogenous polymers blocks held together by covalent bonds. Depending on the number of chemically distinct blocks we can have linear diblock, triblock or multiblock copolymers. If the constituent polymers are immiscible, phase separation is induced, leading to self assembly.

The reason they self assemble into distinct microphases is their unfavorable mixing enthalpy coupled with a small mixing entropy, However at the same time the covalent bond connecting the blocks prevents macroscopic phase separation.

The separation associated with self assembly, and also the order disorder temperature (ODT) depends on some parameters. The total degree of polymerization (N), the flory Huggins parameter (χ) and the volume fraction of homopolymers blocks; all play a role. The degree of segregation is given by the product of χN in the microphase. The dependence of this product can be broadly classified into three different regimes (3, 10):

1) weak segregation limit (WSL) for χN <10

2) intermediate segregation limit for 10<χN <50

3) the strong segregation limit for χN >> 10.5

The different volume fractions give rise to different configurations in the block copolymer microphase separation (11). A volume fraction of around 20%, of the minority block gives a BCC spherical phase in the majority block matrix. At around 38% it changes to hexagonally packed cylinders whereas as we approach 38% we get gyroid or perforated layers at moderate or high temperatures respectively. Alternating lamella is formed at almost equal volume fraction.

So far most of the BCP usage in industry did not take advantage of these self assembling nanostructures. Only very recently, say in the past ten years has research focused on taking advantage of the spatial ordering and orientation of nanodomains :- 1) by using self assembled nanostructures as they are or through chemical isolation/processing of the same

2) via template formation including both the use of copolymer films directly as the template and the fabrication technique, which may be looked upon as a two step process requiring initial template formation and subsequent nanoscale synthesis (12, 13)

2.2 BCP: 3D vs. 2D

BCP morphologies as mentioned earlier are dependent in the bulk on parameters of chain length, volume fraction of involved polymers, the degree of incompatibility and the temperature. However when we take a thin film BCP into consideration, we must take into account additional driving forces, viz. the surface energy and the interfacial energy. The component with lower interfacial energy will tend to adhere to the supporting substrate whereas the one with lower surface energy will preferentially accumulate at the surface.

Additionally, as we will see later, that for some typical film thickness which are integral multiples of polymeric repetition length there exists those morphologies that are expected in the bulk. However at any other film thickness there may be a deviation in morphology from that seen in the bulk. This therefore indicates that thin film BCP phase behavior is more complicated and hence has potential to yield larger number of structures vis-à-vis the bulk.

2.2.1 BCP bulk morphology (3D)

Most studies on BCP have been focused on the simple linear AB diblock copolymer, wherein long sequence of type A monomers are covalently attached to type B monomer. However, triblock and multi block copolymers can be formed using additionally coupled A and B monomers yielding varied branched structures.

Most chemical synthesis give an distribution in molecular weight due to normal chemical kinetics. This of course in BCP synthesis leads to compositional heterogeneity. However, nowadays most BCPs can be prepared with narrower molecular weight distribution. While studying morphology we will assume the ideal case of monodispersed and compositionally uniform molecular architectures.

Microphases

The patterns that result from self assembly are generally referred to as microphases, mesophases or nanophases depending on its length scale. For a simple diblock copolymer the entropy of mixing per unit volume is small due to the large molecular weight associated with macromolecules. Thus the structural properties/morphologies are easily affected by small changes in chemical or structural properties which produce excess free energy not favorable to mixing. This non ideal part of mixing free energy is covered by the Flory Huggins interaction parameter (*14*):

$$\chi_{AB} = (\frac{Z}{K_b T}\left[\varepsilon_{AB} - \frac{1}{2}(\varepsilon_{AA} + \varepsilon_{BB})\right] \qquad ....(1)$$

which gives the free energy cost of contact per monomer between A and B. A positive value indicated net repulsion between A & B and a negative value indicates favorable mixing. Here Z indicates the number of

nearest neighbor monomers and ε is the interaction energy. Generally χ_{AB} is positive barring effect of other forces such as hydrogen bonding. It is also inversely proportional to temperature and hence mixing is favored at higher temperatures.

Most times this parameter itself suffices to explain driving force for phase separation. If the BCP blocks were not covalently bonded this would lead to macrophase separation. However in this case, the covalent bonds balance out the driving force of separation. These entropic forces due to covalent linkages can be equated to elastic forces (14) driven by the Hookean law. With greater number of configurations for a BCP in its inherent randomly coiled state than the number of configurations in extended polymer chains , the phase separation of A and B is only continuous over mesoscopic dimensions. Hence, competing free energies of interaction (given by Flory Huggins parameter) and the elastic free energy, and its intrinsic tendency to minimize decide the most likely configuration and scale lengths for a block copolymer of a given composition at a given temperature.

Illustration of above theory (14):

Now considering a simple linear diblock copolymer we know that:

(1) the degree of polymerization and (2) the composition $f_A = Na/N$, determine the block structure. Now, for a symmetric diblock $f_A = f_B = 1/2$. Also at low temperatures χ_{AB} increases (inversely with temperature) to attain a high value. Thus we can assume strong segregation giving rise to microdomains, effectively pure in A and B. Assuming all chains are uniformly stretched we have an expression relating the elastic and interaction energy per copolymer chain of lamellar phase, given by (14):

$$\frac{F_{lamellar}}{K_b T} = 3\frac{\left(\frac{\lambda}{2}\right)^2}{2N_b{}^2} + \left(\frac{\gamma_{AB}}{K_b T}\right)\Sigma \qquad \dots\dots\dots(2)$$

The first term is the stretching energy for a chain of N total monomers to extend a half period in the lamellar phase. The 2nd term describes interactions that are confined to the narrow interfacial regions between A and B microdomains.

Similarly it has also been proposed that the free energy of a disordered phase per chain can be equated to the A-B contact energy alone by:

$$\frac{F_{disorder}}{K_b T} = \chi_{AB} f_a\, f_b \quad N = \frac{\chi_{AB} N}{4} \quad \dots\dots(3)$$

Equating these two equations ((2) & (3)) we get $\chi_{AB}N = 10.5$ as the defining parameter for ODT. This corresponds closely to ODT proposed by Leibler (3) in his theory of microphase separation. Thus, symmetric diblock copolymers of high molecular weights or with strongly incompatible blocks

$(\chi_{AB}\ N >> 10.5)$ are predicted to be microphase separated, whereas smaller copolymers with more compatible blocks $(\chi_{AB}\ N < 10.5)$ are predicted to show no microphase separation.

More advances to the Leibler theory involve the work done by Mark Matsen and Micheal Schick (*15, 16*). Their phase diagram for a diblock copolymer AB, derived by calculation, closely matches phase diagrams of model diblock copolymers obtained by experimentation (*11*), as illustrated in figure 2.1.

Here for $\chi_{AB}\ N < 10.5$, only a disordered melt is predicted. However for higher $\chi_{AB}N$ beyond the ODT curve, five thermodynamically stable ordered microphase structures are predicted. The five phases are mentioned at the start of the chapter can be divided into:

i)   lamellar (L) phase: stable for nearly symmetric diblocks,

ii)   hexagonally packed cylinder (C) phase: stable for diblocks with intermediate levels of compositional asymmetry for example when, $f_A > 1/2$ the smaller B blocks pack into the interiors of cylinders. This energetically preferable arrangement allows the longer A blocks to reside on the convex side the A-B interface, which affords them more configurational entropy (or, reduces the elastic energy).

iii) body-centered cubic spherical (S) phase: stable for diblocks with higher levels of compositional asymmetry

iv)   narrow region of close-packed spheres (CPS): separating compositional extremes at the disordered and S phases

v)   a complex gyroid (G) phase :between the L and C phases
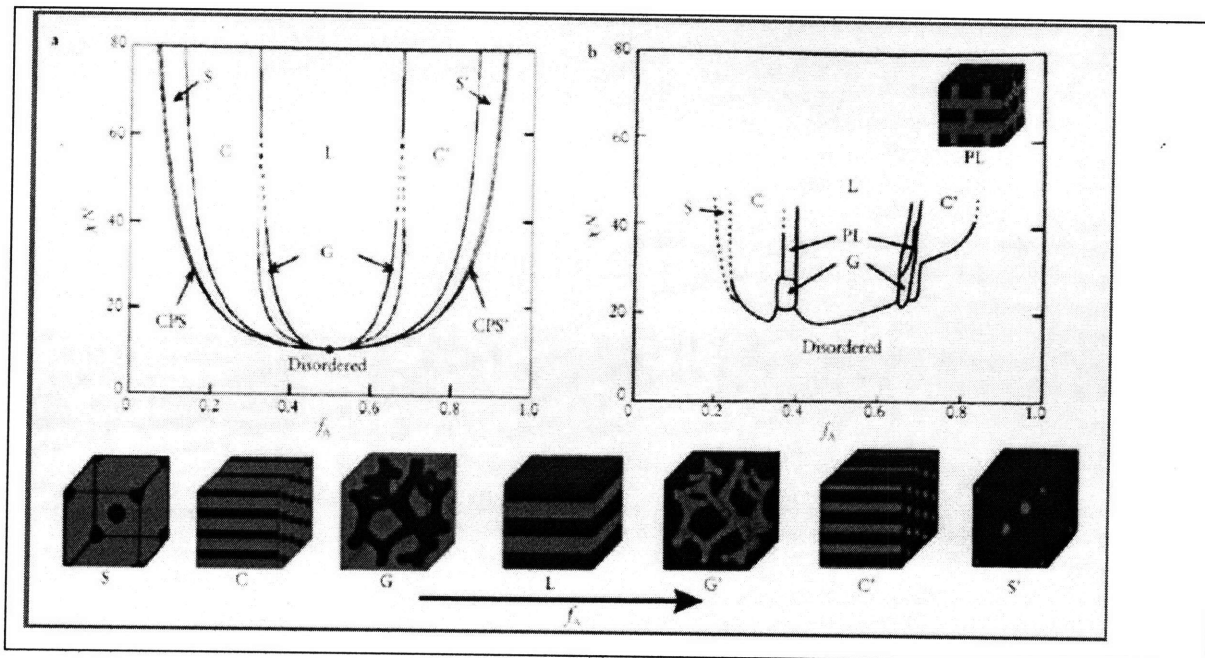
Figure 2. 1: Phase Diagram for linear AB diblock copolymers, theory vis-a-vis experiment :a): Four equilibrium morphologies predicted by self-consistent mean-field theory: spherical (S), cylindrical (C), gyroid (G) and lamellar (L), depending on the composition/and combination parameter χN b): Experimental poly(isoprene-styrene) diblock copolymers phase portrait. Shown at the bottom of the figure is a representation of the equilibrium microdomain structures as f_A is increased for fixed χN , with type A and B monomers confined to blue and red regions, respectively.(11, 14)

Some discrepancies between the theoretical and experimental exist at some points in the figure most notably at the following points. At f_A=0.5, one has asymmetry in experiment as a consequence of probably not getting an accurate value of styrene-isoprene interaction from the single parameter χ_{IS}. Also one see existence of small PL layers in G phase. Theory doesn't predict this but it probably appears only as a short lived region which is not thermodynamically stable (17). A final discrepancy is seen near the ODT regions. In the mean field theory diagram, one sees the lines converging to a (critical) point and thereby only direct phase transitions between the disordered and the ordered (BCC and CPS) phase should be allowed. However by experiment one sees a stable disordered phase beyond χ_{AB} N=10.5 .This is explained by the fact that fluctuations in compositions attain importance in the vicinity of first order ODT curve, esp. for symmetric melts(18).

Despite the above limitations of calculated self consistent mean field theory, the high degree of correlation renders the theory a success.

2.2.2 BCPs in thin films (2D)

As mentioned earlier BCP morphology in thin films is dependent on additional factors such as surface energy and interfacial energy. Research has been focused on understanding this relationship and also the role of the BCP's characteristic length in relation to the film thickness, in deciding BCP morphology, esp. for the case of thin films.

In bulk BCP we have shown clearly defined morphologies as a consequence of volume fraction, degree of polymerization (N), etc. In thin films one observes highly oriented domains as a result of minimization of surface and interfacial energies. In general the most observed trend in thin film BCP is lamella morphology parallel to the substrate esp. when $t > Lo$

These lamella, placed parallel to the surface, do so to minimize the amount of A/B interface while maintaining Lo periodicity. Lamella formation and is classified into symmetric and anti-symmetric wetting, where symmetric wetting involves the same block at each boundary, unlike in anti-symmetric where there are different blocks. It is shown that at equilibrium, symmetric films are stable for a range of characteristic thickness given by nLo, where $n = 1, 2, 3...$ whereas anti symmetric films stable films are formed at $t = (n+1/2) Lo$. Figure 2.2 (*19*) below illustrates the different morphologies for different film thickness.
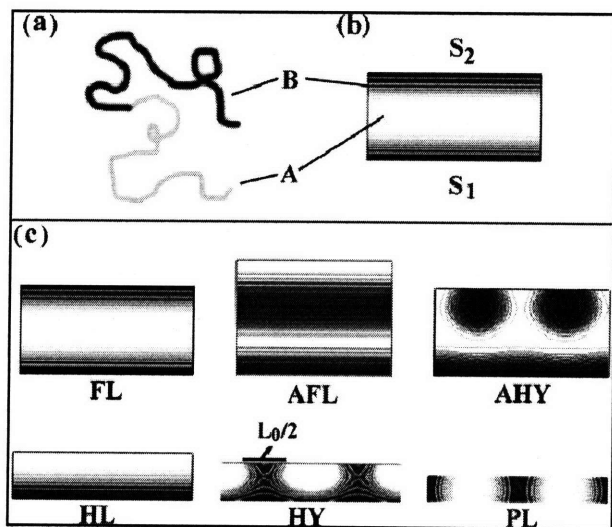
Figure 2. 2: Diblock copolymer thin film morphologies. (a) Schematic representation of symmetric diblock with A(light) and B(dark) type segments. (b) Cross section of BC film system indicating the bottom (1) and top (2) surfaces, with surface interaction energies S1 and S2, respectively. (c) Diblock thin film morphologies, as film thickness decreases from Lo. These calculated cross sections indicate the density of B-type segments, i.e., Black=100% B, white=100% A. These structures are referred to in the text with the abbreviations (19)

Where:

AFL = anti-symmetric surface parallel lamella

AHY = anti symmetric hybrid structure

FL   = symmetric surface parallel full lamella

HL   = half lamella

HY   = symmetric hybrid structure

PL   = surface perpendicular structure

Besides classifying lamella even surface boundary energetics can be classified into symmetric and asymmetric boundary conditions, wherein symmetric system impose identical energetics at each surface and asymmetric which impose different boundary conditions.

Symmetric Boundary Conditions

Research in this area (*20*) has yielded the following trend:

i) Orientation of domain was a function of film thickness. PL was the prominent stable phase when $t \neq nLo$ esp. for $t<Lo$

ii) For neutral surface kinetics PL was dominant and stable for any thickness of film

Further research by Matsen (*21*) and Tang (*22*) also included exploring the possibility of hybrid morphologies for components that were both parallel and perpendicular to the surface. Such hybrid phases were found and believed to be metastable for most cases. Exception to this was shown by work done by Kikuchi and Binder (*23*) who concluded that these hybrid forms could be entirely stable for systems with symmetric boundary conditions and volume symmetry.

For conditions exhibiting boundary symmetry, work done on compositional varying BCPs has been less forthcoming, due to the extra complexity it poses for an analytical solution and also for the greater need of computational muscle. However of particular interest is an analysis of cylinder morphology done by Huinink (*24*), who found that symmetric boundaries having a strong affinity for the cylinder forming (minority) BC components, could induce formation of FL.

Now symmetric Boundary conditions can be attained in lab by either using free standing film or sandwiching it between two like substrates. With the latter confinement technique (*25*) using glassy polymer, it was seen that these boundaries were strongly attractive towards one of the copolymer components, which in turn manifested into stable surface parallel morphologies.

Also as thickness was changed to values incompatible with multiples of Lo, the lamellar period would expand or contract. In fact work done by Kellogg (20) showed transition from lamellar to perpendicular domain orientation due symmetric boundary conditions.

In contrast free standing films too showed particular trends for a system of PS(poly-styrene) and PB(poly-butadiene), as was considered by Radzilowski (26) group. Films of considerable thickness showed surface parallel layering, consisting mainly of half lamellar layer of PB probably as a means of lowering surface tension of component at surface. On the other end, films of minimal thickness, marked a change to volume asymmetric FL from surface parallel PB cylinders. The volume asymmetric core consisted of a thin PB layer between a PS core. This transition is most likely dominated by surface energetics, as the new morphology comes at a higher entropic expense.

Asymmetric Boundary Conditions

In practical cases, most often we encounter substrate supported films which fall under the bracket of having asymmetric boundary conditions. In such film systems, there can be a considerable difference between the surface energy of a monomer and its interfacial energy at the substrate (27).

A study of this effect with t<Lo [2.21] was performed. In this experiment, two boundaries were considered, at substrate where x=0 and the free surface boundary at x=t.
It was noted that the B segments were energetically selective at x=o possessing an interaction energy $S1^B$; whereas at x=t , either the A or B segments were selective, with effect that for either case the interaction energy S2 was lesser than the substrate interaction energy i.e $|S1| \geq |S2|$ [2.21]. Also conditions were imposed such that $S_1^A = -S_1^B$ and $S_2^A = -S_2^B$

The calculated stable morphologies are represented in the following fig. 2.3(*19*) where
AFL = anti-symmetic surface parallel lamella
AHY = anti symmetric hybrid structure
FL   = symmeric surface parallel full lamella
HL   = half lamella
HY   = symmetric hybrid structure
PL   = surface perpendicular structure
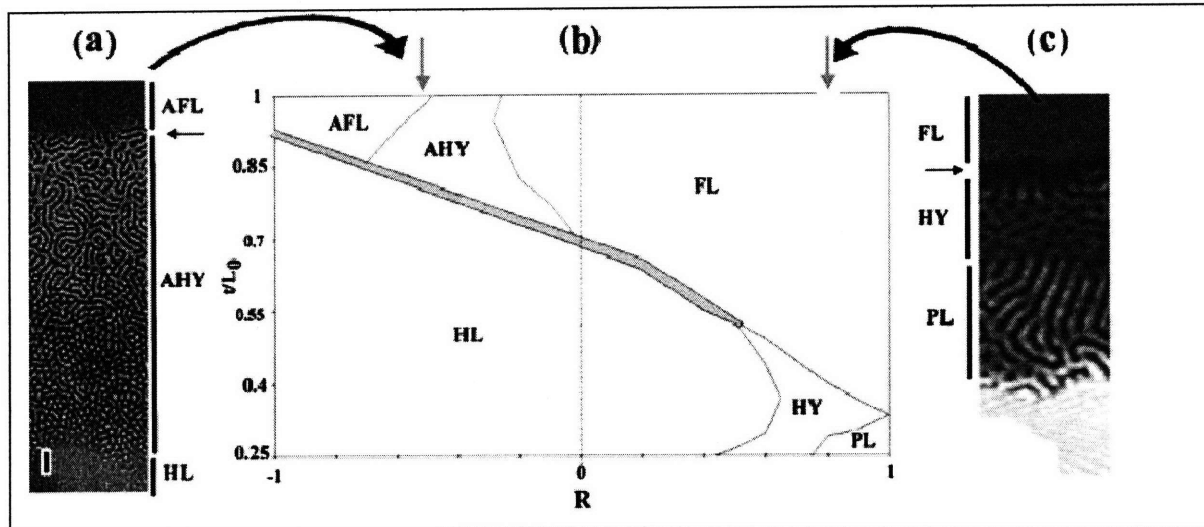
Figure 2. 3: Comparison of predicted morphologies with experimental observations (a)TEM micrograph of PS-b-PMMA thin film exhibiting anti-symmetric wetting, as seen by Morkved et al. Moving from the top the film section decreases in thickness from $3/2L_0$ to $1/2L_0$. PS domains appear dark. The horizontal arrow indicates where a drop in film thickness occurs. (b) Phase diagram of thin film morphologies for: N= 200, $S1^B$ = -0.3 kT, χ_{AB} = 0.1.R= $S2^B/S1^B$. The gray area marks metastable HY morphology. Vertical gray arrows (top) indicate behavior of PS-b-PMMA (left) and PS-b-PLMA (right). (c) AFM phase micrograph of PS-b-PLMA droplet edge. The film thickness decreases from L_0 to 0, from the top. Softer PLMA domains appear dark. Morphologies observed are indicated on the left and the horizontal arrow denotes a sharp drop in film thickness(19, 28)

The positive values of R, are for symmetric wetting. Looking at the figure 2.3 one sees that at R=1 one has 2 phases FL and PL, wherein the former transitions into the latter at certain film thickness. As asymmetry increases i.e. R decreases, we get another phase where at, first the HY structure gains stability, and then the HL morphology. This indicates that with an increase in asymmetry, morphologies lacking horizontal symmetry plane are preferred. Thus a HL phase interludes in a transition from FL to perpendicular structures.

Also as seen in figure 2.3, HY crops between the FL/HL and PL phase. With these latter morphologies being parallel and perpendicular to surface respectively, we can assume HY is a compromise between them.

For R<0, one sees that no perpendicular phases are seen when thickness is less that Lo=2. This is in acceptance of theory where thinner films are predicted to have HL morphology in anti-symmetric systems. When R=-1, AFL morphology is stable considering similar values of affinity of A and B for the surface, and for the substrate respectively. For a smaller negative value of R, one sees a stable FL region with t>0.5Lo. This shows that penalty introduced by localization of B parts near the surface S2 is overcome by

the entropic drive towards Lo periodicity. Similar to R>0, for R<0 one has an AHY region which appears to be a compromise between, in this case, surface parallel states. Matsen (21) indicated that for thickness greater than Lo we have AHY region similarly bounded by anti-symmetric surface parallel lamellar structure.

In figure 2.3(c), depicting an AFM phase micrograph; at Lo one sees a homogeneous layer of FL morphology (indicated be lack of contrast in the figure) which then transits into a region where there's is a sharp drop in thickness of film, akin to a terrace edge

This is often seen in real films supported by a simple substrate. If one casts a film with substrate supported film thickness t_i, and $nLo<ti<(n+1)Lo$, i.e. incommensurate with any kind of equilibrium period, then on annealing one sees a thickness mismatch related directly to this condition where plateaus of $(n+1)Lo$ height are formed on a film nLo thick (27)

Figure 2.3(a) is taken from work done by Morkved and Jaeger (28) who observed (by TEM) films of PS-PMMA deposited on silicon nitride windows which were attractive to PMMA. The section of film shown here decreases in thickness from the top of the image (t==3/2Lo) to the bottom (t== Lo/2).

Most research on BCP thin films deals with bulk-lamellar systems, since it is simpler than the rest, not involving any extra degrees of freedom seen in oft symmetric spheres, cylinders and gyroids. However many of its observed trends can be applied to the other off-symmetric compositions. More experimentation and analytical theory is required for these latter systems.

Experimentation in cylinder morphology though, has been done by various groups, even if theoretical measures are rare. A theory devised by Liu and associates (29) observe that in the case of these cylindrical systems, the persistence of surface parallel layering is limited, esp. as opposed to films of spherical or lamellar systems, which have shown such a layering pattern when thickness of film was many times Lo.

For supported bulk-spherical BC film systems, and the gyroid phase in thin films, little theoretical work has been pursued or published. Spherical BC systems have potential as nanoscopic lithographic masks whereas gyroid morphology is capable of offering unique interconnected structures.

2.3 Summary

This chapter has covered in detail the phenomenon of self assembly both in bulk block copolymers as well as BCPs on thin films. We have seen there are primarily four morphologies observed in such systems, depending on the volume fractions. For applicability in microelectronics, we are more interested in the morphology considerations in thin films. Various models have shown the effect of air, substrate interaction leading to symmetric/asymmetric boundary conditions and their effect on morphology obtained. As BCP self assembly technology heads towards industry integration, it is critical that one is aware of these parameters and their effects, so as to optimize its functionality in industry applications.

Chapter 3: Applications in Microelectronics

Using BCP's self assembling nature and microphase segregation, one can gainfully employ it to generate patterns in nanolithography, and also enable a host of other devices. Conventional lithography uses photon to expose a resist layer, which is then developed. The use of photons limits the feature size formed due to diffraction and sub 50 nm features are hard to get (*12*). For smaller features, we then have the option of e-beam lithography (*2*), but its serial nature makes it economically un-viable for patterning large areas. For this reason a number of other techniques including nanoimprint lithography (*30*), interference lithography (*31*), x-ray lithography (*1*) and BCP lithography has been developed. Block copolymer lithography is simple in principle and has shown to give resolutions as low as 20 nm (*32*).

3.1 Application – As a Lithography Tool

For use in lithography, thin films of BCP when deposited on the substrate can act as a resist material. These films are generally spin cast, baked and then selectively etched. Removal of one block leaves a pattern that can serve as a mask for subtractive patterning (e.g., etching) or additive patterning (e.g., liftoff or electrodeposition) of a functional material, in combination with other planar processing methods. One of its advantages lies in the fact that it can be easily integrated with current semiconductor tooling and processing. Figure 3.1 illustrates BCP enabled lithography. Here the PS-PB BCP, forms spherical microdomains of PB. Depending on sample preparation and processing, an array of holes or dots can be obtained.
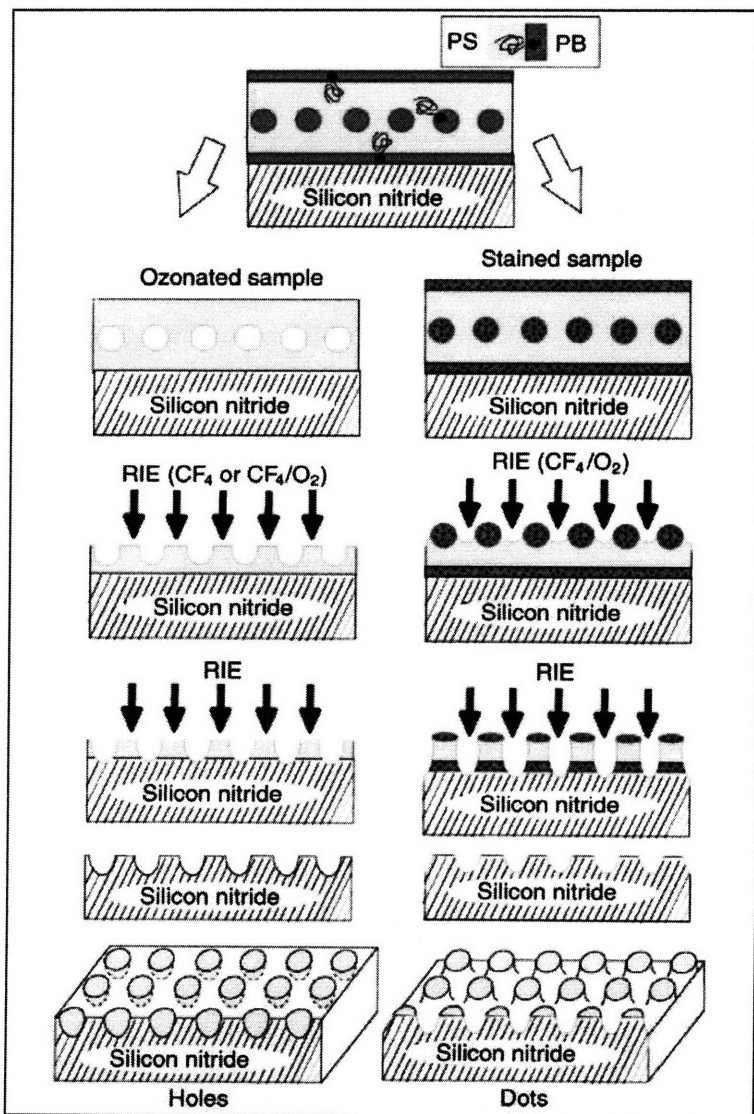
Figure 3. 1:*BCP as a lithographic tool (A) Schematic cross-sectional view of a nanolithography template consisting of a uniform monolayer of PB spherical microdomains on silicon nitride. PB wets the air and substrate interfaces. (B) Process flow using an ozonated copolymer film, so as to used to form holes in silicon nitride. (C) Process flow using an osmium-stained copolymer film, used to form dots in silicon nitride. (D) SEM image of a partially etched, ozonated monolayer film of spherical microdomains. (E) An SEM image of hexagonally ordered arrays of holes in silicon nitride on a thick silicon wafer. The pattern was transferred from a copolymer film such as that in (D). The darker regions are 20-nm-deep holes in silicon nitride, which have been etched out (33)*

A wide array of geometries is possible with BCP lithography depending on the morphology and orientation of the BCP film (*34*). Perpendicularly oriented lamella can give parallel line arrays, so can cylindrical domains lying parallel to the surface. Conversely arrays of dots and holes can be formed by

cylinders lying perpendicular to the plane. Further with the aid of guided self-assembly it is possible to attain uniform well-ordered geometry arrays over larger areas, as will be discussed later.

Selective removal of one block is an important characteristic in BCP self assembly enabled lithography. Volumes of research has focused on PS-PMMA, due to PMMA easy selective removal, availability and well understood full-wafer orientation control methods (35-38) PMMA is selectively removed either by dissolution by acetic acid or degradation by UV (39) or dry reactive-ion etching using oxygen, argon or CF_4 (40). Using acetic acid rinse gives better selectivity between PS and PMMA domains vis-à-vis the plasma etch, but the dry etch prevents the pattern collapse, sometimes associated with wet etch processes. This being said, high aspect ratio hole arrays have been made using wet etch for a PS-PMMA system (39).

The profile of a resulting nanostructures can be greatly improved if one of the blocks has a high etch resistance. One ways to increase etch resistance includes incorporation of inorganic elements into one domain of the BCP. This can be achieved in two ways, One way involves synthesizing a BCP with an inorganic component such as PS-poly-ferrocenyldimethylsilane (PS-PFS) (41), PI-PFS (42, 43), and PS-polydimethylsiloxane (PS-PDMS) (44) to attain high etch selectivity between the organic and the silicon- or iron-containing domains. The second way includes incorporation of an inorganic component, which can be introduced into the BCP system by blending silicon containing polymers or oligomers which are selectively miscible with one domain. One example is, PS-PEO + organosilicate(OS), a hybrid block copolymer system; here OS is selectively miscible with the PEO and forms silicon-containing domains (45, 46). Subsequent oxygen plasma would remove the organic domain leaving behind the inorganic-containing domains on the substrate, effectively producing an oxidized surface layer which would prevent further etching of the inorganic-containing domains.

3.1.1 Patterned Media

As mentioned earlier BCP lithography can reach resolution down to 20 nm, and can also be easily integrated with current semiconductor fabrication technologies. Thus it gives credence to Moore's Law for at least some more years to come, all this at a lower cost and higher throughput compared to serial bottom up processes like EBL(though it has its limitations as will be discussed later). However one should note that BCP lithography is not very flexible in the sense that it can be very effective to form periodic patterns over large area, but cannot be tuned to form specific patterns in specific parts of the substrate.

Even though for simple patterns, cylindrical hole arrays can be applied to elements such as FET gates and wiring levels (via line/space patterns) and/or contact holes (via cylindrical arrays); its main applicability lies in large area periodic patterning.

Patterned media is one such application that meets these criteria. The patterning of magnetic nanostructures is interesting due to its huge potential in data storage (6). The current hard disk stores data in the form of a magnetization pattern written as a continuous thin film of a polycrystalline magnetic alloy. However with ever increasing data density, thermal energy can overcome the anisotropy of the material and result in unwanted erasure of written data. This phenomenon of superparamagnetism limits the data density achievable in thin films (7)

A possible method to extend recording densities is the introduction of patterned media which consist of discrete magnetic dots which are physically separated from each other. Each dot acts as a single magnetic domain, and stores one bit of data (8). For such media to be competitive, data densities on the order of 1 Tbit/in^2 and above would be required (47). This corresponds to a pitch of less than 25 nm, which limits the number of lithographic methods at our disposal. BCP lithography with its ease of application and high resolutions comes into the picture. A prototype for this using BCPs was demonstrated by Toshiba in 2002 (48).

Patterned media as an application has the greatest market potential and will be the focus of this thesis in subsequent sections. Its need, fabrication properties and barriers to implementation will be discussed in detail in the next section.

3.1.2 Limitation of BCP self assembly

In spite of its simplicity, BCP self assembly does have its limitations:

- Limited to generating only periodic patterns such as arrays of holes and dots, gives straight lines
- Period of the block copolymer pattern is governed by length of BCP molecules, hence difficult to make self-assembled patterns with variable periodicity.
- Not useful in the formation of arbitrary patterns.

To increase it applicability tri and multi-block copolymers are being explored, so as to give us a whole new range of morphologies to work with. This is illustrated in fig. 3.2 for a tri-block copolymer system.
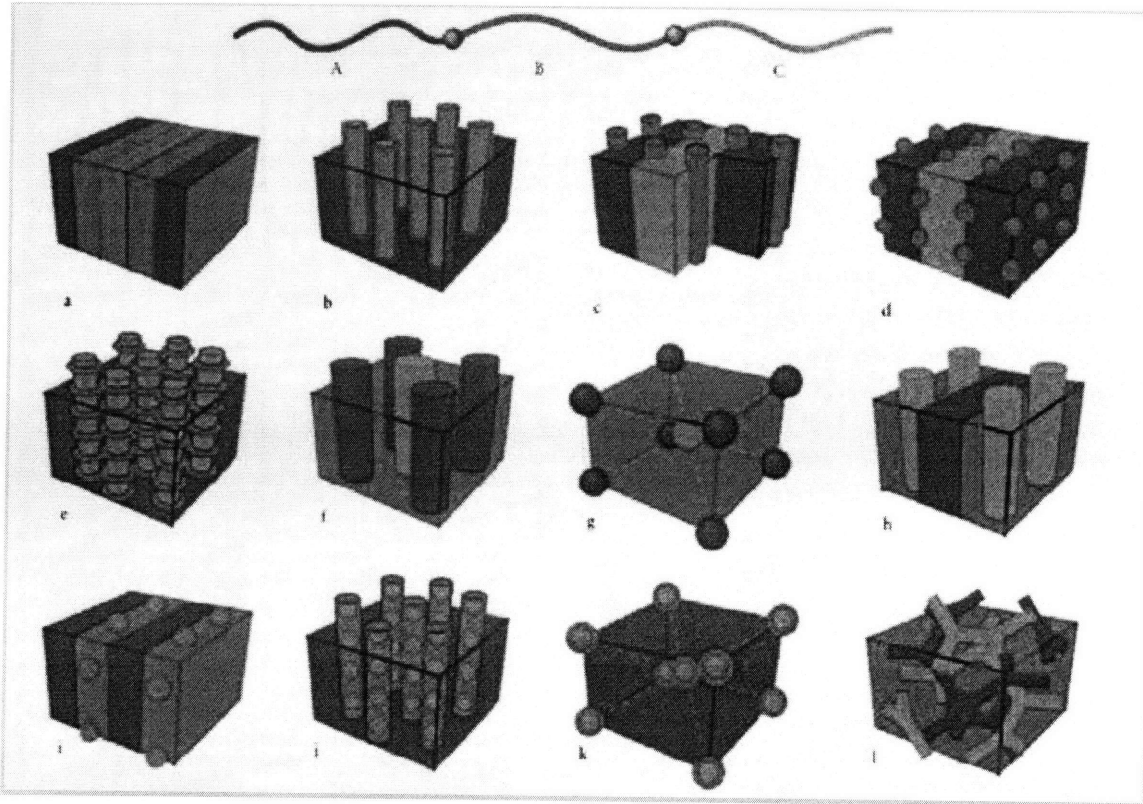
Figure 3. 2: ABC triblock copolymer morphologies. Here the colors blue, red and green represent monomer A, B, C. The combination of block sequence (ABC, ACB, BAC), composition and molecular weight gives substantial leeway in the creation of new morphologies (49)

3.2 Applications in the fabricating nanostructured devices

Besides its use as a lithographic tool, it has been tactfully used to fabricate some interesting nanoscale devices, such as capacitors, flash memories and optical waveguides. These applications have been demonstrated on the research level and will be subsequently discussed.

3.2.1 Capacitors

As devices get smaller and smaller, so do the capacitors embedded in them. With shrinking area there is an obvious decrease in charge carrying capacity of a capacitor as given by its formula. Various techniques have been developed to override this phenomenon, such as deep-trench etching (50), three dimensional stack capacitors (51), surface roughening (52), and high-k dielectrics (53). BCP self assembly proposes a simple way around this hurdle. Using BCP self assembly, one can fabricate a nanostructured capacitor (54) as will be shown here.

Shallow-trench-array gaps were fabricated by transferring the self assembled polymer pattern to a rugged dielectric mask, which is then further used to transfer pattern into device Si counter-electrode. This was followed up by a plasma etch to produce shallow arrays of aspect ratios between 5 to 1 and a mean pore diameter of 20nm (54)This fabrication process has been illustrated in figure 3.2.
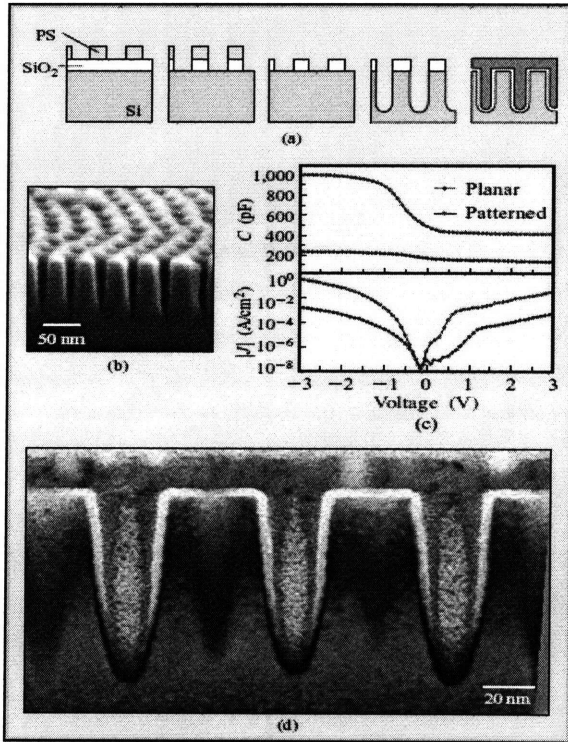
Figure 3. 3: Fabrication and characterization of a shallow trench capacitor:(a) process flow for shallow-trench-array decoupling capacitor fabrication. (b) SEM image of shallow-trench-array (MOS) capacitor bottom Si electrode at 70°; depth of pores is 100 nm. (c) Upper graph: Capacitance versus voltage for planar (solid circles) and patterned (open circles) devices having same lateral area. Lower graph: Leakage current per lateral device area for planar (solid circles) and patterned (open circles) devices. (d) TEM cross-sectional image of completed shallow-trench-array MOS decoupling capacitor (4)

In the TEM image of fig. 3.2d we can see 3 pores of a shallow trench array, which are lined with SiO_2 gate dielectric and filled with a tantalum nitride top electrode. Here the Si electrode surface has comparatively higher area when compared to the planar substrate, due to its roughened surface. The effect on capacitance due to this increased surface area was estimated in the following way (55):

$$\frac{\Delta A}{A_{planar}} = (\pi d h) / (l^2 . sin60) = \frac{2\pi d^2 a}{\sqrt{3}(l^2)} \quad ...(1)$$

where d is the pore diameter, l centre-to centre spacing characteristic to the BCP system, h is the shallow trench array depth and a the trench aspect ratio

The surface area enhancement scales with respect to the trench aspect ratio, which in turn is easily controlled by the etch time. The following equation (2) estimates an increase of close to 500 % (4) for such a device, and capacitance measurements confirm this prediction. Hence this method to increase area and thereby capacitance is effective even with reducing lateral areas of devices.

$$C_{patterned} = C_{planar} \left[1 + \frac{\Delta A}{A_{planar}} \right] \quad \dots\dots\dots (2)$$

$$= C_{planar} \left[1 + \left(\frac{2\pi d^2 a}{\sqrt{3}(l^2)} \right) \right] \quad \dots\dots\dots\dots (3)$$

One drawback of such a device however is the higher leakage current per device viz. approximately 100 times that of a planar capacitor. This is likely to occur due to the higher charge tunneling rates in the high curvature trench bottoms where there exists an enhanced electric field given by equation (3) where,

$$\mu = (1 + 2t_{ox}/d) = (1 + 9/20) = 1.45 \quad \dots\dots(4)$$

where t_{ox} is the gate oxide thickness (4.5 nm) and d is the pore diameter (20 nm) *(4)*.

Besides increasing the trench depth by controlling etch time, one can also control pore diameter by apt selection of BCP template. *(55)*, *(56)*. These devices are compatible with high-performance thin silicon-on-insulator (SOI) circuits, which inherently have smaller intrinsic circuit capacitance and lack of n-well capacitance

3.2.2 Application as an optical waveguide

Optical waveguides consist of a material having higher refractive index embedded between materials with lower refractive index. This provides an omnipresent condition for total internal reflection for light trapped in the medium of higher refractive index. Optical waveguides are present in optical fibers and the basis of optical interconnects for IC chips. These interfaces between materials having different refractive/optical indexes (RI) are generally fabricated from layers of different materials, such that a material of index n_1 sits atop a material of index n_2. The structure of such a waveguide is shown in the figure 3.4.

Figure 3. 4: *Fabrication of an optical waveguide (a) Representation of an optical waveguide with film of optical index n2 below film of optical index n1 (b) Process flow of engineering porosity for fabricating a optical waveguide (c) SEM cross section of unpatterned dielectric film. (d, e) Layered materials having porous top layer obtained through self assembly and etching (4)*

In principle we could use pattern transfer through self assembled polymer to render only a fraction of the underlying dielectric porous, forming a layered structure of this porous dielectric atop a fully dense

dielectric film. A PS-PMMA BCP with cylindrical morphology could be used as a pattern transfer mask, in forming layered dielectric structures of different thickness ratios via controlled etch time. In such a fabrication scheme, the porous dielectric cladding layer atop the non porous dielectric layer provides optical confinement even as the lower non porous layer transports light

The nano scale dimensions imparted by the BCP self assembly are crucial in reducing light scattering by the porous dielectric layer. Scattering S is given by (4)

$$S \propto \frac{d^6}{\lambda^4} \dots\dots\dots\dots\dots\dots\dots (5)$$

With typical dimension of d=20 nm, attainable by BCP lithography, one obtains a low scattering of less than 10^{-3} for a light of wavelength 500nm

A device has been fabricated at IBM Research Labs (4) having a 250nm thick optically transparent material on the substrate, with a base index of refraction, $(n - ik) = (1.56 - i_0)$, for a light of wavelength $\lambda = 632$ nm. Pattern transfer here, was achieved by a self assembled cylindrical phase of PS-PMMA. The thickness of dielectric layer was controlled by different plasma etch times. The porous top dielectric layer therefore had a reduced optical index as compared to the underlying film, creating desired mismatch. In theory the nonporous dielectric layer transports light and the porous dielectric cladding layer on top provides the optical confinement. However this device fabricated, used materials where the underlying substrate has higher RI, and are hence unsuitable for cladding purposes.

In any case, the index of the porous material can be estimated as:

$$\frac{n_{porous}}{n_{nonporous}} = 1 - \left(1 - \frac{1}{n_{nonporous}}\right)v \quad \dots (6)$$

where v is the pore volume fraction in the porous layer.

It is then clear that the optical index change, scales linearly with the extent of film porosity, v; and also that the fractional change increases when considering high-optical-index (nonporous) materials. Self-assembled close-packed hole-array patterns obtained in this demonstration yield layers with v ; 30–50% porosity, so that optical index of this demonstration material changes from a value of 1.39 (for 30% porosity) to 1.28 (for 50% porosity). (4)

However as mentioned earlier, no working device has been fabricated. Also the question remains introduction of porosity will degrade the cladding transparency, thereby introducing degraded performance due to absorption of light. Hence this application is more conceptual in nature as of now.

3.2.3 Nanocrystal based flash memory

Flash memory maintain their non volatility owing to thick gate oxides to prevent any charge leakage through the gate or from the floating gate to the drain/source (57). However in the quest to decrease device area, one has to successively thin down the gate oxide layer, thereby rendering the device susceptible to volatility, due to increased charge leakage through the gate. A solution to this, is using nanocrystals based flash memory, where charge is stored in discrete nano crystals. The efficacy of this device in countering scalability and providing improved retention and reliability and cyclability has been demonstrated by a host of researchers (58).

As mentioned, in this type of device, charge is stored in electrically isolated particles in the floating gate rather than conventional layer setup seen in device today. These nanocrystal enabled memories, builds device redundancy and imparts tolerance against very thin oxide layers. For technologies using fowler-Nordheim processes, such As NAND flash, these devices fit in perfectly, as opposed to NOR devices (59)

BCP self assembly usage to fabricate such devices is illustrated in the following figure 3.5:
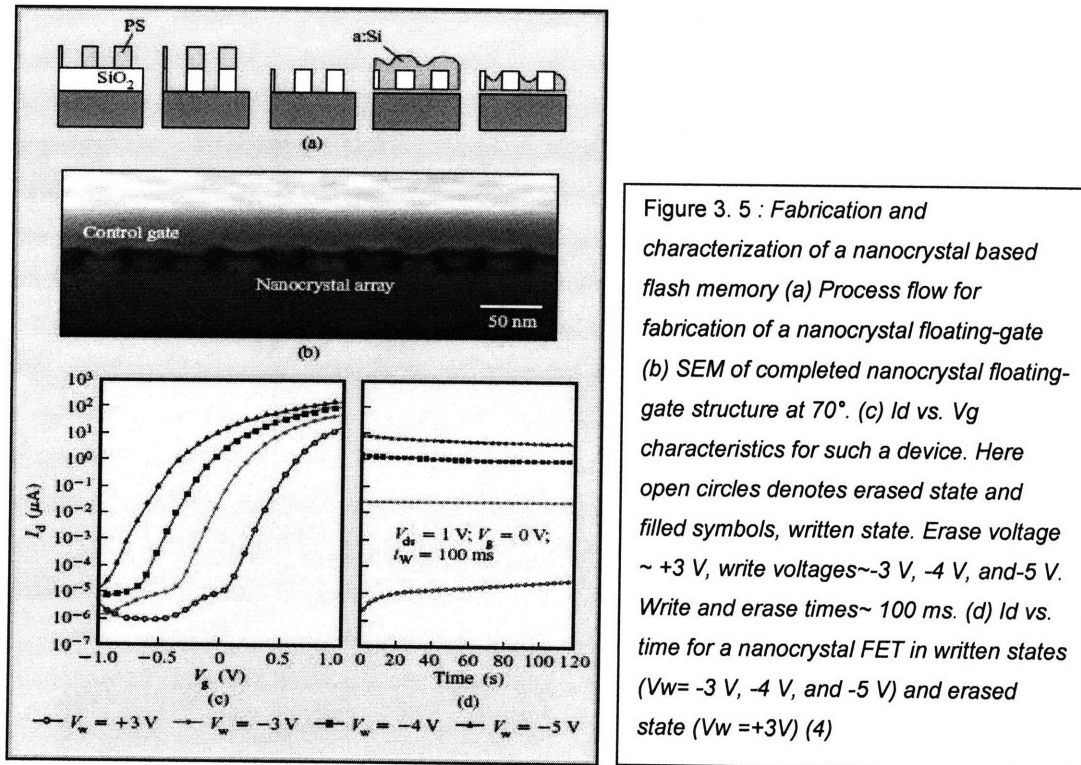
Figure 3. 5 : Fabrication and characterization of a nanocrystal based flash memory (a) Process flow for fabrication of a nanocrystal floating-gate (b) SEM of completed nanocrystal floating-gate structure at 70°. (c) Id vs. Vg characteristics for such a device. Here open circles denotes erased state and filled symbols, written state. Erase voltage ~ +3 V, write voltages~-3 V, -4 V, and-5 V. Write and erase times~ 100 ms. (d) Id vs. time for a nanocrystal FET in written states (Vw= -3 V, -4 V, and -5 V) and erased state (Vw =+3V) (4)

This process (4) showcases devices having crystals at a distance of 20 nm diameter and 40 nm pitch, (60), which are larger than the dimensions one would need for implementation in devices having 50 nm gate length. However, future dimensional scaling in BCP would alleviate this barrier. Also specific to the

nanocrystals technology, is achieving control over nanocrystals size, position and density for uniformity in device performance (61). Effective control of these parameters is also a challenge to BCP assembly.

3.2.4 Nanowire FET

For continued high performance of FET devices, with scaling approaching 10nm, new approaches to FET fabrication have to be taken. One of these designs which show promise to the industry is the nanowire FET (62). This designs gain performance advantages by defining the channel width. With the introduction of such devices, one has to bear in mind the complexities associated with driving different amounts of current, crucial to ICs in which device perform varied functions. Compared to a conventional FET where the current drive is adjusted through lithographically defined width (w), nanowire FET channel width is not easily altered without changing the fundamental device characteristics. Hence multiple channel elements in parallel are needed to operate current drive. BCP's lithographic prowess can be applied here, to attain small channel elements packed in close, regular proximity. Parallel oriented cylinders or perpendicularly oriented lamella can be employed here, to subdivide lithographic patterns of different width, in forming arrays of close packed polymer domains (63). A nanowire FET fabrication process is shown below in figure 3.6.
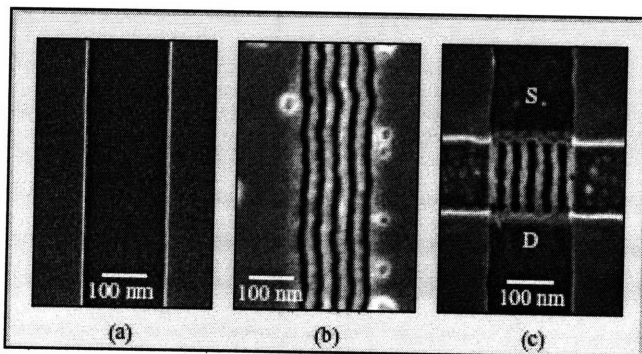
Figure 3. 6: Nanowire array FET
a) Lithographic defined FET channel. (b)BCP self assembly subdivides lithographic feature. (c) Completed six-wire channel nanowire array FET (64)

Here, one can control the number of polymeric lines formed by the lithographic feature width. For a basic PS-PMMA system of parallel cylindrical morphology, the pattern formed can be transferred into a silicon nanowire array through consecutive plasma etch steps (64). Hence polymer self alignment can enable the fabrication of these nanowire FETs, by subdividing random lithographic widths into a numbers of parallel nanowires, thereby easing their current drive scaling.

In fact, Black and researchers (4) have fabricated such a device using PS-PMMA, where they subdivide lithographic regions between 200 and 600nm into five and fifteen periods of 40nms each respectively; where the wire arrays are gated with the substrate through a thick silicon dioxide layer (145nm). However devices thus formed needs a high gate voltage, and short channels effects are observed due to the thick oxide layer, They also exhibit higher than normal (65) on current to off current ratios. This occurs probably

as a result of reduction in parasitic off current paths for leakage, due to complete charge depletion in the nanowire channels *(4)*

3.2.5 IBM air gap

With the industry on the constant look put for new low k dielectric materials, the use of airgaps could be the ultimate solution. (The term air gap here is a misnomer and it reality the gap is actually vacuum). However progress in air gaps technology has been slow and unfruitful.

Just last year IBM has demonstrated a variation of the air gap process, where block copolymer self assembly can be used. Currently ultra low k films have a k~3 which is scaled down to k~2.2-2.3 by nanopore formation. Additional pores cannot be fabricated without degrading yield or reliability, and hence use of a single large" pore, viz. an air gap would be the way forward (*66*).
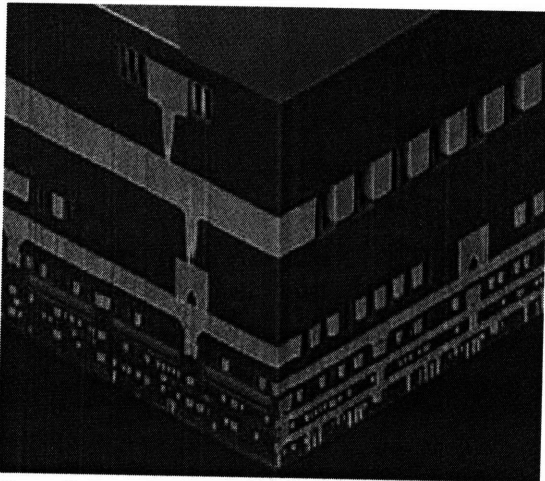
Figure 3. 7: *A color-enhanced SEM cross-section (20k× magnification) shows the airgaps as the holes on each side of the copper wiring.(Source: IBM)*

The IBM air gap process is incorporated into standard dual-damascene copper and SiCOH dielectric process, wherein air gaps are formed by pattern transfer of a hole array from a BCP self assembled system. The hole array has a diameter of 20nm which is most economically achieved by BCP self assembly when compared to other processes. This process is likely to be more useful at lower layers of interconnects, though to lithographic shortcomings(*66*). Its process flow is as follows:

1. Deposit hardmask;

2. Spin-coat an imaging layer; either special new diblock polymer;

3. Create holes using either the self-assembly properties of the diblock lithography;

4. Block out circuit areas to not be etched, using non-critical lithography

5. Transfer holes from the imaging layer to hardmask;

6. Etch: anisotropic RIE to form columnar openings into SiCOH,→plasma damage of the column sidewalls, → isotropic wet etch to remove most of the remaining SiCOH below the hardmask;

7. Strip hardmask; and

8. PECVD of the next SiCOH dielectric level to cap the gaps with a "pinch-off" shape.

IBM claims that, this technique adds only ~1% to chip cost (66) for each dielectric layer gapped. Thus, for an advanced multilevel interconnect, a ~5%-8% cost added should provide 35% faster chips or 15% less power consumption. However in this process, an block out mask is used to protect the underlying metal lines, but being "non-critical" to save costs, the etch chemistry for SiCOH needs to have excellent selectivity to prevent an attack on copper or any metallic barrier layers.

IBM is gunning this technique for 32 nm chips, in tune with the 2009-2010 road map (67). In fact IBM has converted its manufacturing line in East Fishkill, N.Y., where a next-generation Power6 microprocessor has been fabricated, so as to attain a 10 to 15 percent performance enhancement(67). IBM hopes that by 2010, with increases in optimization, system level performance could improve by as much as 30 percent.

3.3 Conclusion

Most of these devise are being designed for the near future, to keep up with scaling laws such as Moore's law, and provide simpler, faster and more economically viable technique. However most of these devices, barring maybe the IBM air gap, cannot be deemed market ready. For flash devices, greater pattern formation density will have to be demonstrated; for FETs desirable current and voltage characteristics have to be obtained; whereas for lithography and patterned media, pattern alignment and uniformity will be the key. Shallow array capacitors are probably least sensitive to such factors (4), however competing technologies (51, 52, 53) are well placed to be implemented too. Optical waveguides akin to FETs are more conceptual than implementable.

In terms of market potential though, the IBM air gap process shows promise for the future. Patterned media as a solution for constant growth in the HDD industry is huge in terms of sheer numbers and market size. For the purpose of showing market potential of BCP self assembly, patterned media has been chosen, and will remain the focus of this thesis, from chapter 5 onwards.

Chapter 4: BCP Self Assembly: Performance Parameters

For implementation of BCP self assembly to a wide range of applications, one has to keep in mind various factors such as microdomain orientation, long range order, maximum possible scaling and defect control. This chapter sheds light on these concerns, termed here as performance parameters.

4.1 Microdomain Orientation

As discussed earlier, depending on the volume concentration of the two BCPs different morphologies such as spheres, cylinders, and lamella can be obtained, provided condition for good microphase separation are met. We also know from the previous chapters, that for the case of thin films, substrate and surface interactions play a role in microdomain orientation.

It is then intuitive that different BCP morphologies will give different nanostructured or nanopatterned devices. The key thus lies in effectively controlling the orientation and lateral order of these domains in thin films.

For the case of an isotropic shape such a sphere, the orientations remains the same in all planes and hence surface energies of the 2 blocks and their interaction with the substrate and air, dictate the film thickness, so that a single layer of spherical microdomains can be obtained.(33, 68, 69)

The same does not hold true for anisotropic shapes like cylinders and lamella. A film spin coated onto a surface, forming cylindrical domains, will most likely have preferred orientation of cylinders lying parallel to the substrate (35, 70, 71) due to the differential interaction at the substrate interface of one block over another. The more technological relevant devices need perpendicular orientation of the cylinders or lamella. (In reality as will be discussed later, besides orientation, long range order is equally if not more important for any devices). In principle this can be done if we can balance out the interfacial interaction of the A and B blocks (of an $-(A_nB_m)-$ BCP) (35) . One way of doing this is to modify the surface. For the case of PS-PMMA where the cylinders are oriented parallel, a thin layer of oxide buffered with HF, applied to the underlying substrate, causes equally non favorable interactions of the substrate surface with the PS- PMMA blocks, and yield perpendicular oriented cylinders on thermal annealing (70).

Another method, involves the use of a polymer brush, wherein an end functionalized random copolymer is anchored to the substrate (35). With the removal of the non attached chains the polymer is now forms a brush of a random copolymer. A BCP film coated onto such a substrate will penetrate into the brush, promoting adhesion, and entailing an average interaction field with the brush for the two constituent blocks of the BCP. The composition of the random polymer brush can be varied by synthesis, which in

turns varies this interaction field. This property is exploited to balance the interactions of the blocks with modified/"brushed" substrate. This surface modification has proven to be robust and can easily be applied to large surfaces (72). Figure 4.1, shows perpendicularly oriented cylinders obtained by this technique for a PS-PMMA di-block system.
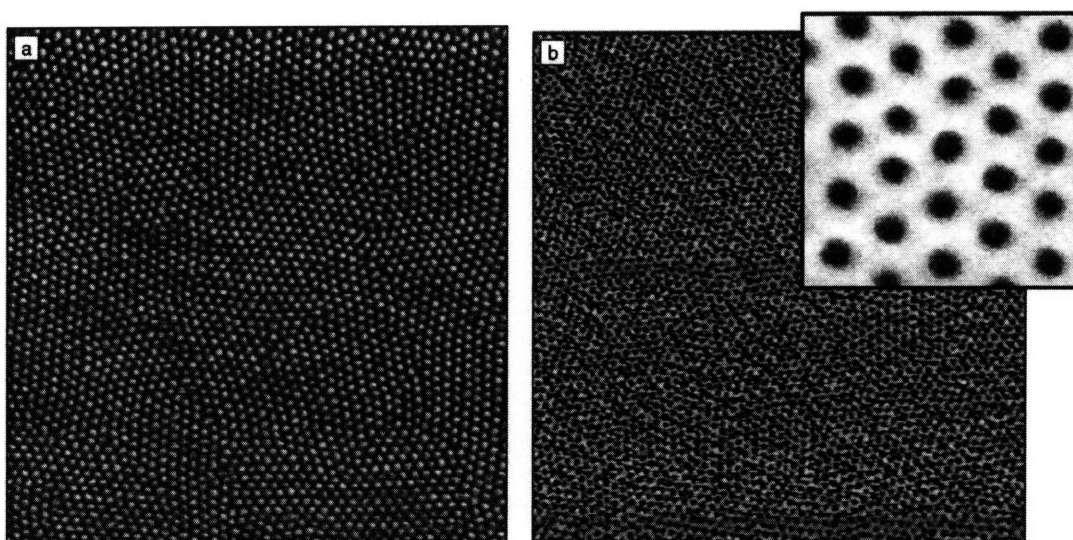
Figure 4. 1 :Perpendicularly oriented PMMA cylinders in a PS-b-PMMA matrix (a) Scanning force micrograph for a 40 nm spin-coated PS-b-PMMA diblock copolymer film where the interfacial interactions were balanced, exhibiting 20-nm perpendicularly oriented cylindrical PMMA microdomains (b) The same film, post UV radiation, and an alcohol rinse. The nanoporous film of cross-linked PS has pores of same size as the PMMA microdomains. inset: field-emission electron micrograph of the film, demonstrating size uniformity of pores The images are 2 µm by 2 µm (35)

In addition to balancing interaction forces, the commensurability between copolymer period and film thickness is also crucial in orienting the microdomains of the copolymer normal to the surface. The effects of incommensurability and film thickness have been demonstrated aptly by Mayes and group, and have been covered in chapter 2 of this thesis.

Other methods to induce microdomain orientation that have been demonstrated are the use of an electric field and solvent evaporation. Electric field plays upon the difference in dielectric constants of the microdomains (73, 74) to achieve orientation, whereas solvent evaporation employs controlled solvent annealing for well formed orientation. In solvent evaporation, one requires a good solvent for both blocks, such that it swells the entire BCP film. Under appropriate conditions, when the solvent is allowed to evaporate, a gradient in the solvent concentration is obtained into the film, with the lowest concentration occurring at air surface. On continued evaporation, the concentration at the surface decreases to a point, such that the BCP microphase-separates. The solvent mediates the surface energies of the blocks, and

defects in the lateral ordering of the domains are rapidly removed, due to the mobile chains (75, 76). Hence an array having long range order is aided by this technique.

4.2 Long Range Order

When polymers microphase separate, the order they assume, is in general only short range. However in most nanolithographical applications where BCP self assembly can be used, we would require a uniform pattern over large distances. To make sure, this happens different approaches have been taken by different researchers to attain, what is known as "long range order".

The two major directed self-assembly methods used in BCP thin films are graphoepitaxy and chemical epitaxy (12). In the graphoepitaxy method, self-organization of block copolymers is guided by prepatterned substrates with topographical features. The lateral confinement of the BCP thin films induces long-range ordering of the domains. In the chemical epitaxy method, the self-assembly of block copolymers is guided by chemical patterns on the substrate. The affinity between the chemical patterns and the BCP domains results in the placement of BCP domains on specific locations. The choice between these methods is dictated by its potential application. Hence they will be discussed in greater detail, when discussing patterned media, in the next section.

4.3 Alignment Issues and Defect Control

Alignment can be broadly classified into: orientational order, translational order and pattern registration. Each parameter stated, is related to some kind of defect in the self assembly pattern.(77, 78)

1) Orientational order

Good orientational order translates into a self-assembled pattern free of gross defects which disrupt the directional orientation. Orientational defects consists basically of circular defects such as disinclinations, target shapes, spirals.

2) Translational order

Sufficient translational order suggest pattern free of dislocation defects and line fluctuations that fall within tolerance levels for that particular application. These tolerance levels are defined in the ITRS Lithographic Roadmap (79).

3) Pattern registration

Pattern registration implies accurate placement of one pattern w.r.t. other predefined features on the substrate. Besides this, it entails control over location of a defect free region.

Defect Annihilation is a complex process, and still needs to be fully understood. Material parameters such as χ, its product with the degree of polymerization(χN), the elastic and Young's modulus all contribute to dynamics of film defect and their annihilation (*77, 78*). The dynamics, however, associated with each type of defect differ for different block copolymer phases, and hence different approaches may be required for different patterns. Also for phase separated morphologies, the diffusion constants in the perpendicular direction can have values much lower than the diffusion constants in the parallel direction (*80, 81*). Hence defect annihilation requires deeper probing of such parameters before one can fully understand it

4.4 Dimensional scaling

In previous discussions we have seen, that giving sub-lithographic resolutions is one of the keys of BCP lithography. In addition to this property one observes that BCP self assembly can also be tailored to give desired resolution. Now, in a BCP, the characteristic domain length scale (L_0) scales with the degree of polymerization as (*82, 83*):

$$L_0 \, \alpha \, N \, \delta$$

where $\delta == 2/3$ in the strong segregation regime. [27]

The degree of polymerization for a <u>symmetric</u> BCP can be calculated with the help of the following formula *(4)*:

$$N = Mn \left(\frac{0.5}{m_1} + \frac{0.5}{m_2} \right)$$

where Mn is the number average molecular weight and m_1 , m_2 are the respective monomer molecular weights of the two constituent blocks.

By looking at the above equations, one could predict or tune the dimensions just by changing the value of N which is a function of the monomer molecular weight. Hence dimensions as low as desired can be obtained. However this is not the case as the constituents' blocks of a BCP have to satisfy several criteria, most importantly the product of their interaction parameter and N. In chapter 2 we had stated that this product should be greater than 10.5,(χN >> 10.5), viz. the condition for strong microphase separation. Only when we have strong microphase separation, will we get distinct pattern transfer. Hence in reality value of N should be high enough to match these criteria.

Now, the value of the flory-Huggins parameter depends on temperature in the following way: (*82, 83*):

$$\chi = c_1 + \frac{c_2}{T}$$

where c_1, c_2 are material constants for certain fractional compositions.

Using the above two equations and $\chi N >> 10.5$ as a necessary criterion we obtain:

$$N_{ODT} = \frac{10.5}{C_1 T + c_2}$$

OR

$$T_{ODT} = \frac{c_2 N}{(10.5 - c_1 N)}$$

Here T_{ODT} is the order-disorder temperature and can be used as a rough guideline for predicting strong segregation limits, for a given N. Besides the value of Lo, another point to consider is the interface width between a microphase separated BCP. This is given as:(*84, 85*)

$$\Delta_\infty = \frac{2}{[6\chi]^{1/2}}$$

$$\Delta = \Delta_\infty \left[1 + \ln 2 \left(\frac{1}{\chi N_A} + \frac{1}{\chi N_B} \right) \right]$$

Where Δ_∞ is the interfacial width in the limit of infinitely long polymers, and *a* is a statistical monomer segment length.

For the case of a simple PS-PMMA block; the value of *a is 0.7 (86)* constituting an interfacial width corresponding to 25% of the domain width, for lamellae morphologies *(86)*.

Another aspect to consider is minimizing defect density. The previous stanzas have described defect and the importance of minimizing them. When it comes to annealing, increased annealing temperatures result in higher polymer diffusivity and thus faster pattern formation. The upper limit on annealing temperature is the polymer decomposition temperature; which for a PS-b-PMMA system is around, Tdec ; 300°C

For the case of defect control, it has been found that its density can greatly be reduced in a two step annealing procedure (*87*), where in the 1st step it is annealed at temperatures slightly over T_{ODT} to promote better intermixing and defect annihilation; followed by a 2nd stage anneal at temperature lower than T_{ODT}. Again, for a PS-PMMA system :

$$\chi = 0.028 + 3.9/T$$

This weak dependence of χ on T leads to an increase in T_{ODT} from below Tg to above decomposition temperature Tdec, over a very small range. Hence this 2 step technique will not be effective. Instead a system where χ is strongly temperature dependent will be desired so as to ensure Tg $<$ T_{ODT} $<$ Tdec over a broad range of molecular weights (N).

From the PS-b-PMMA, N_{min} is calculated as 300(with monomer molecular weights are about 100g/mol); when satisfying the condition of T_{ODT} >Tg; the characteristic length Lo is, (82, 83):

$$Lo = a.\ N^{2/3}\chi^{1/6}$$

By substituting the minimum values (for a minimum molecular weight of 30,000 g/mol) L_{0min} = 18nm. However the N_{min} value considered here, is from the Weak Segregation Limit, and in reality the value of L_{0min} will be greater than 18 nm. Experiments to this effect have been carried out (4) for Mn ranging from 38000-130000, giving minimum values of 27 nm, for a δ=0.77, PS-PMMA system. Further reduction in this value maybe likely, when considering a minimum Mn of 30,000 g/mol, resulting in L_0= 24 nm (4). However this dimension would constitute a 50% domain interface width for a PS-PMMA system (4).

Summarizing, one sees that the domain size or resolution obtainable scales with $N^{2/3}$ but only with $\chi^{1/6}$. Hence, one sees that to achieve a smaller periodicity, a low molecular weight BCP having a high interaction parameter will be best suited, provided the SSL(strong segregation limits) conditions are met. In SSL, a high χ will lead to a lower interfacial width [since interfacial width is a $f(\chi^{-1/2})$] Some typical room temperature χ parameter values are χ~0.04-0.06 for PS-PMMA (88), χ~0.08 for PS-PEO (89), χ~0.09 for PS-PI (87), χ~0.18 for poly(styrene-b-2-vinylpyridine) (PS-P2VP) (87), χ~0.08 for PS-PFS (90)] and χ~0.26 for PS-PDMS (91).

One sees that the χ value of PS-PDMS is much higher than that of PS-PMMA, and therefore they might prove to be the best bet for further decreasing domain width, so that higher resolutions even lower than 20nms are obtained.

4.5 Performance based choice of BCP

As seen above, a lot of parameters decide BCP applicability for any given application. Besides the quest for lower dimensions, other factors ranging from basic chemistry consideration to industry integration requirements also dictate the choice of BCP. These factors are summarized below:

i) Immiscibility

The polymer blocks should have a high flory huggins parameter at Tg, so as to ensure strong segregation for a lower value of N. this will ensure scalability to small pattern dimensions as well as sharp and smooth interfaces in self assembled patterns.

ii) Annealing:

Solvent annealing and thermal annealing are two methods specific to BCP self assembly. Though solvent annealing may provide distinct advantages over thermal annealing, but it may seem than thermal annealing will be easier to fit into industry line. As mentioned earlier, it is best that the material has $T_g < T_{ODT} < T_{dec}$ (with a large temperature window between Tg and Tdec), for a broader temperature space for efficient self assembly. For a system having strong dependence of χ on temperature, one can access both disordered regime and strongly ordered regime by adjusting T, to ensure minimal defects (87).

iii) Etch selectivity:

The chemical composition of the two blocks should vary significantly. The blocks selected should be such that, one can easily remove one block while keeping the other intact. This said, the intact block should have good properties such as high template aspect ratio and chemically resistant template material composition, for further processing needs.

iv) Microdomain Orientation and long range order

This is an important criteria for fabrication and patterning devices. In most cases, perpendicularly oriented morphologies seem more handy for industry implementation. In any case the chosen BCP system must exhibit easy microdomain orientation control and long range order and therefore predefined techniques should have been formulated, suitable for that particular BCP.

v) Process time

The assembly process should be fast enough to be easily integrated with current approaches. A example to this effect was demonstrated (45) where polymer films were spin coated to in controlled vapor environments eliminating the need of thermal annealing.

vi) Solvent Choice

All blocks of the block copolymer should be soluble in a manufacturing-friendly common solvent.

Of the BCP systems investigated, PS-PMMA may seem the best in terms of satisfying maximum criteria *(4)*. However this is probably an off shoot of the fact, that it has been the focus of most research. Alternate materials and techniques such as incorporation of an inorganic component into the BCP (PS-b-(PEO+PMS) *(55)* ; addition of a small homopolymer blend PS-b-(PMMA-PMMA) blend *(92)* , have been investigated to produce an optimized template. An interesting BCP, having high etch selectivity would be PS-PDMS. PS-PDMS with its high χ value may prove to be extremely handy in attaining high resolutions, as more work is done on it.

Chapter 5: Need for Patterned Media, and BCP self assembly for Patterned Media

5. 1 Technological Need for patterned media

The patterning of magnetic nanostructures is interesting due to its huge potential in data storage (6). The current hard disk stores data in the form of a magnetization pattern written as a continuous thin film of a polycrystalline magnetic alloy. However with ever increasing data density, thermal energy can overcome the anisotropy of the material and result in unwanted erasure of written data. This phenomenon of superparamagnetism limits the data density achievable in thin films (7). This is a serious barrier to further growth of areal density using current magnetic recording systems.

5.1.1 Media Storage and Supermagnetism

In continuous media, the bits are defined by the writing head. Each bit consists of many grains, formed as the magnetic film is deposited. These grains act like independent magnets, with independent magnetic vector, which can be flipped by the read-write head. Thus a single bit consists of many grains whose magnetization lies along the same direction.

Now with an increase in areal density, we require that the grains become smaller and smaller, so as to form straight transition regions easing detection of bit cell boundaries. This translates into lower transition noise and more reliable readback signal. However there is only a limit to which we can expect good performance, when we further reduce grain size. Beyond a certain limit (7), magnetization of the grains will tend to be unstable. This instability is an effect of supermagnetism when due at very low sizes, the thermal energy of the grains (k_BT) will overcome its magnetization energy (KuV), causing the grains to reverse spontaneously thereby corrupting the stored data. To circumvent this scenario, we could increase the Ku of our magnetic material. However this will work counter-effectively, as even though we will get good thermal stability, the media coercivity would become too high for any write head to generate a strong enough field to write data onto it. Thus, higher areal density is limited by thermal stability. This brings into picture alternate media storage methods like patterned media.

5.1.2 Patterned Media

Early work on patterned media was done in 1994 (93). Unlike thin film, patterned media consists of pre defined magnetic elements having uniaxial magnetic anisotropy. This differs from conventional media, in the sense that the grains inside a patterned element are coupled, such that effectively the entire predefined element acts like a single magnetic domain. Hence due to this coupling, the thermal stability criterion is postponed as the volume now refers to the entire magnetic element and not to the individual grains of which it is composed. Also in PM, since the magnetic elements constituting one bit are physically separated, exchange coupling is negligible.

Due to patterned media's design it can give much higher areal densities .Quantitatively, the thermal stability criteria is thus postponed to much higher densities of around 10-15 Tb/in^2. (6). Besides its high density storage capacity and lower exchange coupling, it also enjoys the advantage of elimination of transition noise; since the bits are now defined by their physical location and not be any zigzag boundary between two oppositely magnetized domains.

Longitudinal vs. Perpendicular

As in thin film media, patterned media too, can be classified depending on the magnetic orientation of the bits, viz i) longitudinally (in-plane) oriented and ii) oriented perpendicular to the film surface. Research indicates (94) that it will be easier to write islands patterned as longitudinal media as compared to perpendicular media (95). However, it might be more difficult and costly to do this, employing current thin film processes. In contrast it may be easy to orient bits normal to the surface of the film surface. As in the case of thin film media, patterned perpendicular media will probably also be a better choice.

In both cases, it is essential to maintain a thin film of magnetic material so as to ensure lowest aspect ratios of the magnetic elements. The higher the aspect ratio, the greater will be the head field that a neighboring element will experience, making it more susceptible to being inadvertently written. (6) Thus using the shape anisotropy of high aspect ratio magnetic islands to achieve high perpendicular anisotropy may not be a viable option for patterned media.

5.1.3 Resolution requirements for PM

For patterned media to be competitive, data densities on the order of 1 Tbit/in^2 and above would be required (47). This corresponds to a pitch of less than 25 nm, which limits the number of lithographic methods at our disposal. BCP lithography, with its ease of application and high resolutions then comes into the picture. PM using BCP lithography can be achieved in a couple of ways as will be discussed

subsequently. Before that, a short summary is given, using market figures demonstrating the ever growing areal densities and the corollary lithographic needs.

Projections concerning the magnetic recording industry

We have already mentioned the need for newer higher resolution storage media like patterned media as areal density requirements shoot up. The next paragraph along with its set of figures substantiates this claim. Areal Density (expressed as billions of bits per square inch of disk surface area, Gbits/in^2) is the product of linear density (bits of information per inch of track) multiplied by track density (tracks per inch), and varies with disk radius.

The figure (5.1) is from a SPIE conference in 2004 (*96*). It predicts that patterned media will have to become a dominant storage technology if areal density trend has to be maintained. To get areal densities of 1000 Gb/inch^2, conventional fabrication process will have to be replaced by fabrication by process like BCP self assembly. The corresponding lithographic needs are given in the figure alongside which further validates the need for a process like BCP lithography.
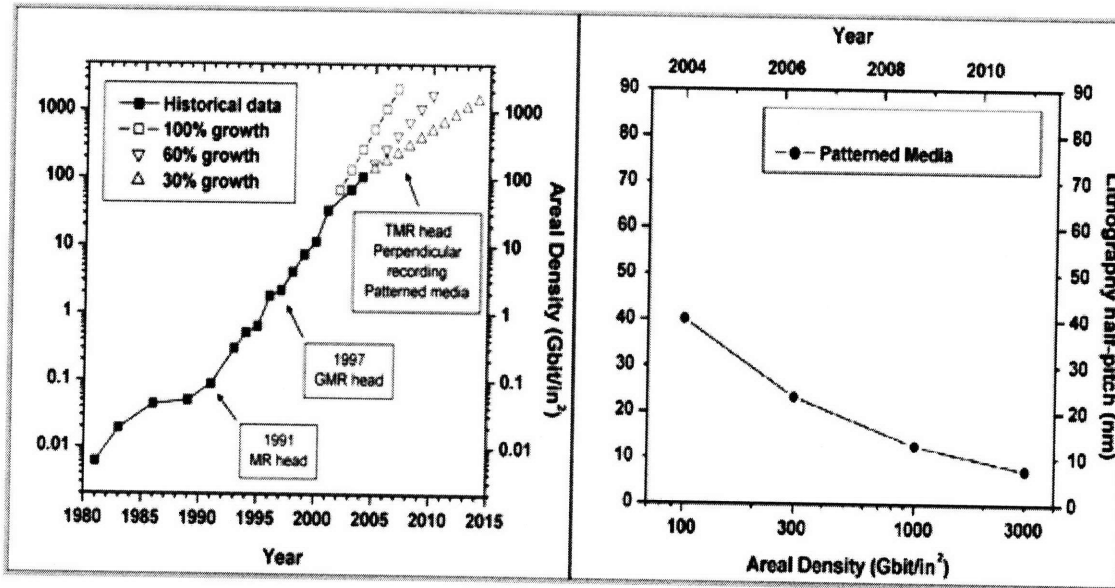

Figure 5. 1: :*Areal Density trends and corresponding lithographic needs: (left) Evolution and projection of areal density in the magnetic recording industry   (right) Lithographical requirements for patterned media (96).*

Typical island sizes and periodicities in patterned media		
Bit areal density (Gb/in2)	Island size (nm)	Periodicity (nm)
300	30	45
500	25	35
1000	18	25
1500	14	20

Table 5. 1: Scaling of island size and periodicities with increasing areal densities (97)

The table 5.1 (*97*) shows periodicities required in patterned media to maintain current areal densities growth trends. Previously one has seen the dimensional scaling typical to a block copolymer system. Periodicities of 25 nm have been easily achieved, for a host of systems, thereby satisfying the 1Tb/inch^2 criterion. Beyond that, a 20 nm resolution can be obtained by proper selection and design of block copolymer system. A system such as PS-PDMS with high χ could be suitable to get even sub 20 nm periodicities, by carefully manipulating synthesis parameters and composition.

5.2 Fabrication Methods via BCP self assembly

Two techniques exist for fabrication of patterned media using BCP lithography, namely subtractive and additive patterning. These are discussed below.

5.2.1 Subtractive patterning methods

Subtractive patterning in general ascribes to removal of part of a material using an etching process, while the desired structures remain protected under the etch mask. In subtractive patterning, the deposition of the magnetic thin film is carried out prior to the deposition and processing of the BCP film, so that we can maintain the magnetic properties of the thin film and optimize the pattern transfer method independently. Subtractive patterning is elucidated in Figure 5.2 where an array of PFS spheres is transferred into an underlying Co film resulting in an array of Co dots with period 55 nm and diameter 35 nm (*41*). The PS-PFS thin film constitutes PFS spheres in a PS matrix. The PS is removed using oxygen plasma (Figure 5.2(1)), and the PFS pattern is transferred into a silica layer with the use of a CHF$_3$ plasma (Figure 5.2(2)). This pattern is then transferred into a W layer using a CF$_4$/O$_2$ plasma (Figure 5.2(3)), and the W pattern is finally transferred into the target Co layer by ion milling using Ne (Figure5.2(4)). This process touches upon some issues related to BCP pattern transfer. The silica layer is present as it enables good wetting of the substrate by the BCP. The Co layer, in common with many transition metals, by itself is impossible to etch using a reactive ion etch process, and hence etched instead by physical sputtering

(known as ion bombardment, ion beam etching or ion milling). For this purpose one needs a layer of W to act as a hard mask and provide good etch contrast with Co under Ne bombardment (*41*). Magnetic measurements of the multilayer showed that the layered structure was preserved through the processing steps.
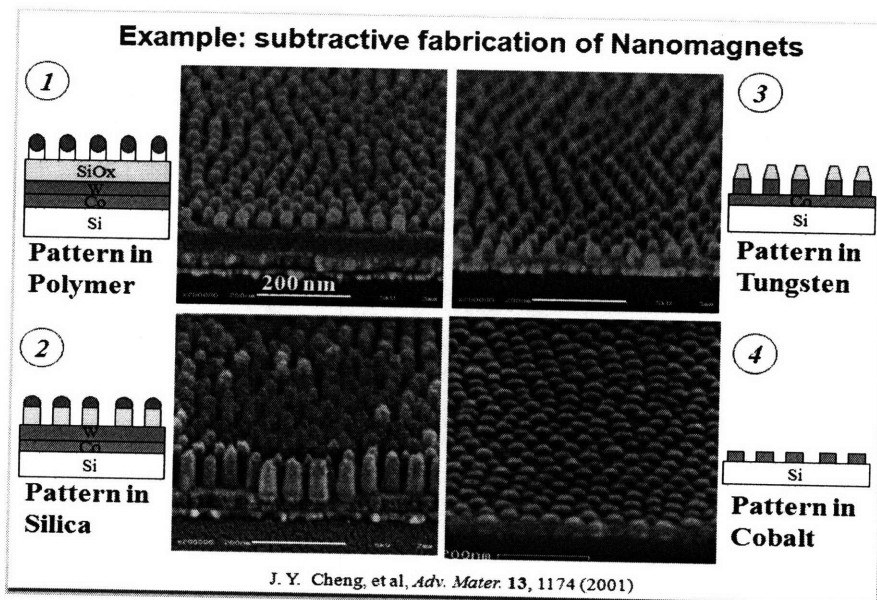

Figure 5. 2: *Illustrating Co dots obtained by subtractive patterning (41).*

In other similar process, CoCrPt or FePt thin films have been patterned using PS-PMMA mask (*48, 98*). In this process, PMMA domains were selectively etched out by oxygen RIE. These voids were then filled using spin on glass which acted as a hard mask in subsequent step, where the magnetic film was etched by argon ion beam into discrete magnetic dots. Other processes involving patterning of multilayers has also been demonstrated, NiFe/Cu/CoFe multilayers patterned by this way, were found to maintain their layered structure(*99*).

5.2.2 Additive Patterning Methods

In additive patterning, the magnetic materials are deposited within or on top of a BCP template, obviating the need for etching the magnetic material. In general for magnetic dot array we can use perpendicularly oriented cylindrical domains by removing the cylindrical domain and then coating the pores by sputtering or electrodeposition with the magnetic material. Magnetic dot arrays can be made by sputtering or evaporating magnetic materials onto etched BCP templates, then lifting off (dissolving) the BCP to leave an array of dots at the locations of the pores in the template. Xiao et al. (*100*) sputtered a 10nm Co layer onto an etched PS-PMMA film.

In additive patterning special attention must be given to the lift off process after metal has been deposited. A standard liftoff process using a long ultrasonic treatment is not advised as was shown by Xiao et al. (*100*). The removal of the continuous Co layer and the PS matrix by the standard liftoff process resulted in defects due to the detachment of magnetic dots (fig. 5.3a). Instead lift offs via mild ion beam etching, followed by oxygen etch displayed better results. (fig 5.3b). Other groups have worked on similar additive patterning using PS-PMMA and PS-P2VP followed by deposition of Ti/Co and CoCr/Pt (*101, 102*).
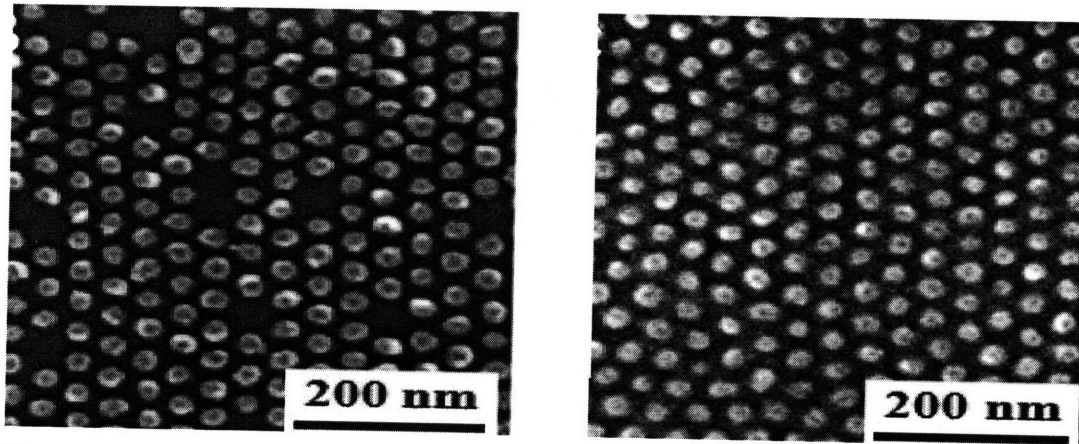
Figure 5. 4:.Magnetic dot placement for additive patterning: (a & b): Top view SEM images of magnetic Co dot arrays on a flat substrate, using PS-PMMA templates after sputtering and lift-off process. (a/left) 'Poor' metal dot arrays after a wet etching process, (b/right) 'Good' metal dot arrays on a flat substrate, after a dry etching process. (100)
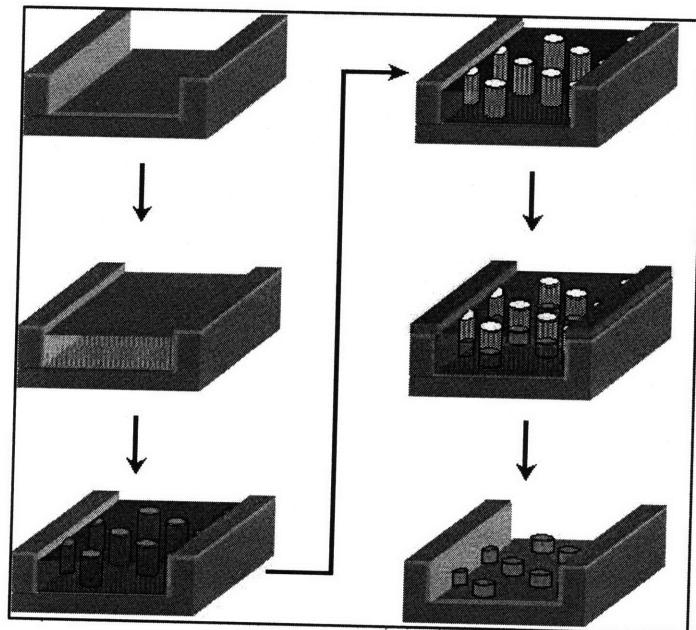
Figure 5. 3: Additive Patterning using vertical PMMA cylinders in a PS matrix *(a) PS-b-PMMA diblock copolymers spin-coated of cylinder-forming onto topographically patterned substrates treated with neutral brushes (green layer: PS-r-PMMA neutral brushes) to form cylinders (b) Annealing of diblock copolymer thin films.(c) Selective etching out of PMMA blocks. (d) Deposition of magnetic cobal metal. (e) Removal of PS matrix including excess metals. (100)*

5.2.3 Subtractive vs. Additive

For the case of additive patterning, the deposition process is similar to conventional deposition process used industry wide. The absence of any etching steps after deposition, lends it similar throughput and cost like the conventional hard disks. However devices made by this technique may suffer from magnetic layer deposition in the recessed region which may influence the read and write process (*103*). Also approaches using perpendicular media recording may not work. A thick soft magnetic underlayer is desirable in PMR. However a thick film stack may not be suitable, since the pattern may become smoother with increasing thickness of the deposited layers (*103*). It also appears that instabilities in the flying could be introduced due to the trenches (*104*), requiring additional planarization.

The case for subtractive patterning has lagged behind additional patterning earlier, due to lack of good RIE chemistry for magnetic materials of interest, and also due to issues of dust generation during ion beam etching process. However recently developments in RIE and ion beam etching for magnetic materials developed for MRAM application (*105*) could significantly tone down this drawback.

Also using subtractive media, perpendicular recording (*103*) can easily be achieved. In the last 1-2 years, the hard drive industry has seen more and more manufacturers shift to perpendicular magnetic recording, and a complete shift from longitudinal recording can be expected soon. It's therefore expected that the same trend of perpendicular magnetic recording will hold true for patterned media as well. Also perpendicularly oriented bits will be easier to orient, as mentioned before.

Hence subtractive patterning may be the more attractive option.

Chapter 6: Technological Hurdles

The implementation of BCP self assembly for patterned media, and patterned media technology itself need to cross several hurdles before they can see a market entry. Probably the biggest hurdle lies in attaining long range order coupled with pattern uniformity and accuracy of the magnetic dots. Besides this patterned media will also constitute some changes in the current hard disk drive (HDD) architecture, which will also need to be sorted out. The crux of these barriers has been explained in this chapter.

6.1 Long Range order

Nearly all areas of application of this technology will require long range order of self assembled BCPs. As formed polymer patterns, such as hole arrays and line space patterns have random positional order and a significant defect density. When speaking of long range order, it indicates that we have the same regularly shaped domains of regular size and at regular intervals throughout the device/ substrate under consideration. For example, in the case of patterned media, we require vertically aligned cylinders to form Co dots, in a ordered arrangement throughout the magnetic media.

Several method have been suggested for attaining long range order, such as electric field (*106*), mechanical shear (*28*) and solvent crystallization (*19*). However pertaining to long range order in thin films of di-BCP, and in terms of semiconductor device fabrication, Graphioepitaxy and chemically pre-patterning methods seem most promising, and will be the main focus here.

6.1.1 Graphioepitaxy

Graphioepitaxy entails a pattern of grooves and mesas of fixed periodicities etched onto the substrate. This can be achieved using standard optical lithographic methods followed by chemical or physical etching. Even PDMS soft stamps and imprint molds (*107*) (*108*) can be used for the same. The grating consisting of the lower 'grooves/channels/trenches' and higher mesas' can induce order into the BCP films. This was earlier demonstrated by Segalman in 2001 (*109*) with the ordering of spheres in the channels of a PVP-PS film. If in the lower channels, the hard wall was found to induce order, the mesas besides, being sites for nucleation, provided flow to the BCPs into the channel. The order observed in this technique, was actually apparent only after the annealing step.

The critical issue here is related to the groove width, and what values it should have to induce desired long range ordering. Experiments to study this effect of varying the channel width were carried out by Cheng (*110, 111*) for a spherical phase PS-b-PFS thin film. Interesting learning has been deduced for the

effect of Ls (width of topographical pattern) on BCP order, relating Ls to Lo, viz the natural periodicity of the block copolymer.

1) For Lo<<Ls, incommensurability is not an issue though spacing of spheres is not distinguishable, i.e it

2) For Lo~Ls, incommensurability does come into picture but is not a deciding factor and ordered microdomains can be formed

The work by Cheng et al studied the number of spherical rows formed for different values of Ls (fig. 6.1 a). For any given microdomain viz. sphere or cylinder, its equilibrium number of rows, for any given spacing will depend on the free energy of polymer chain in confined block against in unconfined block. Graph of free energy vs. confinement width (fig. 6.1b) illustrates this relationship. It was found that free energy is lowest when Ls=nLo and a change in the number of rows is observed when Ls= (n+0.5) Lo. (110, 111) For the polymer and annealing condition, the maximum length of channel width is about $L_S \approx 10 L_O$.
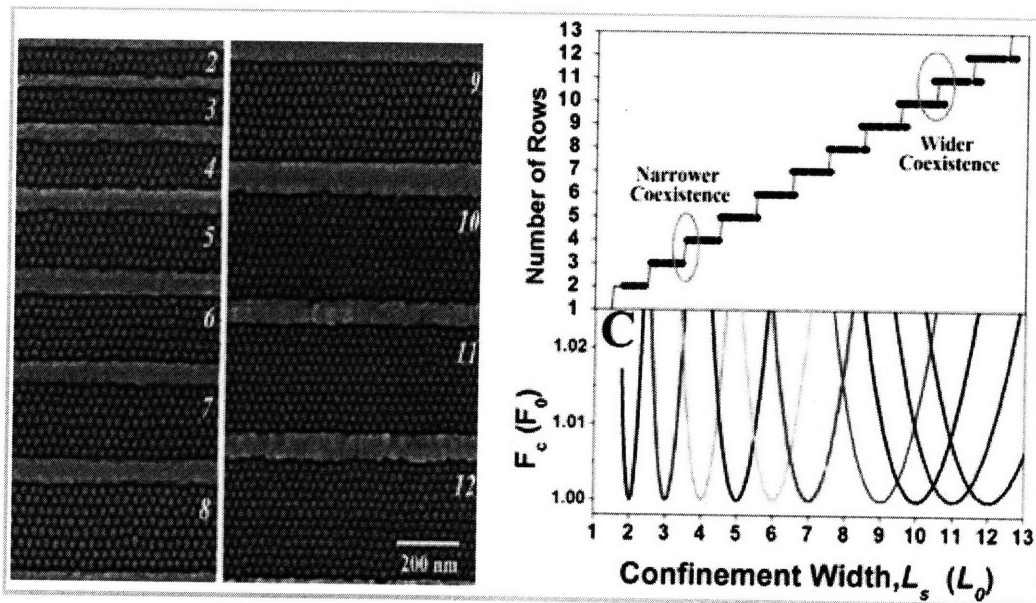
Figure 6. 1: Effect of groove width on long range order :a) SEM image illustrating the effect of varying Ls on number of rows of spherical PFS domains within 1D template [6.9] (b) Graph of number of rows in the groove, N, vs. confinement width, Ls, indicating stability of rows in relation to the systems free energy (110, 111)

Similar long range order for cylindrical microdomains was shown by Sundrani (112), as shown in figure 6.2. Here the cylinders were formed perpendicular to the sidewalls due to the flow of the polymers from the mesas onto the channels, which invariably aligned the axes perpendicular to the walls. However with

subsequent annealing, it lead to coarsening of alignment and eventually perfectly parallel aligned cylindrical domains were observed .

Figure 6. 2: Thin film of cylinder-forming PS-b-PI on a 35 nm deep grating, (width of trough= 960 nm). (a) and (b) show topographic and phase AFM images respectively wherein, in the first case sample is only annealed at 388 K for 2 h (1) whereas for the second case it is additionally annealed at 403 K for 20. Initially, small grains 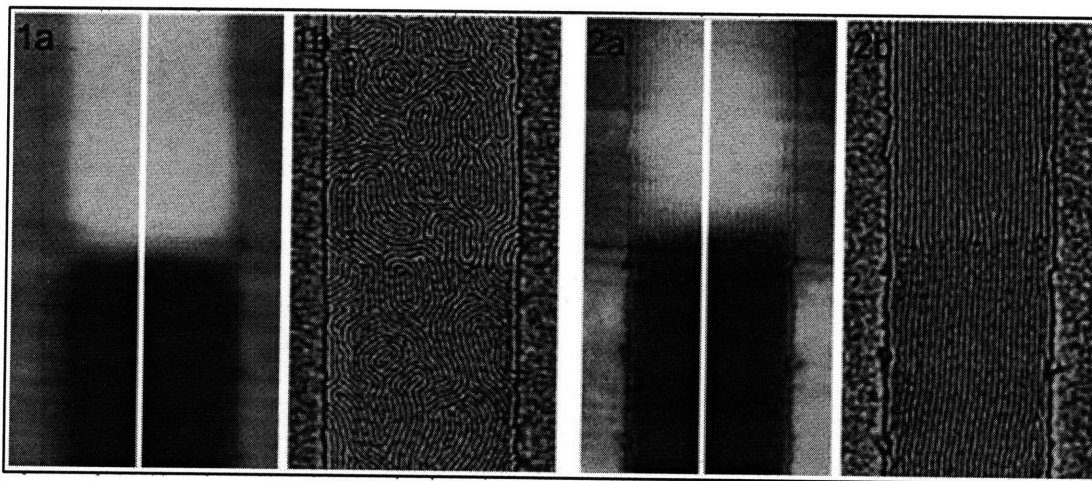of random orientation observed (1b) which then reorient to form a single long grain with cylinders axes parallel to the channel edges. (112)

This being said, the intrinsic limits pertaining to registration accuracy of self aligned polymers are eventually dictated by microphase-separation thermodynamics, compositional and polydispersity effects (*113*)

Graphioepitaxy however remains unique in a way, that it combines the 'bottom up' self assembly of BCPs with 'top down' lithography. Here, relief structure used, can have a length scale much greater than the natural periodicity of the BCP Also this techniques can be implemented without the need of a single crystal substrate.(*114*)

6.1.2 Chemical pre-patterning

In the chemical epitaxy method, the self-assembly of block copolymers is guided by chemical patterns on the substrate. The affinity between the chemical patterns and the BCP domains results in the placement of BCP domains on specific locations. Work in this regard was done by Nealey and co-workers Fig. 6.3 (*115, 116*) where they used interference lithography to periodically pattern a self assembled monolayers on the substrate. PS-PMMA were then spin coated onto the substrate to, wherein PMMA wetted the SAM surface which was modified with polar groups prior to the process. This thus aligns PMMA along the SAM patterned region leaving PS in the non SAM patterned substrates. Even though the periodicities of the

SAM and the periodicity of the polymers has to be similar, a slight variance was shown to be acceptable, by making sure that the interfacial energy gain from preferential wetting adequately compensates the strain energy created by the periodicity diversion.
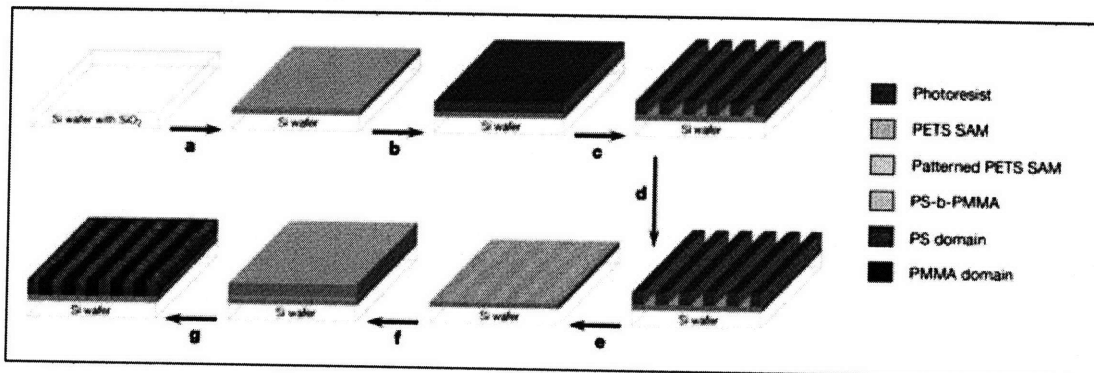

Figure 6. 3: *Schematic representation of the strategy used to create chemically nanopatterned surfaces (115, 116)*

Chemical patterning has the advantages of lower edge roughness and more consistent feature size, due to the polymers self healing nature; but it comes with a drawback that the pattern printed must have dimensions close to intrinsic dimensions of the block copolymer there by needing expensive E-Beam, interference lithography methods to pattern at very small dimensions (which would then beat the purpose of BCP self assembly lithography in the first place)

However the fact that it does smoothen out irregularities in the initial patterning has been exploited to reduce patterning periodicity, by J Cheng et al, as seen in fig. 6.4 (*117*), where they obtained uniform microdomain orientation over long range by using alternate layers of chemically patterned lines on the substrate.

(a)   (b)
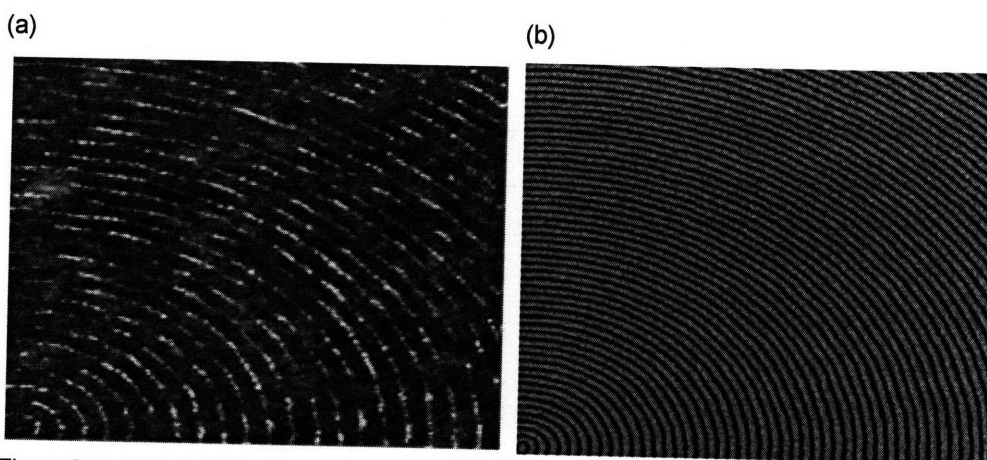

Figure 6. 4: *Effect of chemical patterning width on ordering: Two SEM images with (a) chemically patterned substarte with periodicity 57.5 nm period and (b) Corresponding lamellar BCP with period of 28.8 nm Shows BCP pattern having better line edge roughness than template, and half the period. (117)*

6.1.3 Graphioepitaxy vs. Chemical Pattering

Both graphoepitaxy and chemical epitaxy have shown promise in patterning well-ordered nanostructures over large-area. However there exists a significant difference in their relative length scale between the prepatterned substrate and the natural periodicity of the BCP. For a topographically patterned substrate, this length scale can be much larger than the BCP's periodicity, allowing topography formation by conventional optical methods. For a long time, in chemical epitaxy, the length scale of chemical patterns was restricted to being the same as the periodicity of the BCP, thus requiring expensive patterning steps. The potential to tackle this drawback has been demonstrated earlier (117), however it still remains in a very nascent stage. Chemical patterning holds an edge in reducing line-edge roughness and size variability, due to the 'self-healing' nature of the BCP pattern.

For application in patterned media, graphioepitaxy may be a better bet. There are a couple of reasons for that. As stated above, graphioepitaxy patterns can be easily formed by relatively cheaper methods than chemical patterns due to its greater advantage. Even if chemical patterning were to match up to the graphioepitaxy's length scale, graphioepitaxy could still hold the edge, due to the relative easy integration in industrial device fabrication, in forming topographical patterns as opposed to chemical patterns.

Also patterned media will require a circularly symmetric long range order over the entire area of the disk. Chemical patterning, has so far shown applicability over large areas by interference lithography methods, however interference lithography may not be the best option to get circular patterns, being inherently more suited to cubic shapes.

6.1.4. Annealing

Besides the use of innovative techniques such as graphioepitaxy and chemical patterning, annealing too plays a role in inducing long range order and attaining desired microdomain orientation. Thermal and solvent annealing are two such annealing methods.

6.1.4.1 Thermal annealing:

The efficacy of thermal annealing often depends on the choice of the annealing history. A two step annealing, where annealing in the 1st step is done over T_{ODT} and below T_{ODT} in the next step has shown to improve long range order (87). Use of "zone annealing" which entails processing by moving a hot-cold temperature gradient zone, has also shown improved ordering as well as good in-plane orientational control. Here the 'hot' term refers to temperature above Tg and below T_{ODT}. A moving thermal front (118) has demonstrated a way to speed up the annealing process, such that annealing times approaching a day have been completed within minutes. This may prove valuable, in industrial applications, were overall process time needs to be reduced for higher productivity. Besides temperature considerations, the width of the groove may too play a role in speed of ordering/annealing. Experiments by Sibener and co-workers

(*112*) found that it took longer for parallel cylinders in wider grooves to align compared with narrow grooves.

6.1.4.2 Solvent annealing

In solvent vapor annealing, the BCP thin film is swelled by the solvent, enabling control of domain orientation and BCP morphology, by affecting diffusivity and surface energy of the blocks (*44, 45, 119*). Solvent vapor annealing could be especially useful for attaining ordering in of high molecular-weight, low-diffusivity BCP. It has also shown to decrease defect density substantially, for perpendicularly oriented cylinders of PS-PEO within trenches (*44, 45, 119*) within the first few hours of solvent annealing. For cylindrical morphologies, the cylinder orientation depends on trench geometry and annealing conditions. Parallel cylinders, on annealing are more likely in trenches with wide mesas and a relatively low vapor pressure (*44, 45, 119*).

On the basis of chemistry of ordering, it is not easy to choose between thermal and solvent annealing, though solvent annealing has shown remarkable results (*44, 45, 119*) extending to even high molecular weight BCPs. An industry wise view then would probably be a better outlook. When it comes to time considerations, solvent annealing, by nature may give faster ordering than thermal annealing. However new methods to speed up thermal annealing (*118*) as stated before, would give thermal annealing the edge. More importantly, thermal annealing may seem easier to integrate into a fabrication process than solvent annealing, which would hence make it a much more viable option for the manufacturer.

6.2 Pattern Registration

6.2.1 Pattern Uniformity

In any form of patterned media it is essential to have uniformly formed pattern with accurately placed magnetic elements. For the case of patterned media by BCP lithography, size distribution of the BCP domains will give rise to a variety of undesirable effects such as a distribution of the net magnetic moment and distribution of switching fields. This will introduce jitter in the readback process as well as variability in the switching fields.

Hence it is paramount to obtain uniform size distribution in a BCP thin film. Work in this regard has been done. Cheng et al demonstrated a 9% standard deviation of diameters in magnetic dots made using a PS-PFS spherical BCP (*99*) as an etch mask. For a PS-PMMA film, the distribution of the perpendicularly oriented polymer increased with increased molecular weight. of the BCP. A 10% standard deviation was observed in the cylinder's diameter for a 64 K PS-PMMA mol. Wt whose diameter was around 20 nm

(*120*). Another group reported a standard deviation of 4.3-5.3% for the same cylindrical PS-PMMA case albeit with a molecular weight of 67K.(*121*)

6.2.2 Placement Accuracy

Another important factor in any other kind of patterned media is placement uniformity of the dots. The positioning of the dots is crucial in such a form of storage device, where the magnetic bits are predefined, as it will have a direct effect on the readback jitter as well as the quality of the written pattern. Earlier we have defined chemical epitaxy and graphioepitaxy as key methods to attain long range order. Placement uniformity also depends on the efficacy of these methods. In the case of chemical patterning, the placement accuracy will but naturally depend on the placement accuracy of the guiding patterns, whereas for graphoepitaxy, domain spacing and template edge roughness will hold the key.

In graphioepitaxy; Cheng et al, found that the template edge roughness mainly caused perturbations only in spacing of the spherical BCP domains near the edge, whereas portions away from the edge remained generally unaffected (*122, 123*). This of course stems from the soft domain to domain potential, unique to the BCP assembly system. In fact the perturbations that do exist are a result of limitations on phase separation and the polydispersity effect. To quantify the effect of these factors on the domain placement assembly, the use of pair distribution functions were employed. Results obtained (*122*), showed that the amplitude of oscillation decreased with for a 2D PDF rapidly decreased with distance (fig. 6.5a), for a PS-PFS block on a flat substrate. The correlation length for the same was about 10 Lo. For the 1D PDF, parallel to the groove wall (fig 6.5b), it was shown that precise domain orientation could be predicted at distances even greater than 35 Lo, where Lo is the natural periodicity of the BCP. This particular system, showed only a standard deviation of 0.1 Lo , which implies that the array can be located to within ±6 nm (~0.2L_0) of a registration mark, with 95% confidence.
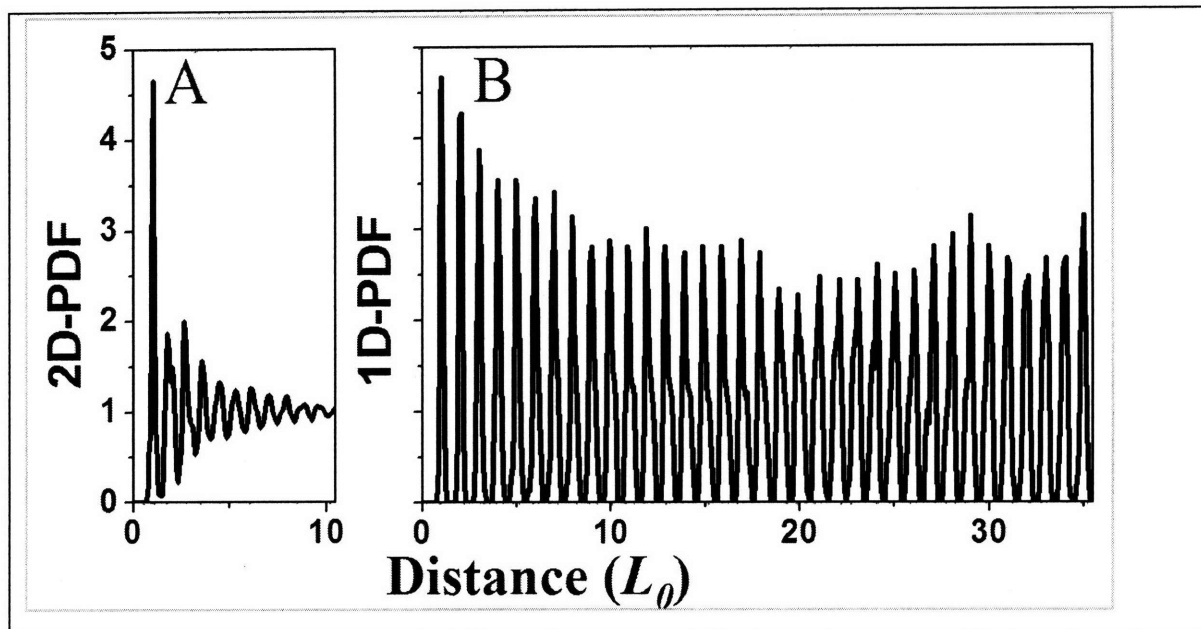
Figure 6. 5: *(a) 2D pair distribution function (PDF) for a film of PS-PFS forming spherical domains on a flat substrate. (B) 1D PDF of annealed PS-PFS spheres in a 1D groove. Peak width in PDF indicates lateral placement accuracy of spherical domains (122)*

6.2.3 Practical Effectiveness

Now we know that in a PM recording system, random deviations, such as dot spacing variations and dot size variations, lead to a finite signal-noise ratio or error probabilities, leading to unrecorded dots (*124*). The maximum sigma/distribution (viz. the standard deviation divided by mean value) of the dot sizes and spacing, for acceptable SNR requirements are around 6%.(*6*)

So, for any given BCP template to be viable, this condition needs to be satisfied. As seen from the previous paragraphs, at least one of the groups have succeeded in attaining sub 6% standard deviations, of 4.3%. This variation in standard deviation among different set of researchers can be attributed to a host of factors such as polymer composition and synthesis method , polydispersity, thickness constrain and annealing conditions (*121*). These factors give us a wide leeway in tailoring BCP templates for PM applications, though more studies on material and annealing effects will determine the ultimate placement accuracy and uniformity achievable in self assembly BCPs for PM.

6.3 Integration with HDD

The pace of Read/Write heads and overall integration of patterned media (PM) into a working system, has not kept up with advances in media fabrication. As fabrication methods of PM become more consistent, there exists a urgent need for system integration. The recording characteristics that need to be sorted are discussed below.

6.3.1 Planarized surfaces

Most R/W systems are characterized by their flyability height, which is the constant distance above the media that the R/W head operates, separated essentially by an air bearing at sub-10 nm spacing. For proper R/W implementation, we need to ensure that this height remains uniform throughout, and hence media are highly planarized. The presence of even the smallest resist residue or particulate contamination can lead to a fatal head crash. PM inherently consists of magnetic dots formed by patterning with resists (or BCPs) and subsequent processes like ion milling, which must be done carefully to avoid damage/contamination of magnetic media. Also some magnetic materials are prone to corrosion and are hence covered by a protective layer. However inspite of these challenges, flying at an 11 nm fly height on discrete track media has been demonstrated by Soeno et al(125).Also reducing flyability height for better disk performance has been an old concern for the HDD industry, and lots of work has gone in experiments and simulations for patterned media (126, 127). In fact an approach where the substrate is patterned before film deposition has shown promising results at sub-10 nm head disk spacing (128).

6.3.2 In Sync Signal Processing

Now unlike in conventional thin film media, the bit locations are not defined by the R/W head in PM but, are prepatterned onto the media. Hence there exists a need to synchronize the head position to the pre existing island locations. Imperfections in the fabrication process will lead to noise, as misplaced islands out of sync with the head will cause R/W errors. It is paramount to be able to write one island without disturbing the neighboring ones. For this purpose, narrow switching field distribution and high write field gradients will be required (129), which corresponds to σ= 10% (124). This σ encompasses parameters like synchronization errors, lithographic and magnetic switching field variations. For higher density close to 10 Tb/inch^2, all the more tighter distributions will be required.

For patterned media a σ of 5 to 8% can be best obtained as illustrated in fig 6.6 (130); though here, the island spacing is much higher than the set target for high areal densities. In general it is seen that switching field distribution (SFD) width increases with decreased island size. Also with decreasing island spacing (131), demagnetizing from neighboring islands will contribute to growing SFD, in addition to

lithographic variations, edge effects or Ku variations. At highest densities this contribution could dominate the SFD, which scaling with M_s, may be difficult to reduce without loss of readback signal. These islands thermal stability will be impacted by broadening Ku or size distributions and a few percent of grains/islands reversing in PM (*131*) will result in a few percent errors and a corresponding undesirable increase in error rate.
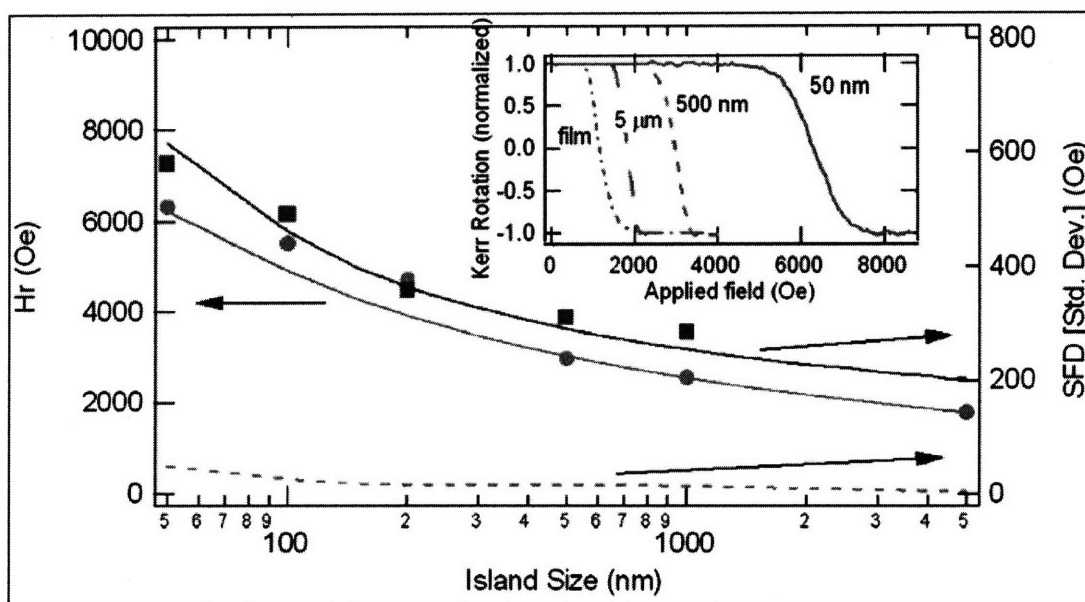

Figure 6. 6: *Left-hand axis; coercivity of island arrays as a function of island size (circles). Right-hand axis; switching field distribution characterized by its standard deviation (squares) Also shown dashed line ,SFD standard deviation caused by differences in magnetostatic environment, viz the switching of neighboring islands. Inset: remanence curves for three island sizes and the continuous film(130)*

This issue related to large Switching filed distributions (SFDs) has been actively researched both for patterned media and for conventional thin film (*132, 133*), and one can expect it to be sorted out in due time. In fact, recent modeling (*134*) suggests that 10 Tb/in^2 may be possible, but the anisotropy required for stability viz. on the order of 10^7 erg/cm^3, will not be writable with current head technologies, and novel mechanism like thermally assisted recording may have to be implemented.

6.3.3 Servo patterning for tracking purposes

The arrangement of these bits and islands must be circularly symmetric so that the head can stay on a single track of islands as it traverses a particular radius. With predefined bit positioning, servos to keep the head on track may also need to be predefined and hence pre-patterned. Hence the methods to produce only pre patterned bits may not be useful without a complimentary technique to pre pattern servos.

In current thin film media servo patterning is done serially with a recording head, and a need for a parallel writing process for larger efficiency has long been felt. A number of approaches have been proposed to sort this, such as pre-embossed rigid magnetic disks (*135*), as early as 1993. Since then, a great amount of study has been devoted to similar techniques. Recent approaches, using magnetic lithography (*136, 137*) wherein the master of the mask is transferred onto a second substrate have shown reasonable success with reagrsd to servo patterning. Hence this criterion too will not be such a big hurdle.

6.3.4 Read/Write Heads

As mentioned earlier synchronization of the bit positioning with the R/W head is the most critical issue to be sorted for market production of PM disks. However, development in recording systems has lagged behind the development of the media.

Spinning Disks are consistent with current hard disk systems, wherein an ultra-narrow magnetoresistive - read/inductive write head is used. The elements can be magnetized longitudinally or vertically as shown in figure 6.7 (*138*). Much of the technology of such systems would be similar to conventional hard drives thereby making it a well understood mechanism. However challenges of synchronization abet the need, to produce heads with extremely narrow widths, so as to follow accurately the lithographically-defined tracks .However the fabrication of ultra-narrow heads remains an issue. Also synchronization will require much greater control of spindle speed than currently used, or simultaneous readback may be necessary to provide position signals for the write process.
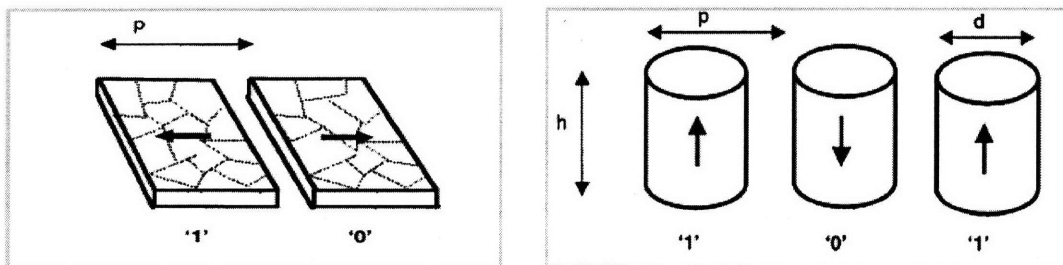

Figure 6. 7: *left- PM with in-plane magnetization showing lithographically defined bits having period p*
right- PM with out-of-plane magnetization with period p, height h and diameter d. Binary one and zero are shown (138)

The reading and writing of patterned media has been demonstrated (*139*) but a practical spinning-disk system has not been made. Simulations/modelling using multi tapered SPT (single pole type) (*140*) as well as using Karlqvist pole heads (*141*) have recently been demonstrated for patterning media 1 Tb/inch^2 by researchers in Japan. As seen from figure 6.8, where a geometric model of a proposed head is shown, head will have minimum dimension of 25 nm for a 1 Tb/inch2 capability. R/W heads are lithographically

manufactured, and attaining high precision heads will continue to remain a challenge; though successful design simulations can be looked upon optimistically, for future implementation.
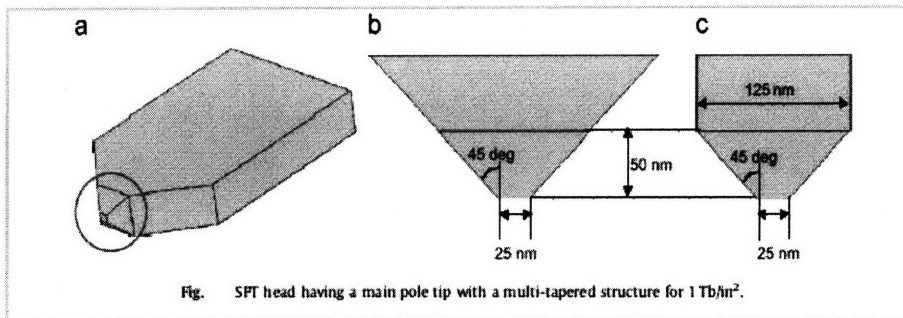

Fig.   SPT head having a main pole tip with a multi-tapered structure for 1 Tb/in².

Figure 6. 8:: Dimensional requirements for a 1 tb/inch2 single pole type head (140)

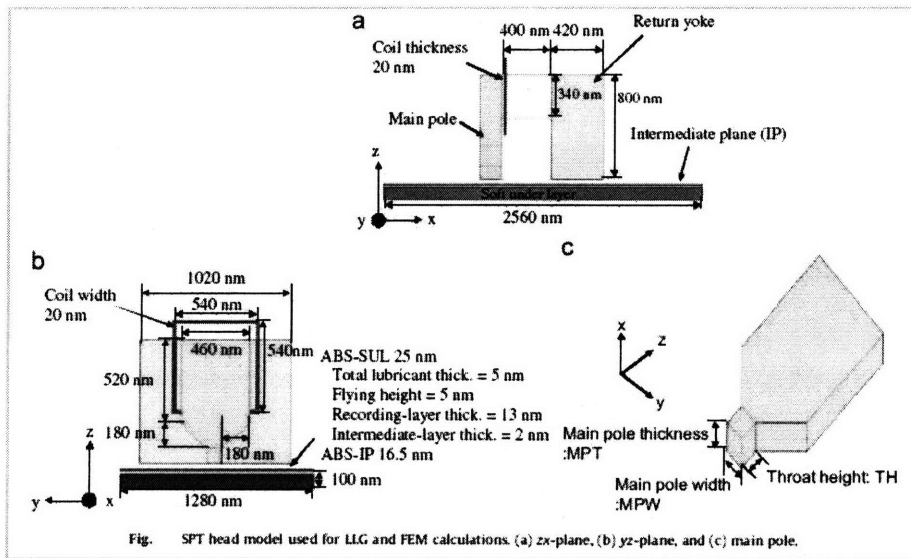Fig.   SPT head model used for LLG and FEM calculations. (a) zx-plane, (b) yz-plane, and (c) main pole.

Figure 6. 9:Design and dimensions for micromagnetic simulations for a high density patterned media head (140)

6.3.5 Future Outlook

It may seem that integration of patterned media into HDD is fraught with difficulties. However for each barrier faced, there are a host of solutions put forward by researchers. Out of all, the barriers mentioned, compatible head technology probably lags behind the rest. However most of these system issues are secondary, and are likely to be overcome (105) as the need for higher areal density (and hence the need for patterned media) becomes pressing, and a methodology to fabricate inexpensive patterned media is fabricated.

Chapter 7: Size of market and opportunity

7.1 Market

The market of HDDs (hard disk drives) is dominated by 5 major players such as Seagate, Western Digital, Samsung, Hitachi and Toshiba.

- The 2 biggest HD OEMs (original equipment manufacturers) - Seagate and Western Digital collectively reported nearly $17 billion (*142*) of HD revenue for the 12 months ending Summer 2007.
- Total revenue of top 5 HDD Companies in 2007= $ 33 Billion

Market has grown steadily since its inception. Growth in the last four years (*142*) (top 5 companies):

- **2004**(net worth) : 18 B$ **2006**(net worth) : 27 B$
- **2005**(net worth) : 22 B$ **2007**(net worth) : 33 B$

Cost per Gb in 2007= 0.3 $s (*143*)

In fact 2007 was actually a good year for the HDD industry and debunked the myth the HDD market was on a decline, and would eventually be replaced by Solid State Devices. The figures (*144*) for 2007 indicate that the number of HDDs shipped grew at an astonishing rate of 18.9 % crossing the half billion barrier. 516 million units were sold up from 434 units in the previous year. At the same time revenue grew by over 4%. In terms of sheer numbers Seagate maintained pole position with the company shipping 175 million HDDs in 2007, up 22 percent from 144 million in 2006. Western Digital Corp. in 2007 shipped 113 million HDDs and Hitachi reversed its operating loss of $93 million in the fourth quarter of 2006 to achieve an operating profit of $95 million in the fourth quarter of 2007. The market share among top companies is represented by the pie chart below:
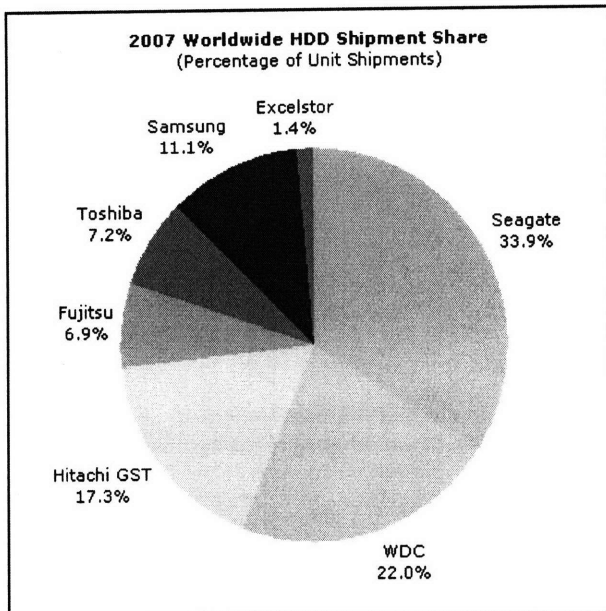
Figure 7. 1: worldwide HDD shipment share (143)

It is interesting to note that from a bleak revenue(*145*) in Q3 2006, the HDD industry has evolved once again into a profitable industry. This revival can be contributed in no mean ways to the growth of the consumer electronics segment. Indeed shipments to consumer electronic applications grew to 17 % in Q3 2007 from 15 % in Q3 2006 (*145*). It is expected to grow up to 22% in Q3 2008. One reason for this is its use in digital video recorders (DVRs) for high definition TVs which are becoming increasing popular.

The segmental sales pattern for 2007 indicated 65 % revenue from the traditional sources of desktops and notebooks. Even in this category, growth is likely to continue upward, due to the emergence of the large economies of countries like India and China, where more and more individuals/corporate are purchasing computers, as the personal computer becomes more accessible with major price cuts.

Even the future of the CE segment looks good. As mentioned earlier DVR has been responsible to drive this segment. DVR will probably continue to drive this growth, as prices drop of HDTV drop. Another factor to be taken into account is that the DVR concept is famous only in North America and Europe as of now. Vast areas of huge population like Asia and South America remain largely unaware of this DVR. However once these markets (*145*) are tapped, we can be rest assured to see an unprecedented growth.

Besides DVR, consumer electronics will also see drivers in personal video recorders, digital A/V players and a host of automobile navigation systems. Figure 7.2, taken off a market report in 2006 (*146*), predicts the increase in HDD usage for consumer electronics in the coming three years, as compared to previous years.
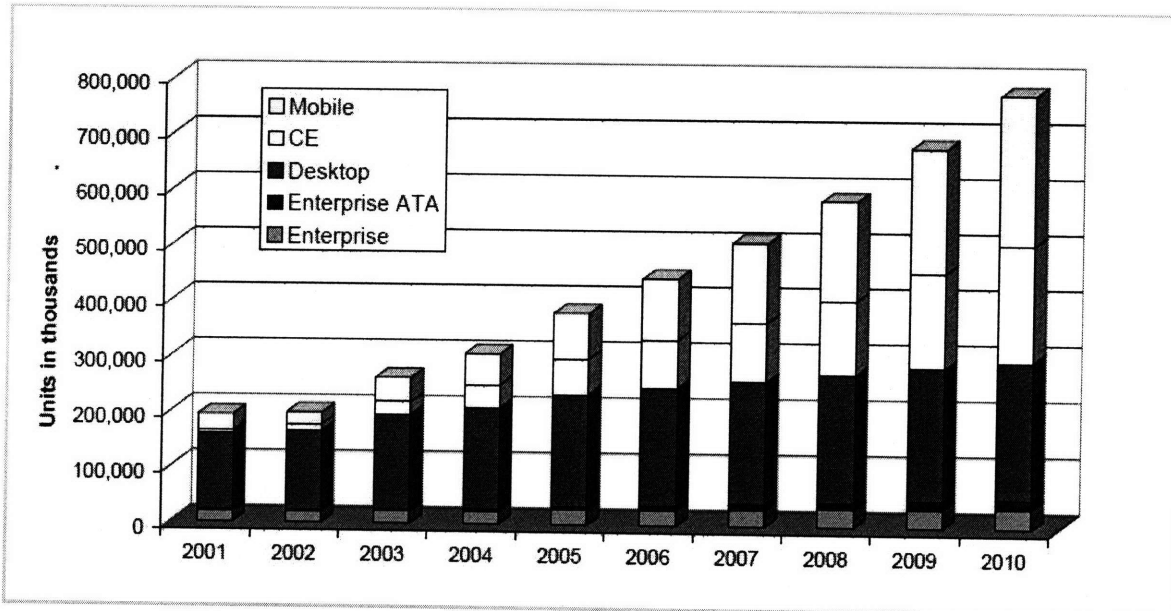
Figure 7. 2: History and projections for HDD unit growth to 2010 per market segment (146)

This dramatic increase in the consumer electronic and mobile computing segment is driven by increasing usage and growth of digital media. The **creation** of all types of digital content (digital photos, video, movies , music), coupled with increasing sales *DVRs, digital music players, gaming consoles, handheld applications, etc.,* for enjoyment, consumption and preservation of such content is one key reason; followed by the **aggregation and distribution** of such content through services such as YouTube(Google), Flickr (Yahoo! Inc), iTunes (Apple)and MySpace (News Corporation).

Besides this, enterprise storage is also seen as a growth factor. Enterprises are increasingly moving away from using server attached storage to network attached storage for storing critical enterprise. SATA (Serial Avacne Technology Architecture) is also making gains in storing non critical data, especially in media companies like Google Inc., Yahoo! Inc with growth in their content aggregation and its distribution

With current growth trends one could estimate that by 2011 the market will be in excess of 50 B $s and will definitely be the "king" of storage technology for many years to come.

7.2 Opportunity

This chapter highlights the ever growing HDD industry. It is also estimated that by 2010 to 2011 (*146*), the HDD industry will have to shift to new techniques like patterned media , and can no longer rely on innovations in the conventional thin film media sector. If the market continues to grow as it has in the past, it presents a huge opportunity, to manufacturers of alternate techniques like patterned media, as the HDD industry will be left with little other option than to purchase or produce patterned media disks to keep their growth intact.

Chapter 8: Supply Chain, Process flow and Cost Model

8.1 Supply chain

The supply chain for HDD manufacture is shown in the chart below.
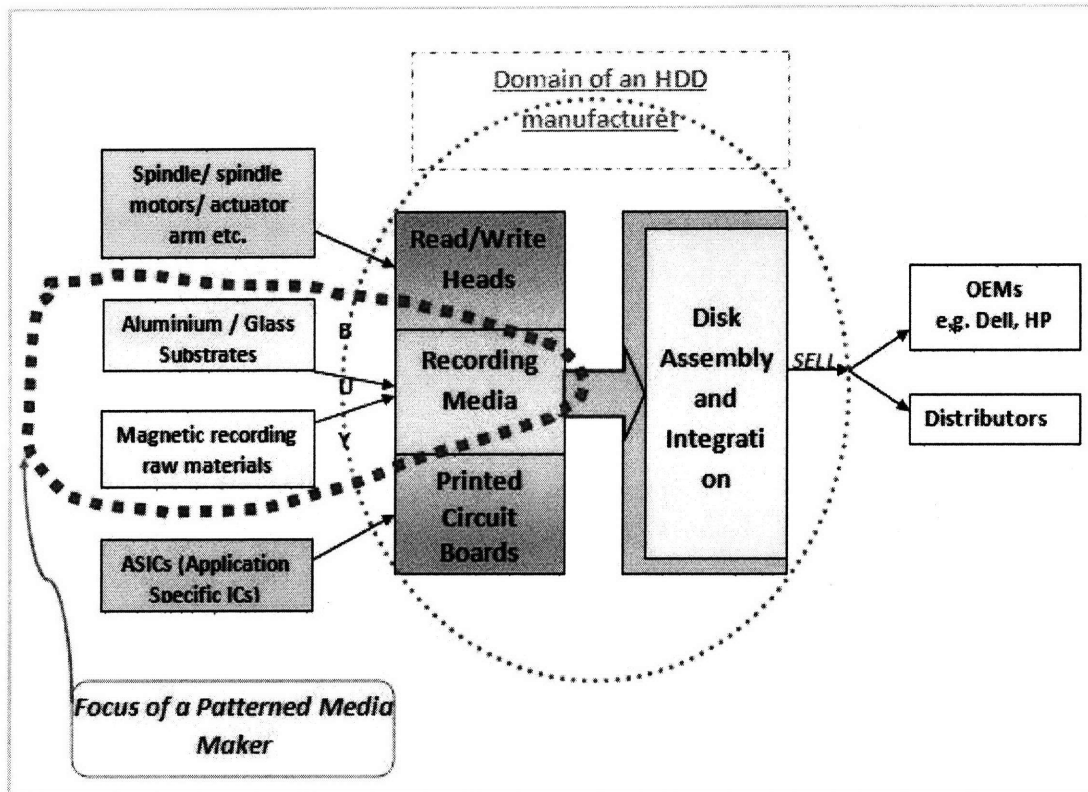

Figure 8. 1: *Schematic illustration of supply chain*

In general an HDD maker will produce its own read/write heads, and printed circuit boards. The recording media fabrication onus could either lie with them or with a third part manufacturer. Other components such as spindle motors, application specific ICs and , aluminium /glass substrates/magnetic recording material(if required) will be purchased from third party vendors. The company will then integrate and assemble these components, packaging their final HDD product to original equipment manufacturers such as Dell and HP.

As a maker of patterned media, we enter this supply chain as suppliers of recording medias. As seen by the zone marked by the "red dotted line", our functions would include buying substrate and magnetic materials and fabricating our own patterned media disks. These disks would then be sold to HDD makers such as Seagate and Western Digital.

8.2 Process Flow

We propose to fundamentally use a subtractive processing step. For subtractive patterning, two cases are considered:

8.2.1 Process 1:
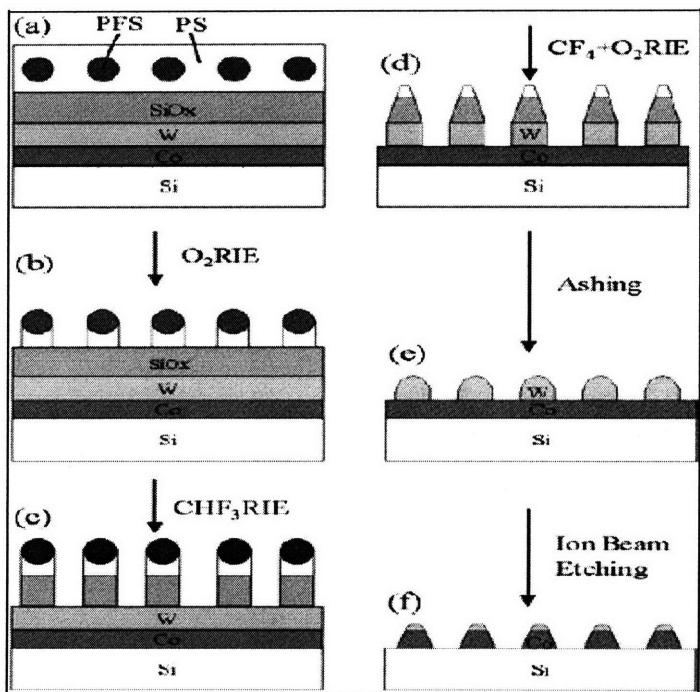
Figure 8. 2: Process 2 employing subtractive patterning using PFS spheres in a PS matrix(41)

Process1 is exactly the same in concept, as the one discussed under subtractive patterning (*41*) in an earlier chapter, where PFS spheres in a PS matrix are used to pattern an underlying magnetic layer.

Optimization of process:

Process 1: instead of using PFS-PS one can use PS-PDMS, and hope to get higher resolutions due to the higher χ associated with the system.

8.2.2 Process 2:

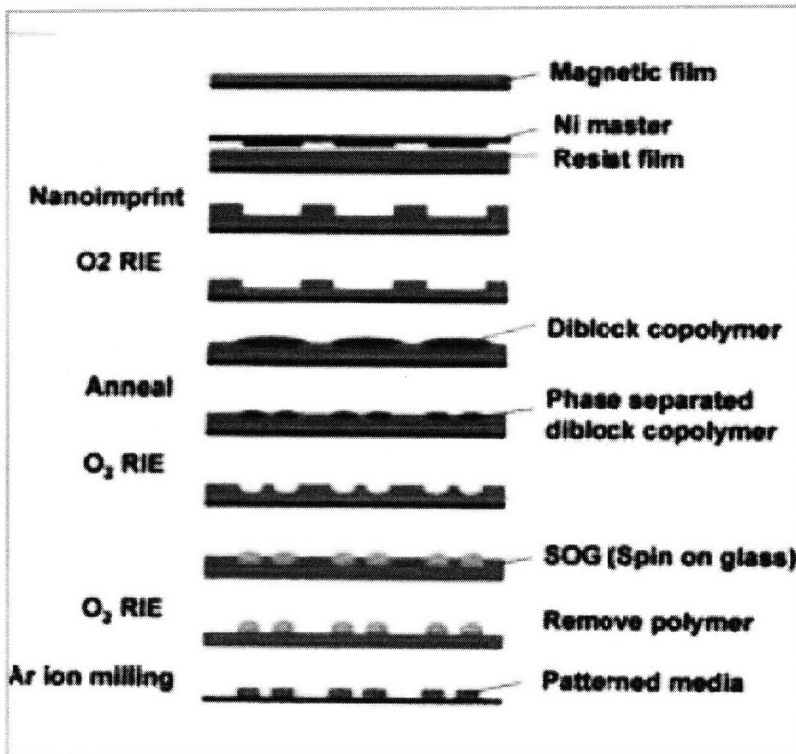*Figure 8. 3: Process 2 using PMMA spheres in a PS matrix. The PMMA spheres are selectively etched and filled with spin-on-glass which is used as a hard mask for further patterning of underlying magnetic film(98)*

Process2 is the process shown by researchers at Toshiba (*98*). Here, using master stamper, spiral patterns are transferred onto an underlying resist layer. Below this resist layer lies a magnetic layer to be etched. Once the spiral grooves are formed onto the resist, the PS-PMMA BCP is spin coated onto the groves to attain long range order on annealing. The PMMA sphere formed in this process is selectively etched, and spin-on-glass is deposited in these holes. This SOG dots then acts as an hard mask for subsequent magnetic dots formation during ion milling; after the PS has been removed by RIE.

Optimization of process:

Process 2: instead of forming spheres of PMMA, it would be better if one can form PMMA cylinders perpendicularly oriented to the substrate. The idea to use vertical cylinders is to avoid the SOG thickness limitations that come with using spherical microdomains. Since the spin-on-glass is used as a mask in further processing steps, we would like it to be at least as thick as the underlying substrate. Using vertical cylinders gives us this flexibility in controlling the thickness of deposited SOG.

8.2.3 Choice of process:

Process 1 is chosen, due to the high etch selectivity provided by the combination of PS-PDMS and also its high Flory Huggins interaction value of 0.26, which gives us a wider leeway in designing higher resolutions, and stay on the predicted areal density growth rate for a longer time.

Besides fabrication concerns, it is essential that the magnetic dots formed, have the desired properties of magnetic anisotropy, single remnant state and independent switching. Positive results regarding the same have been obtained for similar subtractive process as shown by Ross et al recently(147).

8.2.4 Process flow:

A) Building up the Substrate:

i) Sputter deposit Co on Si substrate

ii) Follow this by sputtering tungsten

iii) Grow SiO_2 layer on tungsten

B) Patterning for long range order:

iv) Use SFIL to form spiral trenches. The Mask for SFIL can have periodicities greater than Periodicities of BCP and hence will not require EBL for fabrication

C) BCP self Assembly

v) Spin Coat BCP to get a thin layer, where minority fraction forms a single layer of spheres

Due to underlying mesas/channels, long range order in a circumferential manner can be expected.

vi) Anneal maintaining optimum conditions for long range order defect free pattern.

D) Subtractive Patterning to attain Patterned Media

One of the polymer is selectively etched out. For the sake of illustration we take a PS-PDMS system where PDMS is minority phase and forms spheres in PS matrix.

vii) PS removed by oxygen plasma

viii) PDMS transferred onto SiO_2 layer by CHF_3 plasma

ix) Pattern transferred through to W using CF_4/O_2 plasma

x) Co alloy dots formed by pattern transfer via Ion milling

Considering the process flow here, we note an additional step of patterning the SiO_2 using Step and Flash Imprint Lithography (SFIL). This is done prior to BCP spin coating, so that when the PS-PDMS di-BCP is spun coated onto SiO_2, we can hope to get long range order; via graphioepitaxy, as discussed in earlier chapters. The width of the trenches formed in the SFIL are carefully pre-decided and are an integer

multiple of periodicity of the BCP to be used (*111*). Width of the trenches is kept bigger than the mesas to induce flow of the BCP into trench; it is also big enough such that the original mask can be formed by conventional lithographic methods.

8.3 Cost Modeling

8.3.1 Fixed Cost

For the cost modeling, we have taken into account SFIL machines along with other equipment that will be required, either in the processing step or later as a instrument to test devices, are listed in the table below. (The numbers were obtained* in Singapore dollars and converted to US dollars) The cost of these equipment coupled with the cost of setting up a clean room sized about 5000 sq. feet, constitute the **fixed costs**. *(Modeling is based on Singapore set –up)*.

Equipment	Cost K $s	Equipment	Cost K $s
SFIL machine (180 dph) X 5	4000 x 5	MFM* x 2	60 x 2
(Plasma etchant +RIE machine)* x 5	50 x 5	Ion Milling Machine* x 5	20 x5
Sputtering System* x 5	500 x5	(Spin coater + oven + Mask*) x10	15 x 5
SEM* x 2	1400 x 2	Clean room *(5000 sq ft): Real estate + Set up +R&D lab(1000 sq ft)	50 + 4000+10
		Other equipment	10

Total Fixed Cost* = 28 Million Dollars + any licensing fees

Table 8. 1: fixed cost

these figures were obtained in consultation with Rajamouly,O.S, a 2007 intake phD student under Prof. CHOI, at NUS's ECE department

The cost of an SFIL machine, the Imprio® 100 (*148*) sold by Molecular Imprint® has a price tag of two million dollars (*148*). This machine is however research based, and another tool from the same vendor, the imprio® 2200 is designed specifically for NIL demands of the HDD industry (*149*) The price tag of this

machine is not listed, so has been assumed to cost twice that of the research based tool at 4 million dollars.

Additional machines associated with NIL have been estimated to cost (*148*) between 300,000 to 700,000 USD. Here we have calculated the cost of additional machines (i.e. RIE+ Sputtering System + Ion Milling machine) and calculated a cost of approx. 600,000 USD which is close to market estimates. For our clean room, we have considered a [100] room, which costs around 800USD* per square feet in Singapore.

Currently the HDD Industry produces around 750 disks per hour (*150*) hence we have assumed we will need at least 5 Imprio® 2200 machines who which can produce 180 double sided disk per hour.(*151*)

The total fixed cost is thus a cost of pegged at 28 Million dollars + licensing fees^.

^ *Cost of each patent if assumed to be 5,000 $s and we assume we require licensing agreements for upto 6 patents, then we can easily add another 30K to the fixed costs. Hence the total fixed cost would be in slight excess of 28 Million dollars*

8.3.2 Variable Costs

While calculating **variable costs** we first estimated monthly expenses. We have estimated around 30 pieces of equipment. Assuming we would need 1 technical trained employees + 1 non-technical staff member (to aid in the running of the unit in areas such as supply, operations and marketing); we will need 60 employees. Considering two shifts daily for the technical staff, would add another 30 technical staff taking the total to 90.

The salaries were held at 3850 USD (~5000 SGD) and 2300 USD (~3000 SGD) per month for the technical and non technical staff respectively.

COGS

The cost of goods and services was pegged at 1.2 million USD. Here the main cost associated was the attainment of 2.5" inch glass substrates wafers, which cost around 1.5-2 $S each (assumed). For our production capacity (900 disks per hour) we will need around 625,000 substrates per month leading to an expense of 1 million dollars monthly. The other block copolymer raw material needed PS-PMMA cost around 900$ for 5 gms (source: Polymer Source Inc.) For each 2.5 inch disk, if we assume a polymer layer of 30-40 nm, having density of 1.2 g/cc, then for 625,000 substrates we will need about 56 gms per month, which translates to a cost of about 10,000 USD per month. Power bills and administrative

expenditure were pegged at around 30000 USD and 20000 USD per month respectively. Other materials involved as etch masks are neglected.

Variable costs: Monthly expenses:
- *Manpower (60 technical staff+ 30 non technical staff)= 231K + 69K*
- *COGS(raw materials)~ 1000 K + 10K*
- *Power Bill ~ 30K*
- *Administrative Expenses ~ 20K*

Adding up costs, we have a total monthly cost of 1.35 Million USD

Therefore variable yearly expenses = 16.3 Million Dollars == 16.5 million dollars

8.3.3 Capacity

We are running at a maximum capacity of 900 disks per hour.

However assuming downtime, and defective disks, we are assuming an efficiency of 75%

(Note : In reality our capacity will be affected by annealing time, the actual annealing time can vary widely, and we cannot be sure of it now, hence we assume efficiency decrease due to annealing times, to be included in the figure of 75%)

Thus actual disk produced per hour ~ 650 disk per hour.

Therefore Patterned media disk produced annually = 5.6 Million

8.3.4 Balance Sheet

Now our **total costs** per year are 44.5 (28 + 16.3) Million dollars

Hence to just **break even** we need to sell at **7.9 Dollars per media disk.**

Conclusion

Current conventional media disks are available to manufacturers at around 4-5 $[#] per disk.

Which makes patterned media disks cost at least 3 $ more than the disks sold presently. However it is believed in market circles [8.10] that introduction of patterned media will raise the costs, and with demand for higher areal density, this cost will have to be borne both by the HDD makers as well as the final customers. Also one can expect efficiency improvements in this manufacturing process, which should in probability lower cost, to about 6 dollars per disk within a couple of years of operation.

*Data obtained from at DSI (Data storage Institute), courtesy Dr Liu Chongyang, Singapore*

Chapter 9: Intellectual Property

9.1 List of Relevant Patents

When looking at intellectual property, we come across two types of patents. Those concerned with structure concepts to attain patterned media and those concerned with synthesis methods to attain long range order. Other patents include material based patents and future HDD integration patents. A majority of these have been listed below.

Patent NO.	Date	Assignee	Inventor	Description	Relevance to our product/tech-nology
1. US5820769	Oct. 13, 1998	Regents of the Univ. of Minnesota	Stephen Y. Chou	Method for making magnetic storage having discrete elements with quantized magnetic moments	High
2. US6977108 B2	Dec. 20,2005	Kabushiki Kaisha Toshiba, Tokyo (JP)	Hieda, Naito et al.	Recording medium including patterned tracks and isolation regions	High
3. US2007/028 1220	June 12, 2006	-	Kramer et al	Topography based patterning	High
4. US2006/007 8681	April 13, 2006	Kabushiki Kaisha Toshiba, Tokyo (JP)	Katsuyuki Naito et al	Pattern forming method and method of processing a structure by use of the same	Moderate-High
5. US7186471	Mar 6, 2007	Seagate Technology LLC	Bin Lu, Dieter Weller	Chemically ordered, cobalt-three platinum alloys for magnetic recording	Moderate-High
6. US6777066	Aug 17, 2004	Seagate Technology LLC	Chung-Hee Chang, et al	Perpendicular magnetic recording media with improved interlayer	Moderate-High

7. US5750270	May 12, 1998	Conner Peripherals Inc.	Xiaoxia Tang et al	Multi-layer magnetic recording media	Moderate-High
8. US6468670	Oct 22, 2002	International Business Machines Corporation	Yoshihiro Ikeda et al	Magnetic recording disk with composite perpendicular recording	Moderate
9. US6893705 B53	May 17, 2005	MIT, Cambridge, MA (US)	Edwin Thomas et al	Large area orientation of block copolymers in thin film	Moderate
10. US2006/028 9382AI	Dec. 28, 2006	Kabushiki Kaisha Toshiba, Tokyo (JP)	Akira et al	Method and apparatus for manufacture of patterned media	Low
11. US2006/017 2153AI	Aug. 3, 2006	Kabushiki Kaisha Toshiba, Tokyo (JP)	Akira et al	Patterned magnetic recording media, stamper for manufacture of patterned magnetic recording media, method of manufacturing patterned magnetic recording media and magnetic recording apparatus	Low
12. US6746825 B2	Jun 8, 2004	Wisconsin Alumni Research Foundation, Madison, WI (US)	Nealey et al	Self assembly using interferometricallly nanopatterend substrate	Low
13. US7312939 B2	Dec. 25, 2007	Hitachi GST Netherlands BV, Amsterdam (NL)	Bandic et al.	System , method and apparatus for forming a patterned media disk and related disk drive architecture for head positioning	Low

Table 9. 1: List of patents to be considered

9.2 Degree of Relevance

HIGH:

Patent 1 (US5820769)

This first patent on patterned media was filed by Stephen Chou from the University of Minnesota. It demonstrated a patterned magnetic media prototype for the purpose of data storage and also enlisted one fabrication method. It was issued in 1998, and will have to be licensed by any patterned media manufacturer.

Patent 2 (US6977108B2)

This patent was filed by the inventors at Toshiba following their paper on 2002, in which they patterned a 2.5" circular discussing self assembly of block copolymers, having " (a) a recording track band, and (b) recording cells regularly arrayed in the recording track band to form a plurality rows of sub-tracks".

Our technique of using BCP self assembly for patterned media is similar in ideology to this patent. It will be difficult to supersede this patent and will require and licensing agreement with the inventors at Toshiba.

Patent 3 (US2007/281220)

This patent was filed by Kramer and coworkers when they showed successfully the use of physical templating to attain long range order. So far we intend to implement this technology for our patterned media. Hence licensing agreements will be required here too

Patent 4 (US2006/0078681)

This patent was filed at Toshiba too, by the same inventors involved in patent 1, and also closely related to their paper in 2002. This patent covers exclusively the phase separation of self-assembling block copolymer and minimizing variations in pattern for the given groove structure. I believe, this patent while have to be licensed too along with patent 1, as Toshiba has covered their invention well.

Besides Patent 2 and 4, Toshiba and Naito K., have successfully filed a number of peripheral patents to completely protect their innovation. Some of the more important peripheral patents are listed below. Along with the primary patent, one would need to license a couple of these too.

Toshiba's Backup Patents:

Patent NO.	Date	Assignee	Inventor	Description
US 7,314,833 B2	Jan. 1,2008	Kabushiki Kaisha	Kamata, Naito et al.	Method for manufacturing substrate for discrete track

		Toshiba, Tokyo (JP)		recording media and method for manufacturing discrete track recording media
US 7,306,743 B2	Dec. 11, 2007	Kabushiki Kaisha Toshiba, Tokyo (JP)	Hieda, Naito et al.	Recording Medium, Method of Manufacturing recording medium and recording apparatus
US 7,115,208 B2	Oct. 3, 2006	Kabushiki Kaisha Toshiba, Tokyo (JP)	Hieda, Naito et al.	Method for manufacturing substrate for discrete track recording media and method for manufacturing discrete track recording media

Table 9. 2: Toshiba's Backup Patents

MODERATE TO HIGH:

Patent 5 to 8 have been filed by different company and our related to magnetic alloys for recording media. For the case of perpendicular patterned media, one would desire a high perpendicular anisotropy to the substrate (9). Multilayer film alloys of Co/Pd and Co/Pt are being looked upon as optimal materials for this application (105)

These 4 patents are related to fabrication techniques of these cobalt alloy films. It is likely that one would need a licensing agreement with at least one such patent holder, for using these films in their devices.

MODERATE:

Patent 9: US6893705B53

Filed by Edwin Thomas and group of MIT, this patent extensively covers new ways to orient microdomains, using methods such as directional crystallization by solvent evaporation. This patent describes a efficient to form vertically oriented cylinders in a 1-D BCP thin film, which would be of great use if we were to use additive patterning for our PM discs. However usage of subtractive patterning does not infringe on this patent.

LOW:

Infringement of these patents is highly unlikely, more so if one sticks to manufacturing only the magnetic media disk, and not the whole HDD:

<u>Patent 10 & 11: US2006/0289382AI & US2006/0172153AI</u>

Filed at Toshiba; these patents deals with intricacies of patterned media architecture, apparatus and method of realization. The importance of these patents will only be clear when we actually get into mass scale production, as it deals more with manufacturing techniques.

<u>Patent 12: US6746825B2</u>

Nealey's group invented the use of chemically patterned substrates to attain long range order. We do not propose to use this method, cause as of now, graphioepitaxy seems the better choice.

<u>Patent 13: US7312939B2</u>

Patent 13 was issued to Hitachi very recently. Integration of PM into HDD disks remains a big barrier to market entry. Hitachi address concerns in this patent by putting forward ideas and methods that could be effective in integration. Right now this patent might be superfluous but we must keep in mind, that in all probability we will need a licensing agreement with other similar patents once the problem of integration of PM into HDD is solved, by a research group.

9.3 Getting around the patents

As a start up planning to manufacture patterned media through BCP, patent 1-4 are most important to us.

Patent 1 and Patent 2, 4:

Patent 1 patents the idea of patterned media, and as mentioned before, any patterned media maker will have to license it.

The patents filed by Toshiba (2/4/backup) are pretty comprehensive and a way around these patents is nearly impossible, and one would most definitely require a licensing agreement with Toshiba for them. In fact, one could presume that Toshiba would charge high licensing fees coupled with royalty, and one would have to adhere cause of the leveraging power these series of patents gives Toshiba.

Patent 3:

Now, when it come to long range order, it is most likely we would use patent 3 (this was also the technique we considered when estimating our cost model). Thus would then involve another licensing agreement. However ways around this patent are possible with a ingenious innovations. Very recently Prof. Ross's research group (152) devised a method where they achieved long range order by templating

this experiment were coated with PDMS, to attain long range order in a PS-PDMS spherical di-BCP system, which will then fit very well with our proposed PS-PDMS system for PM.

This is illustrated in the fig 9.1 below:
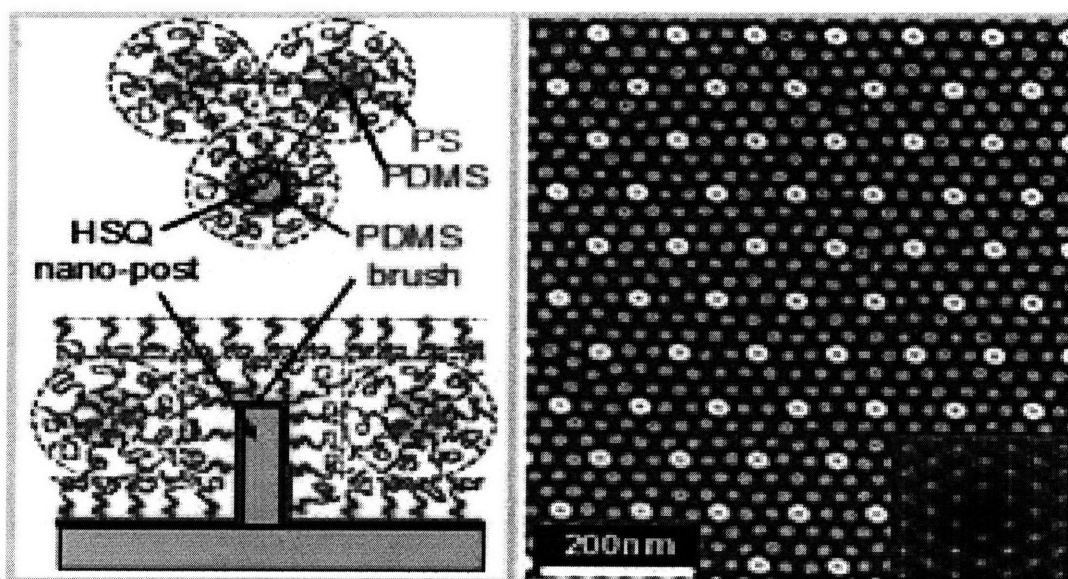
Figure 9. 1: Novel method to attain long rang order using PDMS coated post: PDMS coated posts help align the bcp sphere. The SEM image on the right illustrates this, where the bright dots are actually the posts (152)

The effectiveness of this technique in general hasn't been explored very deeply yet and also its efficacy for patterned media cannot be confirmed for now. One of the main issues surrounding this technique will be the distance between adjacent posts and its effect on pattern formation. Figure 9.2 (*152*) below displays different SEM images for different ratios of the length period of the posts and the periodicity of microphase separated BCP thin film.
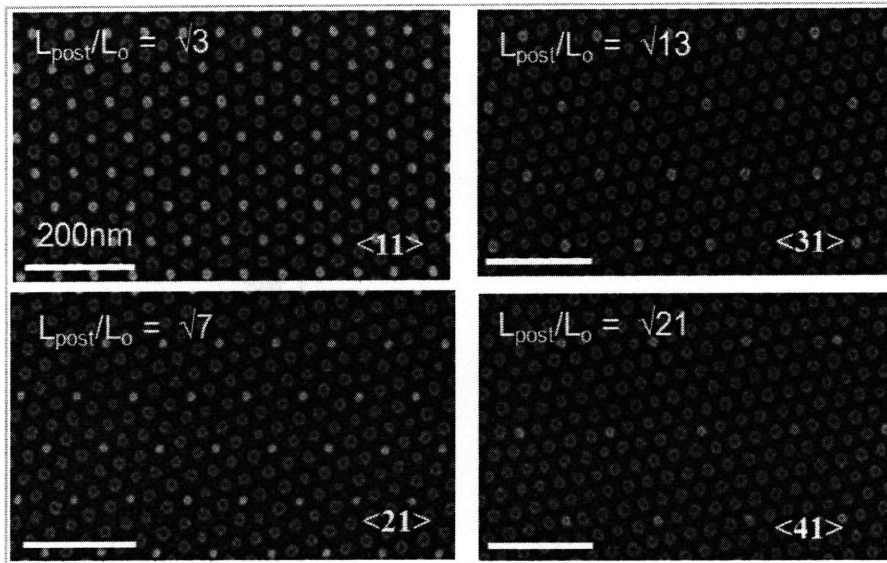
Figure 9. 2: Effect of periodicity ratio on pattern formation (152)

Now if one is able to innovate and produce unique ways for physical templating, one could save a lot of patent licensing costs; best case scenario being that this new technique would turn out to be far better than any existing techniques thus giving one another tool in the form of their own intellectual property which could be used to earn revenue through licensing it out to other manufacturers.

Chapter 10: Competition

Since the competition of patterned media first came into being, a host of methods have been used to describe them ranging from lithographic ones to ones based on self assembly.

I) Lithographic techniques such as optical lithography, E-beam lithography and X-Ray lithography have been proposed. However these techniques suffer from either resolution restrains, cost considerations, throughput limitations or a combination of them.

II) Besides self assembly of block copolymers, some other *self assembly methods* have also been devised. These include:

i) Self assembly via template growth, where self organized porosity of certain microporous membranes (*153*) have been put to use to fabricate magnetic nanodots

Anodized alumina

Anodized alumina can be used as a template to form magnetic elements (*154*). Hexagonally close packed pores , whose size is controlled by anodization conditions such as voltage , solution pH and current density can be formed on the surface of anodized alumina. Pores having diameters of about 9 nm with packing densities close 7×10^{10} cm^{-2}, or 450 Gb in^{-2} have been reported (*155*).Methods focused ion beam exposure (*156*), interference lithography (*157*) or moulding or nanoindenting (*158*) have been suggested to increase length scale of ordering. However anodized alumina techniques have focused more on fabricating long wires (via electrodepositon) (*159*), and so far it has been difficult to obtain low aspect ratio dots, though researchers, are still working on it.

ii) Self assembly of nanoparticles (akin to BCP self assembly) with its high anisotropy has also been forwarded as a technique to attain patterned media. Synthesis and assembly of magnetic nanoparticles can be done without lithographic tools and was first demonstrated by Sun et al (*160*). Various methods such as sputtering, laser ablation and vapor deposition has been demonstrated for the same. However in spite of its advantages of sufficient magnetic anisotropy and high packing density, it does suffer from serious drawbacks (*161, 162*) such as agglomeration of particles during annealing, poor chemical uniformity and poor uniformity of easy axis orientation.

III) Nano-imprint lithography (NIL)

NIL, as a lithographic method was first developed in 1995. Since then it's been touted as a panacea for a range of patterning needs plaguing the industry, and not without reason. It does provide improvement of yield, reliability at lower costs. In fact since its introduction it was quickly adopted by the industry as a way to pattern compact discs and DVD disks, providing mass production at a lower cost.

For patterned media too, NIL is being looked upon as a promising technique. The process of obtaining PM disks using NIL is represented schematically below (97).
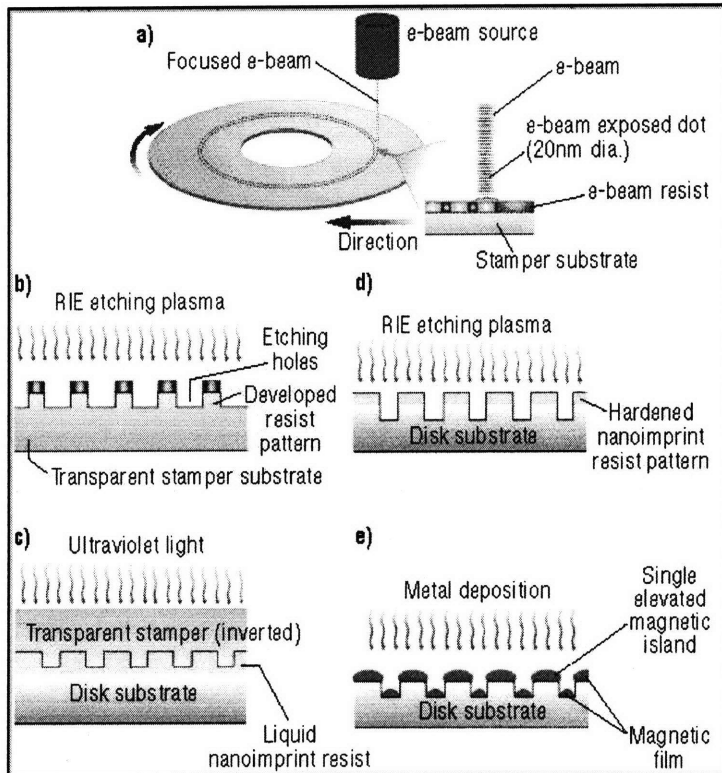
Figure 10. 1: process flow for PM disk fabrication using NIL (97)

E-beam lithography is used to fabricate a high-resolution master mold (Fig. 10.1a). For achieving circular symmetry , an e-beam column in conjunction with a high quality mechanical rotary stage is employed to meet all pattern specifications. After the exposure of the e-beam, the resist is developed, and reactive ion etching (RIE) is employed to transfer pattern into the master mold substrate (Fig.10.1b). This master mold is then pressed against the disk substrate which is coated with liquid nanoimprint resist This resist flows and rearranges itself to conform with the master topography (Fig. 10.1c). Post this step, ultraviolet (UV) light is applied to cure the resist in place and form a solid nanoimprinted *replica*. Post UV curing, pattern transfer onto disk substrate is achieved using RIE (Fig. 10.1d). The imprinted resist topography is a complementary duplicate to the stamper topography. In the final step (Fig. 10.1e), magnetic media is blanket sputter-deposited over the patterned disk substrate.

In spite of its apparent simplicity, NIL still has some issues that need to be sorted. These are listed below:

- Mask for NIL requires E-beam.
- For a required density of 1 Tb/inch^2, 1-2 months for making mask via EBL
- Still many issues to debug in NIL, e.g. mask durability, and the process to remove the resist residual layer while preserving the pattern, are two major issues.

Winners?

For criteria such as highest resolution and maximum density, required for 1Tb/inch^2 densities, BCP lithography and NIL seem to be the best options (*6*) (considering economic viability).

Thus so far, as far as completion is concerned one would have to pick NIL. However as mentioned earlier it too has some defects. For the case of NIL, BCP having higher throughput than e-beam, and being essentially a mask less process (not counting templating) , would be much cheaper and economically viable. In fact if NIL has to become a dominant technology, it would actually do well to employ BCP lithography for the fabrication of its mask over the slower e-beam, hence effectively boosting the market for BCP lithography. In any event, even PM disks through BCP technology can use the NIL method to create trenches for long range order. Hence these technologies are more likely to complement each other than compete.

Chapter 11: Business Model & Entry Strategy

11.1 Manufacturing Model

Whether we enter the market as purely patterned media producers or as complete HDD producers, may vary our business model. However our basic tenets for manufacturing PM disks will remain the same, and are listed below

- Enter in Patent License agreement where needed (case in point-Toshiba)
- Use own patent where possible (e.g. for long range ordering)
- Start small scale manufacturing unit.
- Invest in R&D to attain optimum QC over long range order and defects
- Continue manufacturing alongside with process refinements rooting from the R&D section

Hence ideally our business model would be a good blend of intellectual property, patenting and R&D driven manufacturing.

These tenets will be best served with small scale manufacturing unit with an equally important R&D centre. The proposal of initially setting up a small scale unit vis-s-vis a large manufacturing unit has several advantages, such as lower initial investment, lower set up time, and a good exposure to industry intracacies. A large scale fab unit will most definitely require an initial investment of 1 Billion dollars, and might take upto 3 years to just start produciton. On the small scale, our unit will be ready in less than a year with significantly lower investments, to the tune of 30 Million dollars. Also it will give us a good understanding of which sector (i.e. computer based HDD, consumer electronincs, hand held media etc each requiring different sized media) should we pursue for maximum profitability.

This being said, even before we start production, we should take a hard look at the market we wish to capture. The cycle time of our process may not be very high, considering time consuming steps such as annealing. However the process on a whole is capable of giving very high areal densities. One strategy we could pursue to further increase profitability (and possibly productivity) would be to also make smaller PM disks of around 0.5" to 1" diameter (than the 2.5" considered in the cost model). These could be targeted towards application such as medical drives and portable media which are burgeoning markets but are dominated by solid state devices. These devices would require small sized HDDs of high enough capacities, a criterion which patterned media technology could easily fulfill. This being said, the decision to enter this segment will ultimately depend entirely on the HDD company to whom we supply our patterned media disks.

11.2 In house R & D section

It is important to have a strong R&D section. The business model is not IP based, as most of the technology concerning patterned media through BCP lithography for patterned media, have more or less been covered under previous patents. However when it comes to manufacturing, the process is highly varibale, demanding continuous technology development. It would then be foolish to pursue just an IP based business model. However, continuous research and development will be key to our growth. The whole success of our device lies on getting uniform placement of dots at high densities (dot size <14nm, period <25nm) free of defects. Even with the required templating setup in place, we should take note that a uniform defect free PM disk will depend on more factors than one. Factors such as kinetics of BCP forming, molecular weight, the Flory-Huggins parameter χ, annealing history and domain morphology, will also influence quality of end product. Hence an intensive R&D unit should be attaché d to the manufacturing site so that research on effect of these parameters could be better understood and optimized for this process. Indeed we believe that in a competitive market, the maker who best addresses these areas will be most potent in making the best PM disks. Hence a heavy investment in R&D would be part of our business plan.

In house patenting will come into the picture as more pieces of PM integration fall into place. When this happens and if then, we did devise a unique and efficient prototype methodology, we should in all probability patent it. Patent fees could range between 10K & 15K per patent, but could provide high returns if licensed out to one of the big HDD manufacturers.

11.3 Time line adjustments

One cannot be very sure when patterned media will be implemented in the industry. With the introduction of perpendicular recording, current conventional thin film techniques have been further extended by 4-5 years. However post that, there seems to be no alternative to patterned media, for continued areal density growth. Considering this timeline, we could set-up a purely R&D centre first (say, after a couple of years), and plan on a small scale manufacturing unit later on (when patterned media is due to be implemented). The gains in doing this, would be that we would get adequate time in perfecting our own fabrication method with optimized long range-order, pattern uniformity etc. This would give us a head start (or at least keep us at par) with potential competitors in the future. Any patentable research result, would only justify this cause, especially if it can give us our own licensing rights.
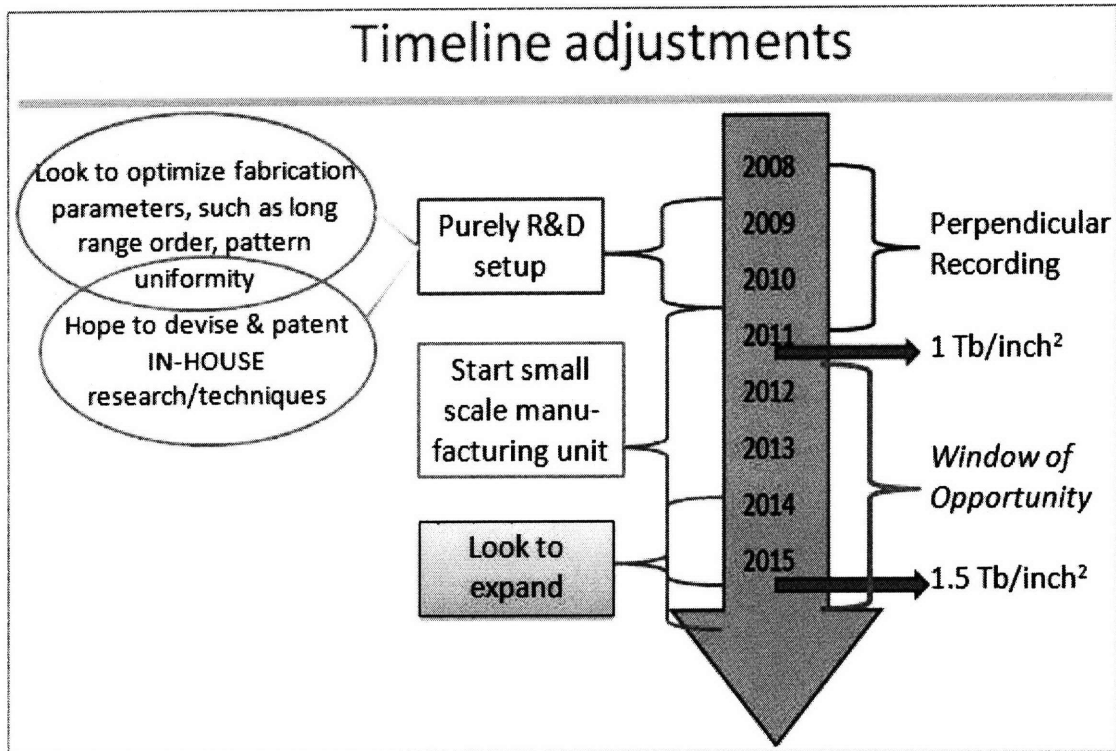
Figure 11. 1: Timeline adjustments for Business model

Chapter 12: Conclusion

We have demonstrated that the field of PM disks as storage devices has great potential. The key to these optimum patterned media disks from the fabrication point of view will be sufficient long range order, good pattern uniformity and placement accuracy. Besides that further research in block copolymer systems will be needed to match the stringent dimensional requirements of patterned media up to and beyond 1 Tb/inch^2. Even if we were able to provide solutions to all these criteria, the question of patterned media integration into HDD disks would still remain. So far integration approaches have lagged fabrication approaches of patterned media. As a potential maker of patterned media, one cannot be exactly sure of the time frame for patterned media implementation. Current methods to produce HDDs are scheduled to keep up with areal density requirements for another 4-5 years, with the introduction of perpendicular media recording. Beyond that, there appears no alternative to patterned media for continued areal density growth. One can assume then, that with patterned media being the need of the hour, integration approaches will be become the main focus, and hopefully rapidly solved. Probably another factor related to the tardiness in progressing integration issues has been the lack of a cost effective patterned media fabrication method. However in our cost model we have calculated the cost of a patterned disk to be just a few dollars over current magnetic media disks. Once this can be verified in practice, all other concerns should eventually even out.

For a patterned media maker, it would make sense to start a small R&D section to fine tune, BCP self assembly processing and optimize one's own personalized approach to fabricate patterned media. If and when patterned media is introduced, the maker who best addresses issues such as pattern uniformity etc will be most likely , selling the most disks and making the most profits.

Also it would make practical sense to explore newer avenues of revenue potential. As shown in this thesis, block copolymer self assembly can be employed to fabricate a host of applications for the electronic and optoelectronic industry. This thesis has covered the market potential for patterned media; similarly other fields should also be equally investigated.

Self assembly in itself has a long existence in everyday living systems and has achieved incredibly ordered structures in nature. Self assembly, then as a fabrication tool, should then be equally effective in a range of nano-technological applications. Self assembly of block copolymers is one such tool, where combining "bottom up" self assembling block copolymers with "top down" lithographic methods has the potential to successfully fabricate or pattern a wide range of precise nanostructures.

References

1. H. I. Smith, D. C. Flanders, *Journal of Vacuum Science & Technology* **17**, 533 (1980).

2. M.A.McCord, M.J.Rooks, *Handbook of Microlithography, Micromachining and Microfabrication,*. C. P.R., Ed., Microlithography (SPIE Optical Engineering Press, 1997), vol. 1.

3. L. Leibler, *Macromolecules* **13**, 1602 (1980).

4. C. T. Black *et al.*, *Ibm Journal of Research and Development* **51**, 605 (Sep, 2007).

5. S. Y. Chou, *Proceedings of the Ieee* **85**, 652 (Apr, 1997).

6. B. D. Terris, T. Thomson, *Journal of Physics D-Applied Physics* **38**, R199 (Jun, 2005).

7. S. H. Charap, P. L. Lu, Y. J. He, *Ieee Transactions on Magnetics* **33**, 978 (Jan, 1997).

8. R. L. White, R. M. H. New, R. F. W. Pease, *Ieee Transactions on Magnetics* **33**, 990 (Jan, 1997).

9. C. Ross, *Annual Review of Materials Research* **31**, 203 (2001).

10. F. S. Bates, *Science* **251**, 898 (Feb, 1991).

11. A. K. Khandpur *et al.*, *Macromolecules* **28**, 8796 (Dec, 1995).

12. C. Park, J. Yoon, E. L. Thomas, *Polymer* **44**, 6725 (Oct, 2003).

13. I. W. Hamley, *Nanotechnology* **14**, R39 (Oct, 2003).

14. F. G. Bates F.S., *Physics Today* **52**, (1998).

15. M. W. Matsen, M. Schick, *Physical Review Letters* **72**, 2660 (Apr, 1994).

16. M. W. Matsen, F. S. Bates, *Macromolecules* **29**, 1091 (Feb, 1996).

17. D. A. Hajduk *et al.*, *Macromolecules* **30**, 3788 (Jun, 1997).

18. F. S. Bates, J. H. Rosedale, G. H. Fredrickson, C. J. Glinka, *Physical Review Letters* **61**, 2229 (Nov, 1988).

19. M. J. Fasolka, A. M. Mayes, *Annual Review of Materials Research* **31**, 323 (2001).

20. D. G. Walton, G. J. Kellogg, A. M. Mayes, P. Lambooy, T. P. Russell, *Macromolecules* **27**, 6225 (Oct, 1994).

21. M. W. Matsen, *Journal of Chemical Physics* **106**, 7781 (May, 1997).

22. W. H. Tang, T. A. Witten, *Macromolecules* **31**, 3130 (May, 1998).

23. M. Kikuchi, K. Binder, *Journal of Chemical Physics* **101**, 3367 (Aug, 1994).

24. H. P. Huinink, J. C. M. Brokken-Zijp, M. A. van Dijk, G. J. A. Sevink, *Journal of Chemical Physics* **112**, 2452 (Feb, 2000).

25. N. Koneripalli *et al.*, *Macromolecules* **28**, 2897 (Apr, 1995).

26. L. H. Radzilowski, B. L. Carvalho, E. L. Thomas, *Journal of Polymer Science Part B-Polymer Physics* **34**, 3081 (Dec, 1996).

27. M. J. Fasolka, P. Banerjee, A. M. Mayes, G. Pickett, A. C. Balazs, *Macromolecules* **33**, 5702 (Jul, 2000).

28. T. L. Morkved, H. M. Jaeger, *Europhysics Letters* **40**, 643 (Dec, 1997).

29. Y. Liu *et al.*, *Macromolecules* **27**, 4000 (Jul, 1994).

30. S. Y. Chou, P. R. Krauss, P. J. Renstrom, *Science* **272**, 85 (Apr, 1996).

31. T. A. Savas, M. L. Schattenburg, J. M. Carter, H. I. Smith, *Journal of Vacuum Science & Technology B* **14**, 4167 (Nov-Dec, 1996).

32. C. T. Black, *Acs Nano* **1**, 147 (Oct, 2007).

33. M. Park, C. Harrison, P. M. Chaikin, R. A. Register, D. H. Adamson, *Science* **276**, 1401 (May, 1997).

34. I. W. Hamley, *Angewandte Chemie-International Edition* **42**, 1692 (2003).

35. P. Mansky, Y. Liu, E. Huang, T. P. Russell, C. J. Hawker, *Science* **275**, 1458 (Mar, 1997).

36. R. D. Peters, X. M. Yang, Q. Wang, J. J. de Pablo, P. F. Nealey, *Journal of Vacuum Science & Technology B* **18**, 3530 (Nov-Dec, 2000).

37. T. Thurn-Albrecht *et al.*, *Advanced Materials* **12**, 787 (Jun, 2000).

38. D. Y. Ryu, K. Shin, E. Drockenmuller, C. J. Hawker, T. P. Russell, *Science* **308**, 236 (Apr, 2005).

39. T. Thurn-Albrecht *et al.*, *Science* **290**, 2126 (Dec, 2000).

40. K. Asakawa, T. Hiraoka, *Japanese Journal of Applied Physics Part 1-Regular Papers Short Notes & Review Papers* **41**, 6112 (Oct, 2002).

41. J. Y. Cheng *et al.*, *Advanced Materials* **13**, 1174 (Aug, 2001).

42. R. G. H. Lammertink *et al.*, *Advanced Materials* **12**, 98 (Jan, 2000).

43. M. Roerdink, M. A. Hempenius, G. J. Vancso, *Chemistry of Materials* **17**, 1275 (Mar, 2005).

44. Y. S. Jung, C. A. Ross, *Nano Letters* **7**, 2046 (Jul, 2007).

45. E. M. Freer *et al.*, *Nano Letters* **5**, 2014 (Oct, 2005).

46. L. Sundstrom *et al.*, *Applied Physics Letters* **88**, (Jun, 2006).

47. H. J. Richter, *Journal of Physics D-Applied Physics* **40**, R149 (May, 2007).

48. K. Naito, H. Hieda, M. Sakurai, Y. Kamata, K. Asakawa, *Ieee Transactions on Magnetics* **38**, 1949 (Sep, 2002).

49. Z. Wei, Z. G. Wang, *Macromolecules* **28**, 7215 (Oct, 1995).

50. K. P Muller *et al.*, paper presented at the Transactions of the IEEE International Electron Devices Meeting, 1996.

51. D. E. Kotecki *et al.*, *Ibm Journal of Research and Development* **43**, 367 (May, 1999).

52. M. Ino *et al.*, *Journal of Vacuum Science & Technology B* **14**, 751 (Mar-Apr, 1996).

53. E. P. Gusev *et al.*, *Microelectronic Engineering* **59**, 341 (Nov, 2001).

54. C. T. Black *et al.*, *Applied Physics Letters* **79**, 409 (Jul, 2001).

55. K. W. Guarini *et al.*, *Journal of Vacuum Science & Technology B* **20**, 2788 (Nov-Dec, 2002).

56. K. W. Guarini, C. T. Black, K. R. Milkove, R. L. Sandstrom, *Journal of Vacuum Science & Technology B* **19**, 2784 (Nov-Dec, 2001).

57. K. Pangai. *et al.*, paper presented at the Proceedings of the IEEE International Symposium on Semiconductor Manufacturing, 2005.

58. S. Tiwari *et al.*, *Applied Physics Letters* **68**, 1377 (Mar, 1996).

59.   S. K. Lai, paper presented at the Proceedings of the 2005 IEEE VLSI–TSA International Symposium on VLSI Technology, 2005.

60.   K. W. Guarini.. et al., in IEEE International Electron Devices Meeting Technical Digest. (2003), pp. 22.2.1–22.2.4.

61.   T. Ishii, T. Osabe, T. Mine, F. Murai, and K. Yano in IEEE International Electron Devices Meeting Technical Digest. (2000), pp. 305–308.

62.   Y. Huang et al., Science 294, 1313 (Nov, 2001).

63.   C. T. Black, O. Bezencenet, IEEE Transactions on Nanotechnology 3, 412 (Sep, 2004).

64.   C. T. Black, Applied Physics Letters 87, (Oct, 2005).

65.   C. Wang, J. P. Snyder, J. R. Tucker, Applied Physics Letters 74, 1174 (Feb, 1999).

66.   Technology News, in Solid State Technology. (2007), vol. 50.

67.   http://www.eetimes.com/showArticle.jhtml?articleID=199203911. (2007).

68.   P. Mansky, C. K. Harrison, P. M. Chaikin, R. A. Register, N. Yao, Applied Physics Letters 68, 2586 (Apr, 1996).

69.   T.P. Russell, E. Huang, L. Rockford., Encyclopedia of Materials: Science and Technology , ed. by T. P. Lodge, Ed. (Elsevier Science Ltd., London, 2001), pp. 676.

70.   H. C. Kim, T. P. Russell, Journal of Polymer Science Part B-Polymer Physics 39, 663 (Mar, 2001).

71.   P. E. Laibinis et al., Journal of the American Chemical Society 113, 7152 (Sep, 1991).

72.   C. J. Hawker, T. P. Russell, Mrs Bulletin 30, 952 (Dec, 2005).

73.   T. Thurn-Albrecht, J. DeRouchey, T. P. Russell, H. M. Jaeger, Macromolecules 33, 3250 (May, 2000).

74.   T. Xu, Y. Q. Zhu, S. P. Gido, T. P. Russell, Macromolecules 37, 2625 (Apr, 2004).

75.   K. Fukunaga, H. Elbs, R. Magerle, G. Krausch, Macromolecules 33, 947 (Feb, 2000).

76.   S. Ludwigs et al., Nature Materials 2, 744 (Nov, 2003).

77.   P.-G. De Gennes and J. Prost., The Physics of Liquid Crystals. (Oxford Science Publications, Clarendon Press,, NewYork, ed. 2nd ed, 1993,).

78.   M. Kleman, O. D. Lavrentovich., Soft Matter Physics: An Introduction. (Springer-Verlag, New York,. ed. 1st ed., 2003).

79.   http://www.itrs.net/Links/2007ITRS/Home2007.htm.

80.   M. C. Dalvi, C. E. Eastman, T. P. Lodge, Physical Review Letters 71, 2591 (Oct, 1993).

81.   T. P. Lodge, M. C. Dalvi, Physical Review Letters 75, 657 (Jul, 1995).

82.   F. S. Bates, G. H. Fredrickson, Annual Review of Physical Chemistry 41, 525 (1990).

83.   A.N.Semenov, Sov. Phys. JETP 61, 733 (1985).

84.   D. Broseta, L. Leibler, L. O. Kaddour, C. Strazielle, Journal of Chemical Physics 87, 7248 (Dec, 1987).

85.   D. Broseta, G. H. Fredrickson, E. Helfand, L. Leibler, Macromolecules 23, 132 (Jan, 1990).

86. S. H. Anastasiadis, T. P. Russell, S. K. Satija, C. F. Majkrzak, *Physical Review Letters* **62**, 1852 (Apr, 1989).

87. M. R. Hammond, E. Cochran, G. H. Fredrickson, E. J. Kramer, *Macromolecules* **38**, 6575 (Jul, 2005).

88. T. L. Bucholz, Y. L. Loo, *Macromolecules* **39**, 6075 (Sep, 2006).

89. H. Frielinghaus *et al.*, *Europhysics Letters* **53**, 680 (Mar, 2001).

90. H. B. Eitouni, N. P. Balsara, H. Hahn, J. A. Pople, M. A. Hempenius, *Macromolecules* **35**, 7765 (Sep, 2002).

91. T. Nose, *Polymer* **36**, 2243 (May, 1995).

92. U. Jeong *et al.*, *Advanced Materials* **16**, 533 (Mar, 2004).

93. S. Y. Chou, M. S. Wei, P. R. Krauss, P. B. Fischer, *Journal of Applied Physics* **76**, 6673 (Nov, 1994).

94. R. M. H. New, R. F. W. Pease, R. L. White, R. M. Osgood, K. Babcock, *Journal of Applied Physics* **79**, 5851 (Apr, 1996).

95. M. Albrecht *et al.*, *Ieee Transactions on Magnetics* **39**, 2323 (Sep, 2003).

96. *Emerging Lithographic Technologies* VIII, ed. by R. Scott Mackay, paper presented at the Proceedings of SPIE, Bellingham, WA, 2004.

97. Z. Z. Bandic, E. A. Dobisz, T. W. Wu, T. R. Albrecht, *Solid State Technology*, S7 (Sep, 2006).

98. H. Hieda, Y. Yanagita, A. Kikitsu, T. Maeda, K. Naito, *Journal of Photopolymer Science and Technology* **19**, 425 (2006).

99. J. Y. Cheng, W. Jung, C. A. Ross, *Physical Review B* **70**, (Aug, 2004).

100. S. G. Xiao, X. M. Yang, E. W. Edwards, Y. H. La, P. F. Nealey, *Nanotechnology* **16**, S324 (Jul, 2005).

101. C. T. Black, K. W. Guarini, R. L. Sandstrom, S. Yeung., paper presented at the Proc. Mater. Res. Soc, 2002.

102. J. R. Jeong, M. C. Choi, M. W. Kim, S. C. Shin, *Physica Status Solidi B-Basic Research* **241**, 1609 (Jun, 2004).

103. A. Kikitsu, Y. Kamata, M. Sakurai, K. Naito, *Ieee Transactions on Magnetics* **43**, 3685 (Sep, 2007).

104. M. Duwensee, S. Suzuki, J. Lin, D. Wachenschwanz, F. E. Talke, *Ieee Transactions on Magnetics* **42**, 2489 (Oct, 2006).

105. B.D.Terris., *J. Magn. Magn. Mater* **Article in press**, (2008, doi:10.1016/j.jmmm.2008.05.046).

106. T. L. Morkved *et al.*, *Science* **273**, 931 (Aug, 1996).

107. T. Deng, Y. H. Ha, J. Y. Cheng, C. A. Ross, E. L. Thomas, *Langmuir* **18**, 6719 (Sep, 2002).

108. H. W. Li, W. T. S. Huck, *Nano Letters* **4**, 1633 (Sep, 2004).

109. R. A. Segalman, H. Yokoyama, E. J. Kramer, *Advanced Materials* **13**, 1152 (Aug, 2001).

110. J. Y. Cheng, C. A. Ross, E. L. Thomas, H. I. Smith, G. J. Vancso, *Applied Physics Letters* **81**, 3657 (Nov, 2002).

111. J. Y. Cheng, A. M. Mayes, C. A. Ross, *Nature Materials* **3**, 823 (Nov, 2004).

112. D. Sundrani, S. B. Darling, S. J. Sibener, *Langmuir* **20**, 5091 (Jun, 2004).

113. L.-W. Chang , H. S. P. Wong in *Proc. SPIE.* vol. 6156, pp. 329.

114. M.W. Geis, D.C. Flanders, H.I. Smith, *J. Vac. Sci. Technology* **16**, 1640 (1979).

115. X. M. Yang, R. D. Peters, P. F. Nealey, H. H. Solak, F. Cerrina, *Macromolecules* **33**, 9575 (Dec, 2000).

116. S. O. Kim *et al.*, *Nature* **424**, 411 (Jul, 2003).

117. J.Y.Cheng et. al. (IBM, 2008, to be submitted).

118. B. C. Berry, A. W. Bosse, J. F. Douglas, R. L. Jones, A. Karim, *Nano Letters* **7**, 2789 (Sep, 2007).

119. S. H. Kim, M. J. Misner, T. Xu, M. Kimura, T. P. Russell, *Advanced Materials* **16**, 226 (Feb, 2004).

120. K. W. Guarini, C. T. Black, S. H. I. Yeuing, *Advanced Materials* **14**, 1290 (Sep, 2002).

121. S. G. Xiao, X. M. Yang, *Journal of Vacuum Science & Technology B* **25**, 1953 (Nov, 2007).

122. J. Y. Cheng, C. A. Ross, H. I. Smith, E. L. Thomas, *Advanced Materials* **18**, 2505 (Oct, 2006).

123. J. Y. Cheng, F. Zhang, H. I. Smith, G. J. Vancso, C. A. Ross, *Advanced Materials* **18**, 597 (Mar, 2006).

124. H. J. Richter *et al.*, *Applied Physics Letters* **88**, (May, 2006).

125. Y. Soeno *et al.*, *Ieee Transactions on Magnetics* **39**, 1967 (Jul, 2003).

126. D. Wachenschwanz *et al.*, *Ieee Transactions on Magnetics* **41**, 670 (Feb, 2005).

127. N. Tagawa, T. Hayashi, A. Mori, *Journal of Tribology-Transactions of the Asme* **123**, 151 (Jan, 2001).

128. J. Moritz *et al.*, *Ieee Transactions on Magnetics* **38**, 1731 (Jul, 2002).

129. M. Albrecht *et al.*, *Applied Physics Letters* **80**, 3409 (May, 2002).

130. T. Thomson, G. Hu, B. D. Terris, *Physical Review Letters* **96**, (Jun, 2006).

131. O. Hellwig *et al.*, *Applied Physics Letters* **90**, (Apr, 2007).

132. C. Brucker *et al.*, *Ieee Transactions on Magnetics* **39**, 673 (Mar, 2003).

133. M. Kitano *et al.*, *Journal of Magnetism and Magnetic Materials* **235**, 459 (Oct, 2001).

134. M. Schabes , *to be published, J. Magn. Magn. Mater. 2008*, (Presented at PMRC 2007).

135. K. Watanabe, T. Takeda, K. Okada, H. Takino, *Ieee Transactions on Magnetics* **29**, 4030 (Nov, 1993).

136. Z. Z. Bandic, H. Xu, Y. M. Hsu, T. R. Albrecht, *Ieee Transactions on Magnetics* **39**, 2231 (Sep, 2003).

137. T. Ishida *et al.*, *Ieee Transactions on Magnetics* **39**, 628 (Mar, 2003).

138. C. A. Ross *et al.*, *Journal of Vacuum Science & Technology B* **17**, 3168 (Nov-Dec, 1999).

139. M. Todorovic, S. Schultz, J. Wong, A. Scherer, *Applied Physics Letters* **74**, 2516 (Apr, 1999).

140. Y. Kanai *et al.*, *Journal of Magnetism and Magnetic Materials* **320**, E287 (Jul, 2008).

141.   N.Honda, S. Takahashi, K.Ouchi, *Journal of Magnetism and Magnetic Materials* **320**, 2195 (2008).

142.   http://www.hoovers.com. (2007).

143.   http://www.pcworld.com/article/id, 1/article.html.

144.   http://www.isuppli.com/news/default.asp?id=8919.

145.   http://www.eetasia.com/ART_8800496826_499486_NT_192bafd4.HTM.

146.   C. Associates, "Hard Disk Drive Capital Equipment Market & Technology Report" (2006).

147.   F. Ilievski, C. A. Ross, G. J. Vancso, *Journal of Applied Physics* **103**, (Apr, 2008).

148.   http://www.eetasia.com/ART_8800293346_480600_NT_7401f7b8.HTM.

149.   http://www.semiconductor.net/articleXml/LN786475151.html.

150.   http://www.semiconductor.net/index.asp?layout=articlePrint&articleID=CA6563343.

151.   http://www.molecularimprints.com/Products/I2200page.html.

152.   Bita *et al.* (MIT, 2008, submitted).

153.   S.Kawai, R.Ueda. *J. Electrochem Soc.* **19**, 32 (1975).

154.   R. M. Metzger *et al.*, *Ieee Transactions on Magnetics* **36**, 30 (Jan, 2000).

155.   Z. B. Zhang, D. Gekhtman, M. S. Dresselhaus, J. Y. Ying, *Chemistry of Materials* **11**, 1659 (Jul, 1999).

156.   N. W. Liu, A. Datta, C. Y. Liu, Y. L. Wang, *Applied Physics Letters* **82**, 1281 (Feb, 2003).

157.   Z. J. Sun, H. K. Kim, *Applied Physics Letters* **81**, 3458 (Oct, 2002).

158.   H. Masuda *et al.*, *Applied Physics Letters* **71**, 2770 (Nov, 1997).

159.   P. Aranda, J. M. Garcia, *Journal of Magnetism and Magnetic Materials* **249**, 214 (Aug, 2002).

160.   S. H. Sun, C. B. Murray, D. Weller, L. Folks, A. Moser, *Science* **287**, 1989 (Mar, 2000).

161.   Y. Ding, S. Yamamuro, D. Farrell, S. A. Majetich, *Journal of Applied Physics* **93**, 7411 (May, 2003).

162.   T. J. Klemmer *et al.*, *Journal of Magnetism and Magnetic Materials* **266**, 79 (Oct, 2003).

163.   C. A. C. Mingqi Li, C. K. Ober, in *Block Copolymers II*. (Springer-Verlag Berlin Heidelberg, 2005), vol. 190, pp. 183-226.
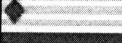
Appendix

Table A. 1: Lithographic requirements as per the ITRS Roadmap 2007: Near Term Lithographic technological requirements (79)

Table LITH3a Lithography Technology Requirements—Near-term Years									
Year of Production	2007	2008	2009	2010	2011	2012	2013	2014	2015
DRAM ½ pitch (nm) (contacted)	65	57	50	45	40	36	32	28	25
DRAM and Flash									
DRAM ½ pitch (nm)	65	57	50	45	40	36	32	28	25
Flash ½ pitch (nm) (un-contacted poly)	54	45	40	36	32	28	25	23	20
Contact in resist (nm)	72	62	55	50	44	39	35	31	28
Contact after etch (nm)	65	57	50	45	40	36	32	28	25
Overlay [A] (3 sigma) (nm)	13	11.3	10.0	9.0	8.0	7.1	6.4	5.7	5.1
CD control (3 sigma) (nm) [B]	5.6	4.7	4.2	3.7	3.3	2.9	2.6	2.3	2.1
MPU									
MPU/ASIC Metal 1 (M1) ½ pitch (nm)	68	59	52	45	40	36	32	28	25
MPU gate in resist (nm)	42	38	34	30	27	24	21	19	17
MPU physical gate length (nm) *	25	23	20	18	16	14	13	11	10
Contact in resist (nm)	84	73	64	56	50	44	39	35	31
Contact after etch (nm)	77	67	58	51	45	40	36	32	28
Gate CD control (3 sigma) (nm) [B] **	2.6	2.3	2.1	1.9	1.7	1.5	1.3	1.2	1.0
Chip size (mm²)									
Maximum exposure field height (mm)	26	26	26	26	26	26	26	26	26
Maximum exposure field length (mm)	33	33	33	33	33	33	33	33	33
Maximum field area printed by exposure tool (mm²)	858	858	858	858	858	858	858	858	858
Wafer site flatness at exposure step (nm) [C]	63	54	50	45	40	32	29	22	17
Number of mask levels MPU	33	35	35	35	35	35	35	37	37
Number of mask levels DRAM	24	24	24	26	26	26	26	26	26
Wafer size (diameter, mm)	300	300	300	300	300	450	450	450	450
NA required for Flash (single exposure)	1.01	1.20	1.35	1.52	1.70	1.91			
NA required for logic (single exposure)	0.91	1.04	1.20	1.38	1.54	1.73	1.94		
NA required for double exposure (Flash)	0.72	0.86	0.96	1.08	1.22	1.36	1.53	1.72	1.93
NA required for double exposure (logic)	0.62	0.72	0.82	0.95	1.06	1.19	1.34	1.50	1.68

Manufacturable solutions exist, and are being optimized

Manufacturable solutions are known
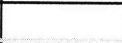
Interim solutions are known
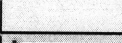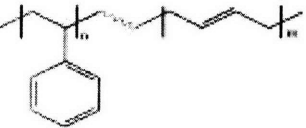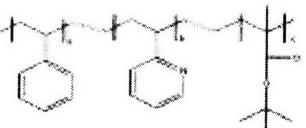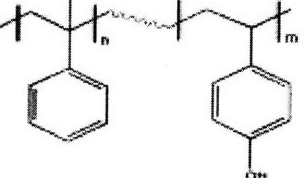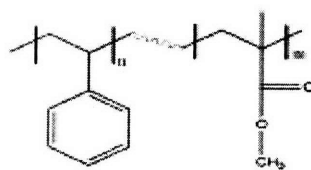
Manufacturable solutions are NOT known

Table A. 2: Lithographic requirements as per the ITRS Roadmap 2007:Long term Lithographic requirements(79)

Table LITH3b Lithography Technology Requirements—Long-term Years							
Year of Production	2016	2017	2018	2019	2020	2021	2022
DRAM ½ pitch (nm) (contacted)	22	20	18	16	14	13	11
DRAM and Flash							
DRAM ½ pitch (nm)	23	20	18	16	14	13	11
Flash ½ pitch (nm) (un-contacted poly)	18	16	14	13	11	10	9
Contact in resist (nm)	25	22	20	18	16	14	12
Contact after etch (nm)	23	20	18	16	14	13	11
Overlay [A] (3 sigma) (nm)	4.5	4.0	3.6	3.2	2.8	2.5	2.3
CD control (3 sigma) (nm) [B]	1.9	1.7	1.5	1.3	1.2	1.0	0.9
MPU							
MPU/ASIC Metal 1 (M1) ½ pitch (nm)	23	20	18	16	14	13	11
MPU gate in resist (nm)	15	13	12	11	9	8	8
MPU physical gate length (nm) *	9	8	7	6	6	5	4
Contact in resist (nm)	28	25	22	20	18	16	14
Contact after etch (nm)	25	23	20	18	16	14	13
Gate CD control (3 sigma) (nm) [B] **	0.9	0.8	0.7	0.7	0.6	0.5	0.5
Chip size (mm²)							
Maximum exposure field height (mm)	26	26	26	26	26	26	26
Maximum exposure field length (mm)	33	33	33	33	33	33	33
Maximum field area printed by exposure tool (mm²)	858	858	858	858	858	858	858
Wafer site flatness at exposure step (nm) [C]							
Number of mask levels MPU	39	39	39	39	39	39	39
Number of mask levels DRAM	26	26	26	26	26	26	26
Wafer size (diameter, mm)	450	450	450	450	450	450	450
NA required for Flash (single exposure)							
NA required for logic (single exposure)							
NA required for double exposure (Flash)							
NA required for double exposure (logic)							
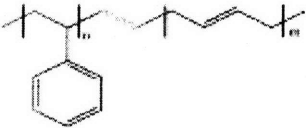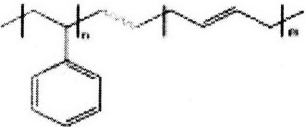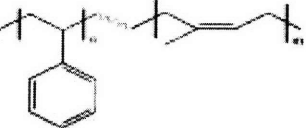
Manufacturable solutions exist, and are being optimized

Manufacturable solutions are known

Interim solutions are known

Manufacturable solutions are NOT known
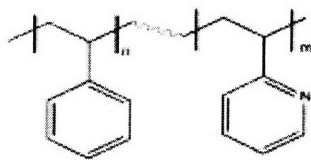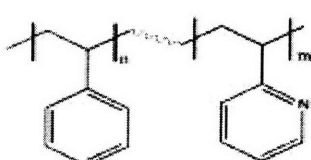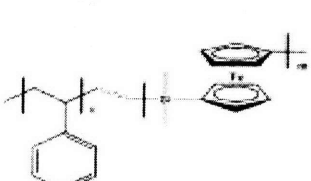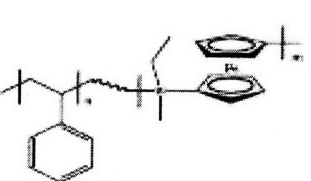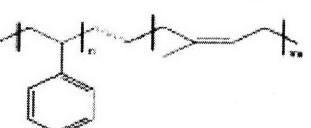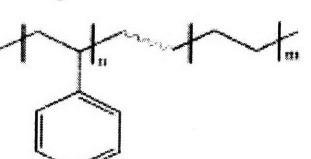
Table A. 3: Summary of methods for microdomain orientations control for block copolymers in thin film state(*163*)

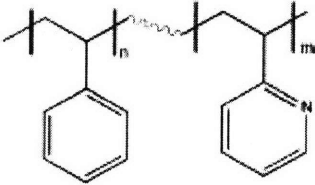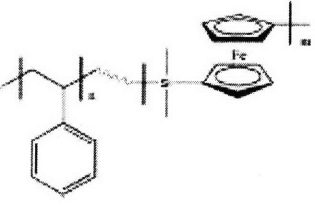| Block copolymer	Structure	Morphology	Orientation method
Poly(butadiene-*b*-ethyleneoxide)		Lamella	Crystallization
Poly(styrene-*b*-butadiene)		Cylinder	Fast solvent evaporation
Poly(styrene-*b*-butadiene)		Lamella, cylinder	Fast solvent evaporation
Poly(styrene-*b*-butadiene)		Cylinder	Orthogonal flow field
Poly(styrene-*b*-isoprene)		Cylinder	Directional crystallization with Graphoepitaxy
Poly(styrene-*b*-ethyleneoxide)		Cylinder	Fast solvent evaporation
Poly(styrene-*b*-2-vinylpyridine-*b*-*tert*-butylmethacrylate)		Lamella	Fast solvent evaporation
Poly(styrene-*b*-butadiene-b-styrene)		Cylinder	Fast solvent evaporation
Poly(*α*-methylstyrene-*b*-4-hydroxystyrene)		Cylinder	Fast solvent evaporation

Poly(styrene-*b*-*n*-alkylmethacrylate)		Multiple	Film thickness
Poly(styrene-*b*-*n*-butylmethacrylate)		Lamella	Substrate topography
Poly(styrene-*b*-methylmethacrylate)		Lamella, cylinder	Neutral surface
Poly(styrene-*b*-methylmethacrylate)		Lamella	Control interfacial interaction
Poly(styrene-*b*-methylmethacrylate)		Lamella	Chemical patterned substrate
Poly(styrene-*b*-methylmethacrylate)		Cylinder	Electric field
Poly(styrene-*b*-methylmethacrylate)		Lamella	Orthogonal electric field
Poly(styrene-*b*-methylmethacrylate)		Sphere	Graphoepitaxy

Poly(styrene-*b*-methylmethacrylate)		Lamella	Directional crystallization
Poly(styrene-*b*-2-vinylpyridine)		Sphere	Graphoepitaxy
Poly(styrene-*b*-2-vinyl pyridine)		Lamella	Chemical patterned substrate
Poly(styrene-*b*-ferrocenyldimethyl-silane)		Sphere	Graphoepitaxy
Poly(ferrocenyldime-thylsilane-*b*-dimethylsiloxane)		Cylinder	Graphoepitaxy
Poly(styrene-*b*-ferrocenylethyl-methylsilane)		Cylinder	Fast solvent evaporation
Poly(styrene-*b*-isoprene-b-styrene)		Cylinder	Electric field
Poly(styrene-*b*-isoprene)		Cylinder	Directional crystallization
Poly(styrene-*b*-ethylene)		Cylinder	Directional crystallization

Table A. 4: Summary of block copolymers studied for template nanolithographic applications (*163*)

Block copolymer	Structure	Morphology	Application
Poly(styrene-*b*-butadiene)		Cylinder	Silicon nitride, germanium nanodots
Poly(styrene-*b*-isoprene)		Sphere	Silicon nitride, germanium nanodots
Poly(styrene-*b*-isoprene)		Sphere	Metal nanodots
Poly(styrene-*b*-isoprene)		Sphere	GaAs nanodots
Poly(styrene-*b*-methylmethacrylate)		Sphere	$Co_{74}Pt_{26}$ and $Co_{74}Cr_6Pt_{20}$ magnetic media
Poly(styrene-*b*-methylmethacrylate)		Cylinder	Semiconductor capacitor
Poly(styrene-*b*-methylmethacrylate)		Cylinder	Nanoscopic templates
Poly(styrene-*b*-2-vinylpyridine)		Spherical micelles	GaAs quantum dots
Poly(styrene-*b*-2-vinylpyridine)		Spherical micelles	Diamond nanocolumns

Poly(styrene-*b*-2-vinylpyridine)		Spherical micelles	Nanoporous gold films
Poly(styrene-*b*-ferrocenyldimethyl-silane)		Sphere	Silica nanopillars
Poly(isoprene-*b*-ferrocenyldimethyl-silane)		Cylinder	Cobalt magnetic media

--X--